NUCLEAR MAGNETIC RESONANCE IN LIQUID METALS AND ALLOYS

by

James Heighway B.Sc.

A thesis submitted for the degree of
Doctor of Philosophy of the
University of Warwick.

School of Physics,
University of Warwick.

November, 1969.

Memorandum

This dissertation is submitted to the University of Warwick in support of my application for admission to the degree of Doctor of Philosophy. It contains an account of my own work performed at the School of Physics of the University of Warwick in the period October 1966 to October 1969 under the supervision of Prof. E. F. W. Seymour. No part of it has been used previously in a degree thesis submitted to this or any other university. The work described in this thesis is the result of my own independent research except where specifically acknowledged in the text. A preliminary account of the liquid alloy results has been published in Phys. Letts., 29A, (1969), 282, and the calculation of the Knight shift of sodium has been published in Colloque Ampere XV, North Holland, Amsterdam, 1969. It is anticipated that the detailed liquid alloy results, the full results of the Knight shift calculations and the Pb - Bi results of Chapter 6 will be published presently.

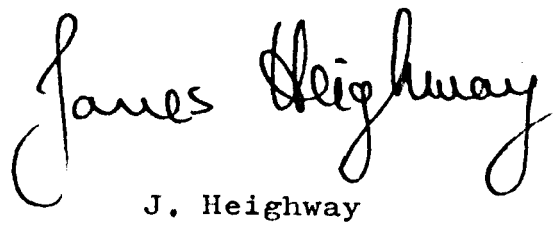

J. Heighway

November, 1969.

To my father, my mother and my wife Diane,
without whose patient encouragement,
support and unending love this work would
never have come to fruition.

Author's Note

The S.I. system of units has been used throughout this thesis except as mentioned below. In this system the units of magnetic intensity are tesla and

$$10^{-4} \text{ tesla} \equiv 1 \text{ gauss.}$$

Wavefunctions are most normally expressed in atomic units

$$a_0 = 0.52_9 \times 10^{-10} \text{m}$$

amd these have been used in the calculations of Chapter 4. In a similar vein, the spin susceptibility has been expressed in c.g.s. "volume" units, because theorists usually employ this system.

Acknowledgements

I am indebted to Prof. E. F. W. Seymour for his interest, advice and help, which has been a continual source of inspiration to me during the course of this work and in the preparation of this thesis. I would like, also, to acknowledge the patient guidance given to me by Dr. G. A. Styles in all matters concerning nuclear resonance. In addition I would like to thank Dr. E. M. Dickson who repeatedly gave me useful and stimulating advice concerning, amongst many other resonance phenomena, quadrupolar relaxation, and Dr. B. W. Holland whose patience with my ignorance of theoretical matters was a continual source of encouragement. Further, I thank Professor A. J. Forty for allowing me to use the facilities of the School of Physics.

My thanks are due to the Science Research Council for providing a Research Studentship, and to Mrs. Bobbie Ann Kerton and Miss Christine A. Phillips for the preparation of this manuscript.

ABSTRACT

Nuclear magnetic resonance measurements in pure lead and in dilute binary alloys of lead are reported.

(i) Measurements of the ^{207}Pb linewidth and Knight shift (K) in solid and liquid lead are presented. The linewidth shows a narrowing at 550 K and this is interpreted in terms of a motional narrowing phenomenon. The value obtained for the pseudo-dipolar contribution to the linewidth is $\sim 3 \times 10^{-4}$ tesla and this is shown to be consistent with estimates available in the literature. The values of $(1/K)(dK/dT)$ for both the solid and liquid phases are $+6.3(\pm 0.4) \times 10^{-5}$ and $-7.6(\pm 0.9) \times 10^{-5}$ $(\text{kelvin})^{-1}$ respectively. The result in the solid is consistent with a value deduced from spot measurements available in the literature.

The absolute value of the ^{207}Pb Knight shift in pure lead, together with the values for 12 other pure metals, is discussed in terms of a zero-order pseudopotential formulation. Holland has recently discussed the evaluation of K from a single O.P.W. formulation with the approximation that the pseudofunction is constant over an ion core. This approximation is now removed and good agreement with experiment is obtained using interacting electron spin susceptibilities (χ_p). It is shown that very little change in K is expected on melting if χ_p remains constant. It is thus concluded that when K remains constant through the melting point the spin susceptibility, and therefore the density of states, ~~has very~~ usually has nearly the free-electron value in the solid.

The extension of the Holland theory introduces a dependence of the Knight shift on the Fermi wave vector, k_F. The temperature dependence of K, produced by expansion effects, is evaluated but in every case is an order of magnitude smaller than is observed. It is shown that the major temperature dependence arises from the term to first-order in the pseudopotential and this has been evaluated for 6 liquid metals from the expression of Faber.

(ii) Measurements of the ^{207}Pb Knight shift in dilute liquid alloys of lead with Ag, Cd, In, Sb, Au, Hg, Tl and Bi are reported. The results for the liquid at 625 K are larger in magnitude and of opposite sign to those on lead solid solutions at room temperature. The way in which these differences occur is investigated for the two alloys Pb - 18% Bi and Pb - 20% Tl. The experimental results for the liquid are discussed in turn, in terms of the zero-order pseudopotential theory, the first-order theory and the Friedel theory. It is deduced that a reasonable explanation can be obtained from the Friedel model if the semi-empirical choice of phase shifts, deduced by Flynn, is used.

(iii) Measurements of the ^{207}Pb and ^{209}Bi Knight shifts and ^{209}Bi linewidths in the Pb - Bi system are reported. Experimental studies of the concentration dependence and the temperature dependence are presented. The ^{209}Bi linewidth versus concentration shows a maximum at approximately 50% and around this maximum, the linewidth versus temperature plot shows a sharp minimum. This is interpreted in terms of a quadrupolar contribution to the linewidth. This quadrupolar relaxation is also observed in pure bismuth and the enhancement on alloying is

discussed in terms of a crude diffusing ion model. On the basis of this model a qualitatively correct description of the alloying effects is obtained.

Finally, in a general discussion, it is concluded that the nearly-free-electron picture is adequate for a description of Knight shifts in liquid metals and alloys if allowance for electron-electron interactions is included into the spin susceptibility.

CONTENTS

		Page
CHAPTER ONE	INTRODUCTION	
1.01	Introduction	1
1.02	Experimental situation	2
1.02.1	The Hall coefficient	2
1.02.2	Optical properties	3
1.02.3	Resistivity and thermopower	4
1.02.4	Magnetic susceptibility	4
1.02.5	The Knight shift for pure metals	5
1.02.6	Positron annihilation and soft x-ray emission	7
1.02.7	The atomic structure	8
1.03	Theoretical situation	10
1.03.1	The electronic states in a liquid metal	10
1.03.2	Nearly-free-electron model	12
1.04	Nuclear Magnetic Resonance	13
1.04.1	Basic theory	13
1.04.2	N.M.R. in metals	15
	(i) The Knight shift	16
	(ii) The relaxation rate and the Korringa product	17
1.04.3	N.M.R. in liquid metals and alloys	19
References		22
CHAPTER TWO	EXPERIMENTAL DETAILS	27
2.01	Basic experimental arrangement	27
2.02	Auxiliary apparatus	30
2.02.1	The magnet	30
2.02.2	Computer of Average Transients	31

Page

2.02.3 Frequency and field calibration 32

2.02.4 The furnace 33

2.03 Sample preparation 34

(a) Ultrasonic dispersion 35

(b) Aerosol technique 36

2.04 Measuring technique 37

References 39

CHAPTER THREE EXPERIMENTAL RESULTS 40

3.01 Introduction 40

3.02 Pure lead 41

3.03 Liquid alloys 42

3.03.1 Concentration dependence of the Knight shift 42

3.03.2 Temperature dependence of the Knight shift 44

3.03.3 Temperature dependence of the ^{207}Pb linewidth 44

References 45

CHAPTER FOUR DISCUSSION OF THE OBSERVATIONS FOR PURE METALS 46

4.01 Introduction 46

4.02 ^{207}Pb linewidth 46

4.03 Knight shifts in liquid metals 51

4.03.1 Introduction 51

4.03.2 The theory of Holland 53

4.03.3 Extension of the zero-order theory to take account of incomplete 'constancy' 56

4.03.4 Results for Knight shifts - evaluated to second order in the displacements 59

4.03.5 Discussion 61

4.04 The temperature dependence of the Knight shift 63

4.04.1 General considerations 63

4.04.2 The temperature coefficient from the zero-order pseudopotential expression 65

4.04.3 The temperature coefficient from the first-order pseudopotential term 67

4.05 Conclusions 71

References 72

CHAPTER FIVE DISCUSSION OF THE OBSERVATIONS FOR LIQUID ALLOYS 75

5.01 Introduction 75

5.02 ^{207}Pb linewidth in Pb - 18% Bi and Pb - 20% Tl 76

5.03 The variation of the ^{207}Pb Knight shift with solute concentration 78

5.03.1 Volume and electron/atom ratio effects 78

5.03.2 Changes in P_F - to zero-order in the pseudopotential 79

5.03.3 Changes in P_F - to first-order in the pseudopotential 81

5.03.4 Changes in P_F - the Friedel model 86

5.04 General Discussion 92

5.05 The variation of the ^{207}Pb Knight shift with temperature in Pb - 18% Bi and Pb - 20% Tl 94

5.06 Conclusions 99

References 100

CHAPTER SIX THE LEAD-BISMUTH SYSTEM 102

6.01 Introduction 102

6.02 Experimental results 104

6.02.1 Knight shifts 104

6.02.2 Linewidth 105

6.03 Knight shifts - comparison with earlier data 106

6.04 Discussion of the linewidth 108

Page

6.04.1 The Korringa relation 108

6.04.2 Quadrupolar relaxation 111

6.04.3 Results for pure bismuth 115

6.04.4 Conclusions for pure bismuth 117

6.04.5 Relaxation in liquid alloys 117

6.04.6 ^{209}Bi linewidths in liquid alloys - identification of quadrupolar component 120

6.04.7 ^{209}Bi linewidths in liquid alloys - origin of enhanced quadrupolar component 123

6.04.8 Conclusions 128

References 130

CHAPTER SEVEN SYNOPSIS 133

APPENDIX I Data appendix

APPENDIX II ALGOL 60 program

APPENDIX III Sternheimer antishielding factors

CHAPTER ONE

INTRODUCTION

1.01 Liquid Metals

The study of liquid metals has followed two converging paths; studies of the electronic properties (resistivity, Hall effect and Knight shift) and studies of atomic arrangements (theoretical models being tested using X-ray and neutron diffraction techniques). The development of liquid metal physics has followed, very closely, that of solids in that the long range periodicity of the solid lattice was found to produce bands of allowed and forbidden energies, and many authors have looked at liquids in an analogous fashion, hoping to obtain from a structural model an understanding of electronic properties. In essence the main question has been: 'How free-electron like are liquid metals ?' The role of electronic studies is secondary in the sense that they provide a test of the predictions of a structural model; it is difficult to deduce structural information reliably from measured electronic properties. For instance, from the fact that the Knight shift changed little on melting for many metals (see section 1.02.5), a microcrystalline model of a liquid was postulated at one stage, but this now is no longer current.

The wide diversity of the results of investigations of the electronic properties of liquids makes it possible that one structural model will not be found to explain all the data. Perhaps, in analogy to solids, various structures exist and each liquid metal must be considered independently. Liquid metal

physics is not able to provide an answer to this question at present and future advances still depend, to a large extent, upon experimental data both of atomic arrangements and, less directly but more importantly, of electronic properties.

The work reported in this thesis concerns further studies of the electronic properties of liquid metals - particularly the Knight shift - and the emphasis of this introduction will thus be on the current experimental and theoretical situation in this field. This has been the subject of a number of comprehensive reviews and a brief discussion only will be given here. The situation up to 1963 was extensively reviewed by Cusack[1]. Since then Mott (1965)[2] has given a short discussion of transport properties and Wilson (1965)[3] an extensive discussion including the thermodynamic properties of liquid metals and alloys. More recently, the whole field of the properties of liquid metals has been covered by the Proceedings of the Brookhaven Conference[4].

1.02 Experimental situation

The majority of the experimental results on the electronic properties of liquid metals supports the free-electron model.

1.02.1 The Hall coefficient In general the Hall coefficient R_H of liquid metals agrees with the free-electron value, often needing a large change on melting to do so. The temperature dependence of R_H has been measured for a number of liquid metals and within experimental uncertainty follows that predicted by the free-electron model; volume changes being the sole effect. The tendency of R_H to revert to a free-electron value was first investigated by Cusack and Kendall[5] who attributed the change on melting to the increase of disorder.

As long as the electron mean free path is greater than the range of any order that exists then a spherical Fermi surface results and this is more than sufficient to produce a free-electron value of R_H; the necessary conditions being an ellipsoidal Fermi surface and an isotropic relaxation time. When the mean free-path becomes shorter (for instance, in polyvalent metals) R_H has been observed to diverge from the free-electron value. However, the full explanation is not quite as simple as this suggests for, whereas the value of R_H for the metals Hg, Sn, Zn and Cd is in excellent agreement with the free-electron prediction, that for Bi, Pb, Tl, In and Ga is not. From this simple discussion it seems surprising that any polyvalent metal exhibits a free-electron Hall coefficient but, certainly, the majority of liquid metals do conform.

The situation in alloys is much less well documented. For Hg - In[6] no agreement with a free-electron prediction is obtained even though Hg and In themselves agree reasonably well; for Ag - In Busch and Guntherodt[7] find R_H lower than, but within experimental uncertainty of, the free-electron value; and for Cu - Sn, Enderby et al.[8] suggest that bound state formation eliminates the possibility of free-electron behaviour. The situation is thus not conclusive at the present time.

1.02.2 Optical properties Measurements of the optical properties support the conclusions deduced from the Hall effect data for pure metals. The optical data can be interpreted in terms of the Drude theory; both effective mass values and relaxation times agree with the free-electron values. Further, the degree of agreement seems to be independent of the valence.

However, recently, Rice[9] has suggested that in general the wavelength range over which measurements have been made is insufficient to provide a sensitive test of the Drude theory. This casts some doubt upon the reliability of the evidence from the optical measurements but the general agreement of optical and Hall coefficient data seems indicative of free-electron behaviour.

Again the situation for liquid alloys is less documented. The measurements of Schultz[10] on Hg - In certainly agree with those for R_H in showing that an alloy may not necessarily be free-electron like even if the pure components are, but few data are available.

1.02.3 Resistivity and thermopower The resistivity and thermopower of both liquid metals and alloys has been well documented. The introduction of a nearly-free-electron theory, the pseudopotential method of Ziman et al.[11] has led to, at least, a qualitative if not fully quantitative explanation of the observations. The changes of resistivity with temperature and on melting are explained in terms of a changing atomic radial distribution function (see section 1.02.7) which is a measure of the atomic disorder. The full theory, which will be discussed in more detail in section 1.03.2, must be considered as giving support to an almost-free-electron picture.

1.02.4 Magnetic susceptibility It has often been said that if liquid metals are free-electron like then the density of states at the Fermi surface $\rho(E_F)$, and therefore the Pauli spin susceptibility χ_p, must change on melting. The density

of states in the solid is deduced from values of γ, the electronic specific heat coefficient, which is unfortunately affected, generally to an unknown extent, by electron-phonon and electron-electron effects. Only recently has a more direct method of obtaining χ_p and therefore $\rho(E_F)$ become available. Before, it was necessary to estimate the ionic and conduction electron diamagnetic contributions to the total susceptibility, and subtract their sum from the measured total to get an estimate of χ_p. With the uncertainties of the estimates, together with the experimental error, the end result was little more than a reasonable guess. However, with the improvements of electron spin resonance spectrometry it is now possible to measure χ_p directly in a limited number of liquid metals; Li, Na and K seem to be the only serious possibilities and measurements on Li only have so far been reported[12]. The result, that $(\chi_p)_{liquid}/(\chi_p)_{solid} = 1.04(\pm 0.05)$, suggests, in view of the decrease of the total susceptibility on melting, that the diamagnetism of the conduction electrons may be modified by the disorder. Further, the lack of any change in the Knight shift (see below) or in the soft X-ray data of Skinner[13] confirms the similarity between solid and liquid Li. Similar experiments have been performed on Na where Devine and Dupree (private communication) show that, if anything, a small increase of χ_p on melting occurs, $(\chi_p)_{liquid}/(\chi_p)_{solid} = 1.1(\pm 0.1)$. It is concluded that in Li and Na, at least, the change in the electronic properties on melting is not marked; both χ_p and the Knight shift remaining virtually unaffected by melting.

1.02.5 The Knight shift for pure metals The Knight shift[14], the theory of which will be discussed in more detail

in section 1.04.2, can be written

$$K = \frac{8\pi}{3}\Omega\chi_p P_F \qquad 1.1$$

where Ω is the atomic volume, and $P_F \equiv \langle|\Upsilon(0)|^2\rangle_F$ the probability density at the nucleus averaged over all electrons on the Fermi surface. The Knight shift changes by less than 5% on melting for Li, Na, Rb, Cs, Al, Hg, Sn, Cu, Pb, Tl and In and by a large amount on melting for Ga, Cd, Sb and Bi. The situation with regard to the Knight shift change on melting is clearer now than it was at the time of Cusack's review. The large change in K on melting for Cd coincides with a large change in R_H, and this is also the case for Bi and Sb. However there is still a discrepancy for the cases of Pb and Sn where R_H changes on melting but K does not. Perhaps the situation is as discussed by Ziman[15] who suggests that the constancy of K through the melting point indicates a constancy of both P_F and χ_p. Since in the liquid state the density of states seems to be free-electron like, whereas the value of γ in the solid appears not to be, the question is why χ_p does not change on melting. The answer probably lies in the interpretation of γ. For Pb and Li, γ has been found to be greater than twice the free-electron value. Such large values have been explained by Ashcroft and Wilkins[16] as arising from a strong electron-phonon interaction. (For Na, Al and Pb they obtain effective masses, in the solid, very near to the free-electron value.) In addition, Anderson and Gold[17] have fitted the experimental Fermi surface of lead on the basis of 4 electrons/atom and deduced that band structure effects only reduce $\rho(E_F)$ by $\sim 10\%$. The suggestion is that only in a few cases does χ_p change markedly on melting and this change is then reflected in the Knight shift. Since K involves an average over the Fermi

surface (through $\chi_p P_F$) it might be expected to be relatively insensitive to deviations from sphericity so that a free-electron Knight shift might be obtained (e.g. for Pb) even where a significant change in other properties, such as R_H, are found to occur. The anomalous results are thus those where a large change in K occurs on melting and an explanation must be looked for. In the case of Bi, a semi-metal, the density of states is very low in the solid phase, whereas in the liquid the Knight shift results suggest a free-electron value. A similar explanation has been given for Cd by Kasowski and Falicov[18] where the density of states changes with temperature due to a wash-out of the strong pseudopotential.

Certainly, a full discussion of the situation is more complicated than the above brief statements imply but it is apparent that, for pure metals, the lack of any change in K on melting is not at variance with the Hall effect and optical data. The situation in alloys is more complex still and a discussion is deferred until section 1.04.3.

1.02.6 Positron annihilation and soft X-ray emission

There are some potentially very interesting data being obtained using the techniques of positron annihilation and soft X-ray spectra. In positron annihilation experiments, the angular correlation of the two annihilation γ-rays, for a thermalised positron, gives information on the linear momentum distribution of the electrons. Stewart and Kusmiss[19] have reported positron annihilation results for 15 solid and liquid metals, at varying temperatures in both phases. These can be divided into three groups according to whether they show a change on

melting, on heating below the melting point, or on heating above the melting point. It is interesting that Sb, Bi and Ga (which all show large changes in K on melting) should fall into the first group. However, Hg and Sn also fall into this group and thus destroy any hope of a simple correspondence with Knight shift changes. Further experiments are in progress and perhaps a better understanding of the implications of the results (possibly in terms of an increasing vacancy concentration on heating) will become available.

There seems to have been a remarkable lack of activity in soft X-ray studies; the experimental results seem to be limited to Li[13] and Al[20]. This type of experiment would be expected to give a very good test of the free-electron picture in that it measures the density of states curve. However what is really measured is $\rho(E)$ multiplied by the probability of a transition occurring and this latter quantity is very difficult to calculate. Still, the assumption that it remains constant on melting may be made[21] and a comparison of liquid and solid becomes useful. In both Li and Al there is little change on melting and neither show close correlation with the free-electron prediction in the liquid phase. There seems to be a lot of scope for further investigations of liquid metals using both positron annihilation and soft X-ray emission techniques.

1.02.7 The atomic structure The atomic structure of liquid metals has been investigated using both X-ray and neutron diffraction experiments. The pattern obtained is a series of diffuse, circular haloes. From the results, using a Fourier transformation, the pair distribution function P(r) can be

obtained which represents the probability of finding an atom at a distance r from a chosen atom. Certain additional information, discussed by Furukawa[22] in his review, can be determined from P(r). For instance, the position of the first maximum gives the mean inter-atomic distance, the 'width' of this first maximum gives the mean 'jump' distance involved in thermal motion, and the area beneath it the mean number of nearest neighbours (the coordination number). Furukawa suggests that the uncertainties in determining the coordination number from the experimental P(r) are large and that it is better to obtain a value from the density and the inter-atomic spacing. Using this latter technique he obtains a coordination number of $\sim$ 11 for most liquid metals. These diffraction patterns do not contain enough information to permit the derivation of a structural model but, of course, must be reproduced by any postulated model. The microcrystalline model proposed by Knight et al.[23] to explain the constancy of K on melting, does not reproduce the diffraction data without excessive motional blurring, whereas the random packing model of Bernal[24] gives good agreement with the observed diffraction patterns.

Although experimental diffraction patterns have been reported for many metals the list is by no means exhaustive and model pair distribution functions are very useful (or, more commonly, their Fourier transform, called the structure factor and denoted by a(K)). The most widely used are those of Ashcroft et al.[25] based on the solution of the Percus-Yevick equation for hard spheres. Ashcroft derived structure factors for varying temperatures and found values which agreed well with measured results up to the first maximum. Beyond this the model

and experimental results get out of phase. As will be discussed in Chapter 4, this has the effect of producing a marked uncertainty in the predicted temperature dependence of the Knight shift.

For a liquid alloy system the situation is more complicated. For a complete discussion of binary alloys, three partial structure factors are required, $a_{00}(K)$, $a_{01}(K)$ and $a_{11}(K)$ corresponding to solvent-solvent, solvent-solute and solute-solute distributions. Again model factors are available based on a hard sphere model with two different sized spheres; and in addition there exists a limited number of measured results that have been deduced from a three-radiation experiment[26]. The precision of these partial structure factors is not yet sufficient to warrant the extra complication involved in their use (compared with the approximation of using merely the a(K) for the pure metal) for the calculation of Knight shifts in dilute alloys.

Finally, it should be mentioned that, X-ray measurements in some liquid alloys have been interpreted as showing the retention of solid-like structure above the liquidus (for instance, in InBi and In_2Bi[27]) and as showing changes in coordination number (for instance, in Pb - Bi[28]) across the concentration range. The possibility of observing the influence of such effects on the electronic properties is discussed in Chapter 6.

1.03 Theoretical situation

1.03.1 The electronic states in a liquid metal The most extensive treatment of the electronic states in a liquid metal is that of Edwards[21,29]. He defines a quantity $\rho(E,\underline{k})$

which gives the probability that an electron of energy E has a Fourier component of wave number $\underline{k}$ in its wave function. Edwards evaluates an expression for $\rho(E,\underline{k})$ in a liquid by a complicated perturbation procedure expressed in terms of Greens functions. The writer does not intend to suggest that he understands the Edwards formalism completely but the results may be visualised as follows. The $\rho(E,\underline{k})$ gives the height of a surface above the E - $\underline{k}$ plane, which for a simple free-electron case degenerates into a line whose projection is the normal parabola. For complete disorder the surface is humped around the free-electron line, corresponding to a spectrum of possible $\underline{k}$ - values for any given energy E. For a more realistic structure factor the resulting E - $\underline{k}$ curves are blurred and kinked. Near to the origin the curves are free-electron like but at particular higher energy regions (which will be occupied in polyvalent metals) the kinks occur and cause deviations from free-electron behaviour. The extent of the kinks depends on the ratio of the electron mean free path to the range of order, for a mean free path $\gg$ the range of order, free-electron ideas are valid. This approach is very general and the case for each metal must be considered in more detail before a full explanation (for instance of the different value of R_H in Pb and Sn) is available.

The theory of Edwards is complicated and not amenable to calculations. Cusack[1] has shown that the nearly-free-electron theories are special cases of the Edwards formalism and calculations based on free-electron ideas will be used to discuss the experimental results in this thesis. There is still no theoretical justification of this for polyvalent metals.

1.03.2 Nearly-free-electron model The earliest attempts to apply this method to the liquid state[30] failed for two reasons: firstly, the structure factor of the liquid, a(K), was insufficiently well known, and secondly, little was known about the scattering potential. Only when Ziman[11] considered the problem, was full attention given to the nature of the scattering potential.

Using a perturbation method starting from a plane wave description, and thus ensuring a free-electron value of R_H and agreement with the optical results, Ziman wanted to see if the resistivity, and its change with temperature, could be explained. To do this he used the concept of the pseudopotential[31]. Using this as a weak perturbing potential he justified the plane wave approximation via the smoothness of the pseudowavefunction. As model potentials became available[32] extensive calculations of the resistivity and thermopower of pure metals were made[33] using the Ziman formalism. The agreement with experiment was good considering the uncertainties in the Fourier transform of the pseudopotential U(K) and in the structure factor a(K). Improved agreement was obtained when corrections were made by Animalu for spin-orbit coupling[34] and non-local screening[35]. The temperature coefficient of the resistivity, which arose mainly from that of a(K), was evaluated and again the agreement was very reasonable. In addition, it is of interest, that for solid Pb the agreement between the Animalu potential and the matrix elements determining the Fermi surface as measured by Anderson and Gold[17] is excellent. This adds support to the applicability of the approach but also introduces a need for caution because temperature and melting effects might appreciably

modify the potential so that the model potential of Animalu might not be so good for the liquid phase. However, the overall agreement between experiment and theory for the resistivity, and the smallness of the pseudopotential at present in use, suggests that the potentials are fairly reliable and in fact the Animalu potentials have been used in the present work to describe a number of liquid polyvalent metals.

1.04 Nuclear magnetic resonance

The phenomenon of nuclear magnetic resonance (n.m.r.) was first observed in 1945[36,37] and since has been the subject of a number of text books[38,39,40]. The description given here will therefore be brief, emphasis being placed on those facets of n.m.r. that are particularly relevant to the study of electrons in metals.

1.04.1 Basic theory It is known that a nucleus with spin $\underline{I}$ (in units of $\hbar$, where h is Planck's constant) greater than zero can possess a magnetic moment $\underline{\mu}$. The application of a steady magnetic field $\underline{B}_0$ to an isolated nucleus gives rise to an interaction energy $-\underline{\mu}.\underline{B}_0$. If the steady field is along the z-direction the Hamiltonian can be written

$$\mathcal{H} = -\gamma_n \hbar B_0 I_z \qquad 1.2$$

where γ_n is the 'gyromagnetic ratio' (i.e. the ratio of the magnetic moment to the spin angular momentum) and I_z is the z-component of the spin. The allowed energies form $2I_z + 1$ equally spaced 'Zeeman' levels separated in energy by $\gamma_n \hbar B_0$. Transitions between these levels can be induced by supplying electromagnetic radiation of angular frequency ω given by

$\hbar\omega = \gamma_n \hbar B_0$ or $\omega = \gamma_n B_0$, the 'resonance condition'. It can readily be shown that the external radiation must be circularly polarised with its magnetic vector $\underline{B}_1$ in a plane perpendicular to $\underline{B}_0$. However, if the populations of adjacent levels do not differ (for instance, by the Boltzmann factor $\exp(\gamma_n \hbar B_0/kT)$ which obtains when the system is in thermal equilibrium), no net absorption of energy will be observed because upward and downward transitions have the same probability.

An assembly of spins achieves internal thermal equilibrium by various spin-spin interactions, the approach to equlibrium being characterised by a relaxation time T_2. The spin-spin interactions broaden the absorption line through two processes; (i) the spread in local z-fields produced at a nucleus by its neighbours (ii) the component of the local field at the resonant frequency which causes mutual flipping of pairs of identical spins and thus limits the lifetime of any spin state. By virtue of the uncertainty principle this lifetime limiting process broadens the line and T_2, which is the time for two spins initially precessing in phase to get out of phase by one radian, is related to the width by

$$T_2 = \frac{1}{2} g(\nu)_{max}$$

where $g(\nu)$ is the lineshape function.

The spin system achieves thermal equilibrium with the lattice through spin-lattice interactions and the coupling is characterised by a relaxation time T_1. Spin-lattice relaxation is effected by local magnetic fields that have a component fluctuating at the resonant frequency. There are a variety of mechanisms that can produce such fields, the dominant effect in

metals almost always being the contact interaction with conduction electrons.

At low temperatures the width of the absorption line is dominated by the spread in local z-fields. At sufficiently high temperatures the increased thermal motion causes all local fields to be averaged to zero and 'motional narrowing' occurs. The linewidth is then determined by lifetime limiting processes, the width, $\Delta\nu$, from absorption derivative extrema is given by

$$\Delta\nu = \frac{1}{\sqrt{3}\,\pi} \cdot \frac{1}{T_2} \qquad 1.3$$

and $T_1 = T_2$. A more detailed discussion of the various contributions to the linewidth of ^{207}Pb in the solid metallic state is given in Chapter 4.

1.04.2 N.M.R. in metals[41] The addition of a conduction electron sea to an assembly of nuclei has two major effects: firstly, the frequency of the resonance absorption in the applied field $\underline{B}_0$ is shifted, and secondly, the conduction electrons dominate the spin-lattice relaxation processes.

For a nucleus interacting with an electron the simple Hamiltonian of eqn. 1.2 must be replaced by a more extensive expression

$$\mathcal{H} = -\gamma_n \hbar \underline{B}_0 . \underline{I} + \gamma_e \gamma_n \hbar^2 \underline{I} . \left[\frac{8\pi}{3} \underline{s}\, \delta(\underline{r}) + \left\{ \frac{3\underline{r}(\underline{s}.\underline{r})}{r^5} - \frac{\underline{s}}{r^3} \right\} + \frac{\underline{l}}{r^3} \right] \qquad 1.4$$

where $\underline{s}$ and $\underline{l}$ are the electronic spin and orbital angular momenta and $\underline{r}$ is the radius vector from the nucleus to an electron.

(i) The Knight shift This is the shift in resonance position in a metal with reference to a non-conducting compound. The most important contribution to this shift is contained in the second term of eqn. 1.4 which represents the hyperfine contact interaction with a conduction electron. The external magnetic field polarises the conduction electrons through their paramagnetic susceptibility. The effect of this polarisation is to produce a small extra field $\Delta \underline{B}_0$ at the nucleus and the effective field experienced by the nucleus becomes $\underline{B}_0 + \Delta \underline{B}_0$. The Zeeman interaction energy $-\underline{\mu}.\underline{B}_0$ must now be expressed as $-\underline{\mu}.(\underline{B}_0 + \Delta \underline{B}_0)$ and, for a given frequency, the resonance absorption occurs at a lower applied field than is the case in an insulator. The incremental field is proportional to the applied field and the fractional shift is generally written

$$K \equiv \frac{\Delta B_0}{B_0} = \frac{8\pi\Omega\chi_p}{3} \langle|\Psi(0)|^2\rangle_F \qquad 1.5$$

where the parameters are as defined in section 1.02.5

A further contribution, K_{cp}, to the shift can occur from the contact interaction with core electrons, polarised by interaction with conduction electrons. The spin-up and spin-down core electrons feel a different exchange force and this alters their spatial wavefunctions in different ways. The resulting imbalance of core spin density at the nucleus can give either positive or negative contributions to the shift. For example, Das et al.[42] found that the s-character of the conduction electrons in Al induced a positive contribution from both 1s and 2s core states, the p-character induced a negative contribution from 1s and a positive contribution from 2s, and the d-character a positive contribution from 1s and a negative

from 2s. The calculated total effect was $K_{cp} \sim -K_s/12$ a value that might be expected to increase for heavy metals.

The third term in eqn. 1.4 is the spin-dipolar term. For cubic metals, symmetry ensures that the effect of this term is zero. For non-cubic crystals this contribution, which arises from the non s-character of the conduction electrons, produces an orientation-dependent shift. In view of the fact that liquids are isotropic, this contribution averages to zero for liquid metals; it will not be considered further.

The last term in eqn. 1.4 is the orbital hyperfine term and results in a contribution K_o to the measured shift. Dickson[43] has used a simple expression (see Chapter 6) for this term and has deduced that in Sn and Cd the effect is not negligible. Because it is not usually possible to separate the core polarisation and orbital contributions the nomenclature of Dickson will be adopted:

$$K_{expt.} = K_s + K_{cp} + K_o = K_s + K_{other}.$$

(ii) The relaxation rate and the Korringa product In liquid metals spin-lattice relaxation is usually dominated by the contact hyperfine interaction. The energy exchange can be considered as a scattering process, the incident electron being scattered by the hyperfine potential into some final state with a change in energy of both the nucleus and the electron. Slichter[39] shows that the relaxation rate arising from the second term in eqn. 1.4 is given by

$$\frac{1}{T_1} = \frac{64}{9}\pi^3\hbar^3\gamma_e^2\gamma_n^2\left[\langle|\psi(0)|^2\rangle_F \rho(E_F)\right]^2 kT \qquad 1.6$$

where k is Boltzmann's constant.

The relation between the Knight shift due to the contact interaction and T_1 was first given by Korringa[44] as

$$T_1 T(K_s)^2 = \left[\frac{\chi_p}{\rho(E_F)}\right]^2 \frac{1}{\pi k} \frac{1}{\gamma_e^2 \gamma_n^2 \hbar^3} \qquad 1.7$$

a result that can be simplified for a non-interacting gas of electrons to

$$T_1 T(K_s)^2 = \frac{\hbar}{4\pi k} \left\{\frac{\gamma_e}{\gamma_n}\right\}^2 \qquad 1.8$$

It should be emphasised that T_1 and K_s refer only to those parts of the observed values that are due to the contact interaction; as this is generally the dominant contribution to both quantities eqn. 1.8 is expected to give a reasonable fit to the experimental data. However it was found that the measured Knight shift predicted values of T_1 that were consistently shorter than those observed; the measured Korringa product was enhanced. It was realised that this discrepancy was due to the effect of electron-electron interactions on both χ_p and ρ. Hence Pines[45] and Silverstein[46] obtained an expression

$$T_1 T(K_s)^2 = \frac{\hbar}{4\pi k} \left\{\frac{\gamma_e}{\gamma_n}\right\}^2 \left[\frac{\chi_p}{\chi_p^0} \frac{\rho^0(E_F)}{\rho(E_F)}\right]^2 \qquad 1.9$$

where the superscript '0' refers to the non-interacting case. The Knight shift depends on the static susceptibility $\chi_p(0,0)$ and is affected by electron-electron interactions giving $K = K^0 (1 - \alpha)^{-1}$ where α is a measure of the screened inter-electronic potential.

In addition to this modification Moriya[47] realised that T_1 responds not to $\chi_p(0,0)$ but to the dynamic susceptibility

$\chi_p(\underline{q},\omega)$ evaluated at the nuclear resonance frequency and appropriately averaged over all q's connecting states on the Fermi surface. Equation 1.9 can then be expressed

$$T_1 T(K_s)^2 = \frac{\hbar}{4\pi k}\left\{\frac{\gamma_e}{\gamma_n}\right\}^2 x \frac{1}{\mathcal{K}(\alpha)} \qquad 1.10$$

where $\mathcal{K}(\alpha)$ is always < 1. A typical value of $\mathcal{K}(\alpha)$ (see Chapter 6) has been found to be 0.75 for liquid metals. For a complete discussion of electron-electron interactions in n.m.r. the reader is referred to Narath[48]. The effect of K_{other} on the Korringa product is discussed in Chapter 6.

1.04.3 N.M.R. in liquid metals and alloys Because K is determined by the conduction electron-nuclear interaction n.m.r. is a useful tool for the investigation of the electronic structure of liquid metals. Hitherto, most of the experimental work has concerned the Knight shift change on melting and, indeed, an understanding of the relative constancy of K with temperature has been the most important single contribution that n.m.r. has made to liquid metal physics. Nevertheless, small changes in K with temperature are detectable. At the time when this work was begun a theoretical expression (Watabe and Tanaka[49], Faber, private communication) for the temperature dependence of the Knight shift had appeared. This was expressed in terms of the Fourier transform of the pseudopotential U(K) and the structure factor a(K), the main change with temperature being the dependence of the structure factor. However, this theory had not been seriously tested by comparison with experiment; a rough comparison for sodium was all that had been attempted. In view of this, one metal, pure lead, has been fully investigated

experimentally as a function of temperature (the results are discussed in Chapter 4) and a comparison with the theory made, both for lead and for a series of other liquid metals for which results are available in the literature.

It was also apparent from the literature that, if attention was paid to precise values, K was sensitive to the local order of systems more complex than pure metals; for instance, Knight shift changes had been used to observe phase changes in the solid[50], liquidus-solidus effects[51] and, in one case, non-random atomic associations in the liquid[52]. An investigation of the Pb - Bi system is reported in Chapter 6 with a view to finding how useful the Knight shift is as a probe for structural effects in the liquid state. It was hoped that such investigations might cast light on the state of local order and lead to a better understanding of liquid structure.

A number of investigations of changes of solvent shifts had been reported. It had been shown that a simple change in the density of states, deduced from a free-electron model, with no change in P_F, could not explain the observed Knight shift changes in alloys. However, the nearly-free-electron theory of Friedel et al.[53] which considers that P_F changes associated with screening clouds round solute ions are the most important effect, had been reasonably successful for liquid alloys based on monovalent solvents. When the same theory was applied to polyvalent-base liquid alloys[54] no agreement with experiment was obtained. However Flynn[55] proposed an alternative, semi-empirical method of characterising the screening charge and obtained qualitative, but not quantitative, agreement with almost all the experimental results then available. These

predictions were only seriously in error for the solvent lead where theory was of opposite sign to and an order of magnitude bigger than the experimental values of Snodgrass and Bennett[56] on lead solid solutions. An investigation of the ^{207}Pb Knight shift in a series of Pb-base liquid alloys is discussed in Chapter 5 of this thesis. These were undertaken to find whether the discrepancy might be associated with the band structure in the solid, which would be expected to disappear on melting.

The situation had arisen where the temperature dependence of K had been discussed in terms of a pseudopotential whereas the concentration dependence in alloys had been described in terms of the apparently different formulation of Friedel and later workers. This is clearly unsatisfactory. In fact a few authors had attempted to use the pseudopotential method to account for concentration dependences in liquid alloys. For dilute alloys of sodium the attempt was reasonably successful[57]. On the other hand, Moulson[58] had less success for alloys of polyvalent metals - for instance, the predicted dependence of the Knight shift of ^{115}In in In - Sn and In - Pb is very similar but the experimental results have opposite signs - even though the method is potentially able to take account of differing core structures of solutes of the same valence (like Sn and Pb). It is clear that a further attempt to test the applicability of this theoretical approach is warranted; such an attempt is made for the new results on Pb-base liquid alloys.

References

(1) Cusack N. E., Rep. Progr. Phys., 36, (1963), 361.

(2) Mott N. F., Liquids:Structure, Properties and solid interactions, (ed. Hughel 1965), Elsevier, 152.

(3) Wilson J. R., Met. Rev., 10, (1965), 381.

(4) The Properties of Liquid Metals, Proc. Int. Conf. at Brookhaven, Adv. in Phys., 16, (1967), ed. Adams, Davies and Epstein, Taylor and Francis Ltd., London.

(5) Cusack N. E. and Kendall P. W., Phil. Mag., 6, (1961), 419.

(6) Cusack N. E. and Kendall P. W., Phil. Mag., 8, (1963), 157.

(7) Busch G. and Guntherodt H.-J., Adv. in Phys., 16, (1967), 651.

(8) Enderby J. E., Hasan S. B. and Simmons C. J., Adv. in Phys., 16, (1967), 667.

(9) Rice S. A., Liquids:Structure, properties and solid interactions, (ed. Hughel 1965), Elsevier, 167.

(10) Schultz L. G., Adv. in Phys., 6, (1957), 102.

(11) Ziman J. M., Phil. Mag., 6, (1961), 1013.
Bradley C. C., Faber T. E., Wilson E. G., and Ziman J. M., Phil. Mag., 7, (1962), 865.
Faber T. E. and Ziman J. M., Phil. Mag., 11, (1965).

(12) Enderby J. E., Titman J. M. and Wignall G. D., Phil. Mag., 10, (1964), 633.

(13) Skinner H. W. B., Phil. Trans., 239, (1940), 95.

(14) Townes C. H., Herring C. and Knight W. D., Phys. Rev., 77, (1950), 852.

(15) Ziman J. M., Adv. in Phys., 16, (1967), 421.

(16) Ashcroft N. W. and Wilkins J. W., Phys. Letts., 14, (1965), 285.

(17) Anderson J. R. and Gold A. V., Phys. Rev., 139A, (1965), 1459.

(18) Kasowski R. V. and Falicov L. M., Phys. Rev. Letts., 22, (1969), 1001.

(19) Kusmiss J. H. and Stewart A. T., Adv. in Phys., 16, (1967), 471.

(20) Catterall J. A. and Trotter J., Phil. Mag., 8, (1963), 897.

(21) Edwards S. F., Adv. in Phys., 16, (1967), 359.

(22) Furukawa K., Rep. Prog. Phys., 25, (1962), 395.

(23) Knight W. D., Berger A. G. and Heine V., Annals of Phys., 8, (1959), 173.

(24) Bernal J. D., Nature, 188, (1960), 910.

(25) Ashcroft N. W. and Lekner J., Phys. Rev., 145, (1966), 83.

Ashcroft N. W. and Langreth D. C., Phys. Rev., 156, (1967), 685. Ibid., 159, (1967), 500.

(26) Enderby J. E., North D. M. and Egelstaff P. A., Phil. Mag., 14, (1966), 961.

(27) Dutchak Ya. I., Mykolaychuk A. G. and Klym N. M., Phys. Metals Metall., 14, (1962), 132.

(28) Sharrah P. C., Petz J. I. and Kruh R. F., J. Chem. Phys., 32, (1960), 241.

(29) Edwards S. F., Phil. Mag., 3, (1958), 1020; Ibid., 6, (1961), 617; Proc. R. Soc. A,267, (1962), 518; Proc. Phys. Soc., 85, (1965), 1.

(30) Gerstenkorn H., Ann. Phys., Leipzig, 10, (1952), 49.

(31) Cohen M. H. and Heine V., Adv. in Phys., 7, (1961), 395.

(32) Heine V. and Abarenkov I. V. Phil. Mag., 9, (1964), 451; Ibid., 12, (1965), 529.

(33) Sundström L. J., Phil. Mag., 11, (1965), 657.

(34) Animalu A. O. E., Phil. Mag., 11, (1965), 379; Ibid., 13, (1966), 53.

(35) Animalu A. O. E. and Heine V., Phil. Mag., 12, (1965), 1249.

(36) Purcell E. M., Torrey H. C. and Pound R. V., Phys. Rev., 69, (1946), 37.

(37) Bloch F., Hansen W. W. and Packard M. E., Phys. Rev., 69, (1946), 127.

(38) Andrew E. R., Nuclear Magnetic Resonance, (C.U.P.1958).

(39) Slichter C. P., Principles of Magnetic Resonance, (Harper and Row, N.Y., 1963).

(40) Abragam A., The Principles of Nuclear Magnetism, (Oxford, 1961).

(41) Rowland T. J., N.M.R. in metals, Prog. in Materials Science, 9, (1961), Pergaman.

(42) Shyu W. M., Das T. P. and Gaspari G. D., Phys. Rev., 152, (1966), 270.

(43) Dickson E. M., Ph.D. Thesis, Berkeley, (1969).

(44) Korringa J., Physica, 16, (1950), 601.

(45) Pines D., Solid State Physics, 1, (N.Y. Acad. Press, 1955), 367.

(46) Silverstein S. D., Phys. Rev., 128, (1962), 631; Ibid; 130, (1963), 912.

(47) Moriya T., J. Phys. Soc. Japan, 18, (1963), 516.

(48) Narath A., Hyperfine Interactions, (Acad. Press, 1967), 287.

(49) Watabe M. and Tanaka W., Phil. Mag., 12, (1965), 347.

(50) Drain L. E., Phil. Mag., 4, (1959), 484.

(51) Takahashi T. and Tiller W. A., Acta Met., 17, (1966), 657.

(52) Styles G. A., Adv. in Phys., 16, (1967), 275.

(53) Blandin A., Daniel E. and Friedel J., Phil. Mag., 4, (1959), 180.

Blandin A. and Daniel E., J. Phys. Chem. Sol., 10, (1959), 126.

Daniel E., J. Phys. Rad., 20, (1959), 769 and 849.

(54) Styles G. A., Ph.D. Thesis, Leeds, (1964).

(55) Odle R. L. and Flynn C. P., Phil. Mag., 13, (1966), 699.

(56) Snodgrass R. J. and Bennett L. H., Phys. Rev., 134, (1964), 1294.

(57) Kellington S. H. and Titman J. M., Phil. Mag., 15, (1967), 1045.

(58) Moulson D. J., Ph.D. Thesis, Leeds, (1966).

CHAPTER TWO

EXPERIMENTAL DETAILS

2.01 Basic Experimental Arrangement

The gyromagnetic ratio of nuclei is such that at typical laboratory magnetic fields ($\sim$1 tesla) the frequency for resonant absorption is approximately 10 MHz. The basic system is, therefore, a radio-frequency transmitter and receiver, coupled through a device that detects the nuclear signal, as the polarising magnetic field is varied through the resonance value $\omega = \gamma_n B_0$.

A block diagram of the apparatus used is shown in fig. 2.1. This is a commercially available wide-line n.m.r. spectrometer and magnet made by Varian Associates Inc.. The V.F.16 wide-line spectrometer is suitable for measuring lines wider than 5×10^{-6} tesla; in fact, when used with the Varian V-3600 series 12" electromagnet, field stability over long terms is such that lines less than 5×10^{-5} tesla wide can not be measured accurately.

The heart of the spectrometer is the radio-frequency probe; three are available covering the frequency ranges 2 $\rightarrow$ 4 MHz, 4 $\rightarrow$ 8 MHz and 8 $\rightarrow$ 16 MHz. These probes use the nuclear induction method of detecting the resonant condition. (For details of this system, references to original papers, and details of other detecting systems see Andrew[1].) To briefly describe the nuclear induction (crossed-coil) system it is convenient to consider the

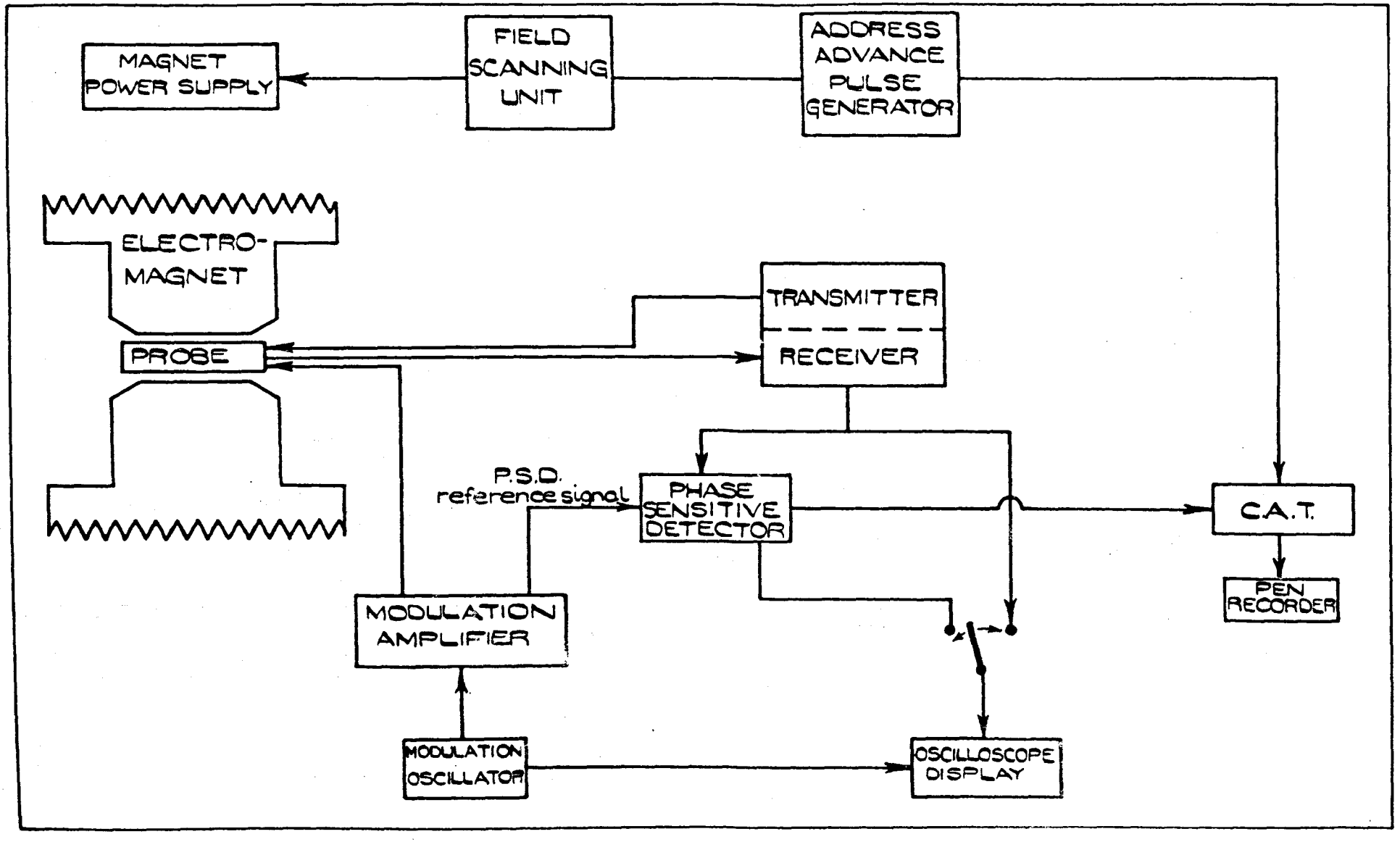

Figure 2.1. BLOCK DIAGRAM OF THE N.M.R. SPECTROMETER.

vector model of a precessing magnetic moment. If B_0, the resonant field, is along the z-axis and the r.f. field B_1 parallel to the x-axis in the usual rotating frame co-ordinate system, there will, in general, be both an x-component and a y-component of the magnetic moment. It is possible to adjust the leakage flux, between two nearly orthogonal coils, to be either in phase with the much smaller flux, due to M_x (dispersion mode of operation), or due to M_y (absorption mode). Each probe, then, contains a transmitter coil, a receiver coil and two sets of paddles for adjusting the leakage between the transmitter and receiver coils. These coils are built to be as nearly orthogonal as is mechanically possible and the paddles are used for final fine adjustment of the amplitude and phase of the leakage flux. Because it is at this stage that the ultimate signal-to-noise ratio is determined great care is taken in the construction. The probes are milled from a solid block of Duralumin to avoid unwanted microphonics. To avoid capacitive coupling between the transmitter and receiver, a Faraday shield is inserted, and the whole probe is carefully sealed to exclude any impurities. In making measurements the leakage level is reduced to a minimum and a small amount of imbalance is then introduced by means of one paddle.

The first stage of the amplification of the resonance signal is a tuned r.f. amplifier. This is followed by a broad band r.f. amplifier and the signal is then detected. It is common to modulate the 'steady' polarising magnetic field at an audio-frequency with a small amplitude ($\sim 10^{-3}$ tesla). The radio frequency carrier is then amplitude modulated when the 'steady' field is near to the resonant value B_0. After detection

the audio signal passes to a phase sensitive detector. This is simply a synchronous switch, and allows only signals, whose frequency and phase is close to that of a reference signal, to pass. It is important, in order to get maximum output from this switch, to adjust the switching to occur at zeros of the signal voltage. This correct phase can be adjusted, using resonance signals that are visible on the oscilloscope. The output waveform from the switch is similar to that from a full-wave rectifier, and can either be passed direct to the y-axis of an oscilloscope (x-axis driven by the modulation oscillator) or through an R-C network to a graphic recorder.

Because of the short spin-lattice relaxation times in liquid metals and alloys, saturation was not a serious problem and high transmitter levels could be used. Typically a level of 800 μA was used with the lead samples, which at 12 MHz is equivalent to a value of 0.2×10^{-4} tesla for B_1. This meant that a considerable gain in the signal-to-noise ratio was obtained, provided the probe balance could be stably maintained. For each nuclear species, a preliminary experiment was performed to determine the optimum r.f. level.

When using the 8 → 16 MHz probe the maximum modulation amplitude obtainable was 32×10^{-4} tesla peak-to-peak. Normally a very small modulation amplitude compared to the linewidth is used and an undistorted first derivative of the resonance lineshape is recorded. However, the signal-to-noise ratio can be improved by increasing the modulation amplitude. The amplitude can be optimized but in this case the recorded linewidth must be corrected for modulation broadening. These optimum conditions

have been discussed in the literature[2, 3 & 4], including ways of correcting the broadening obtained. Typically, for a Lorentzian lineshape, the optimum peak-to-peak modulation amplitude is equal to the width of the line. The correction to a recorded width of 5×10^{-4} tesla, when using a modulation amplitude (p - p) of 3.6×10^{-4} tesla, amounts to about 15%. The magnetic field must be swept through the linewidth in a time long compared to the time constant of the apparatus, or further distortion will occur. In practice, for a sweep of 25×10^{-4} tesla, in a time of 30 seconds and a width of 5×10^{-4} tesla, a time constant of 0.5 seconds will avoid this distortion. In fact, the magnetic field stability limits the maximum sweep time that can be used in practice, and, consequently, the minimum signal strength observable. The signal-to-noise ratio can also be affected, to a small extent, by the modulation frequency. At low frequencies, 'flicker' noise is increased; at high frequencies 'adiabatic fast passage' produces a distortion of the lineshape. For metal samples the optimum frequency, of those available, was found to be 80 Hz, and this value was used throughout the measurements.

2.02 Auxiliary Apparatus

2.02.1 The Magnet The maximum field available with the V-3600 12" electromagnet, with plane pole faces coned to 9" and a gap of $1\frac{3}{4}$" was 1.5 tesla. With this arrangement the homogeneity and stability claimed by the manufacturers is fully realised; homogeneity of 1 part in 10^5 over the specimen volume, and stability of 1 part in 10^5 over one hour were obtained once ambient conditions had been reached.

The field is continuously variable from 0 → 1.5 tesla. It can be swept over several ranges, 0.5, 1.0, 2.5, 5, 10 ..... x 10^{-4} tesla, in times varying from 0.5 minutes, by similar steps, to 100 minutes. The signal-to-noise ratio can be improved by increasing the response time of the apparatus with a corresponding increase in the sweep time. The maximum sweep time available on the instrument is 100 minutes and is thus a fundamental limitation to sensitivity. A further limitation on sweep time is the stability of the field, frequency and probe balance.

2.02.2 Computer of Average Transients The restrictions of sensitivity mentioned above can be removed by the use of a computer of average transients (CAT). In effect, the CAT is a device for the summation of successive sweeps, and so, instead of a single sweep lasting for 30 minutes, say, with a response time of 30 seconds, 60 sweeps are made, with a sweep time of 30 seconds and a response time of 0.3 seconds. The coherent signal adds directly as the number of sweeps, and the random noise, as the square root of the number of sweeps. The signal is literally 'pulled out' of the background noise. The method has the two advantages of theoretically infinite sweep time, and the facility for stopping the 'count', resetting all the important parameters and thus eliminating drift errors.

The CAT used was a Northern NS-544 Digital Memory Oscilloscope. This has 1,024 channels that can be opened by an address advance pulse generator, in sequence, so that each channel stores information relating to a small section of the sweep. The pulse generator was run from the x-axis drive of

the field sweep unit. The CAT has both visual and graphic output facilities, and a Bryans 21000 series recorder unit was used in conjunction with it.

2.02.3 Frequency and Field Calibration The two parameters essential to magnetic resonance are the r.f. frequency and the magnetic field. The frequency can be determined directly from the transmitter by means of a counter. A Venner TSA 3436 counter was used and with this, together with a divider unit, it is possible to measure frequencies of 10 MHz to 1 part in 10^7. To avoid interference from the counter crystal it is important that the counter is not operated whilst a sweep is in progress.

To determine the magnetic field as precisely is more difficult. In fact, the n.m.r. signal from a heavy water sample is used, because the deuteron magnetic moment is precisely known, the Larmor precession frequency of ^2H nuclei is convenient for fields of $\sim$1 tesla, and the resonance is very narrow. Two arrangements were used. In one mode of working, the deuterium sample was directly substituted for the metal sample. However, at high temperatures this was very inconvenient, and the deuterium sample was placed in a subsidiary probe. This was positioned immediately adjacent to the Varian probe in the magnet gap and fitted with its own modulation coils. The resonance was observed using a Watkins-Pound marginal oscillator[1] built by Styles[5]. The deuterium sample could be racked into the position normally occupied by the metal sample by means of a screw mechanism, and, in this way, the systematic error due to field inhomogeneity could be avoided. (In fact this movement was not essential for many of the measurements to be described.)

2.02.4 The Furnace The Varian probe body temperature must not be allowed to exceed 338 K (65°C). This means, that for working at high temperatures, either an alternative system must be used, that can operate inside a furnace, or a dewar system (similar to that described by Schreiber[6]) must be inserted into the probe. This latter suggestion necessarily reduces the filling factor, and, in practice, the reduction was found to be about a factor of 3. A serious attempt was made, therefore, to construct an alternative system that could operate with the Varian spectrometer without such a loss of filling factor. A radio-frequency twin-T bridge based on the design of Anderson[7] was constructed and extensively tested. Poor impedance matching of the transmitter output to the bridge input, and the bridge output to the receiver input meant that the full power of the spectrometer could not be used. The best signal-to-noise ratio obtained was a factor of 4 poorer than that obtained when using a dewar furnace inserted into the Varian probe.

The particular furnace used had been designed by G. A. Styles and I would like to acknowledge his kindness in allowing the use of it. During the experimental work, the centring mechanism, the sample tube design and the top cap were modified and the arrangement is shown in fig. 2.2. An L-shaped dewar, the shape being chosen to allow for differential expansion between the inner and outer vessels, was centred in the probe by means of two brass flanges. The lower one also served to suck air past the outside of the dewar; the upper one allowed hot air to be sucked past the specimen and also enabled evacuation of the sample tube, and the introduction of an inert atmosphere. The dewar is silvered in the conventional way, except where it fitted

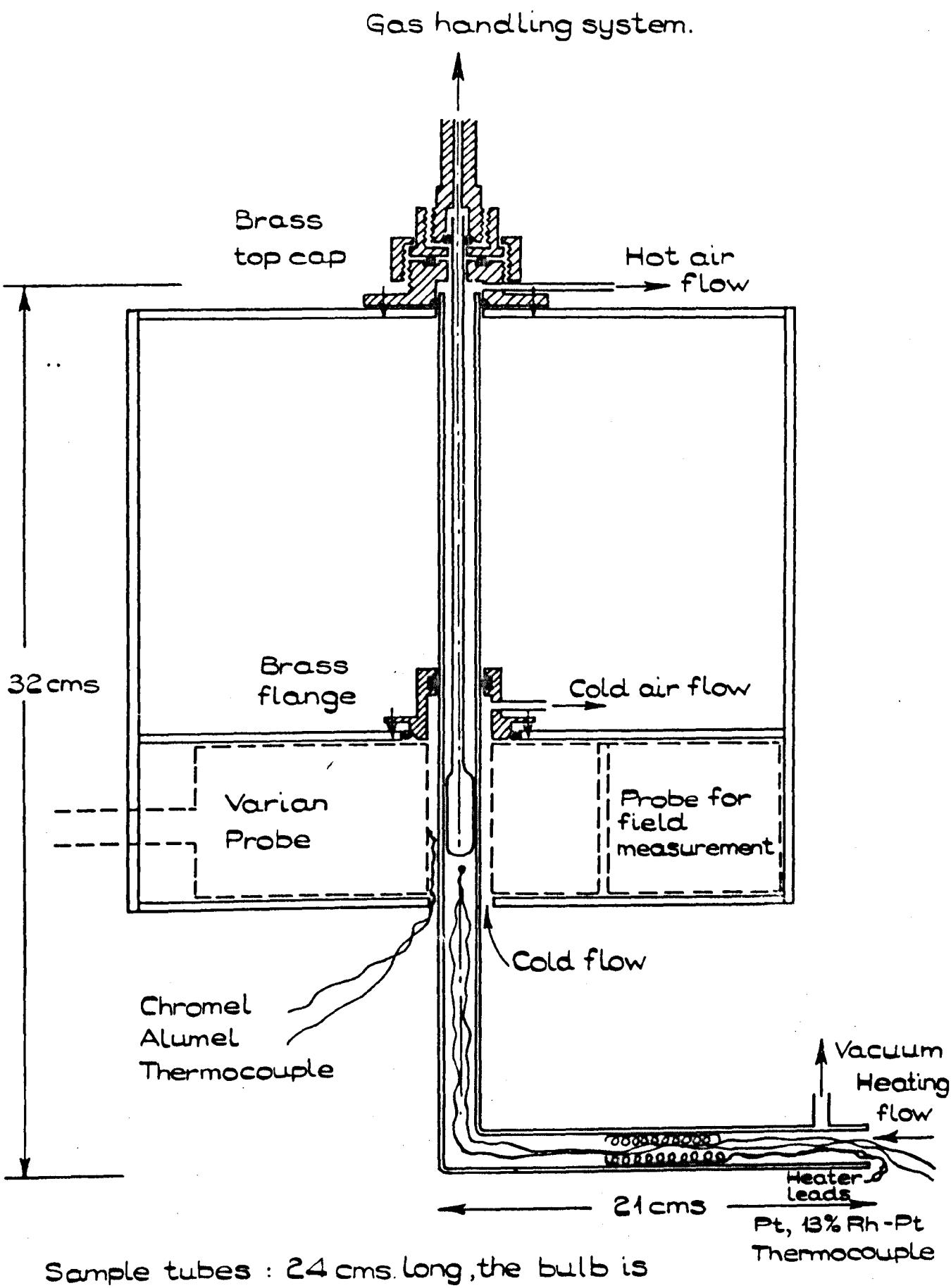

Figure 2.2. THE FURNACE SYSTEM USED FOR MEASUREMENTS OF LIQUID METALS.

inside the probe, this region being hatched in ~ 3mm squares to reduce eddy current effects. The dewar interspace was pumped continuously during operation. The heating coil was simply pushed into the inner vessel, and comprised nichrome wire covered with refrasil sleeving, and power was supplied by a Roband 50 V 10 A power supply. Air was drawn over this heater by a compressor, operated on the suck mode. With an air flow of 5 l min^{-1}, a temperature of 800 K could be reached, before the probe body attained its maximum allowed temperature. Because the metals and alloys investigated were of low melting point this maximum temperature was quite adequate.

The sample temperature was monitored by a Pt, 13% Rh-Pt thermocouple fixed immediately below the specimen. A control experiment showed that the temperature gradient across the sample did not exceed 5 K at 800 K, which compares favourably with that quoted by Schreiber[6] for his design. The temperature of the probe was monitored by a chromel-alumel thermocouple, and both thermocouple outputs were displayed on a Sunvic pen recorder.

2.03 Sample Preparation

One difficulty in the investigation of n.m.r. in metallic samples is the radio-frequency skin effect, which prevents the penetration of r.f. radiation into a sample. If the sample is larger than the skin depth a poor filling factor results as only a fraction of the available spins contribute and, moreover, an admixture of dispersion and absorption signals is normally obtained, resulting in an apparent shift of the line centre. This distortion has been discussed by Chapman, Rhodes and Seymour[8] who show, for powders of spherical particles of

diameter less than the r.f. skin depth, that negligible distortion results. For a material with a permeability that is approximately unity, the skin depth is given by

$$\delta = 5.03 \times 10^{-3}(\rho/\nu)^{\frac{1}{2}}$$

where δ is in cm, ρ is the resistivity in μohm cm and ν the frequency in MHz. In the present investigation δ was never less than 60 μm.

All the alloys were made from 5 N pure materials obtained from Koch-Light laboratories. The constituents were carefully weighed, melted together under an argon atmosphere and quenched in a copper mould. This was done using a simple pyrex glass crucible, with a side arm, which allowed both evacuation and the introduction of argon into the system. The neck of the crucible fitted, with an 'o'-ring seal, into the heavy copper mould. The sample was heated under half an atmosphere of argon and then held molten for up to 10 minutes, shaking continuously to ensure good mixing. The ingot was cast by inverting the whole apparatus. Metallographic inspection of the alloy, by polishing and etching, showed that a certain amount of coring did occur. Powders were produced from these ingots in two ways:-

(a) Ultrasonic dispersion. The ingots were carefully cut into slices, taking a cross section of the ingot in each slice. It was thought that, although radial concentration gradients existed, longitudinal gradients were unlikely. By taking thin cross sections, the average concentration of the alloy was retained. Each slice was placed in a 6 cm by 1 cm specimen tube under silicone fluid MS550. The tube was carefully heated and the alloy melted. The tip of an ultrasonic stirrer

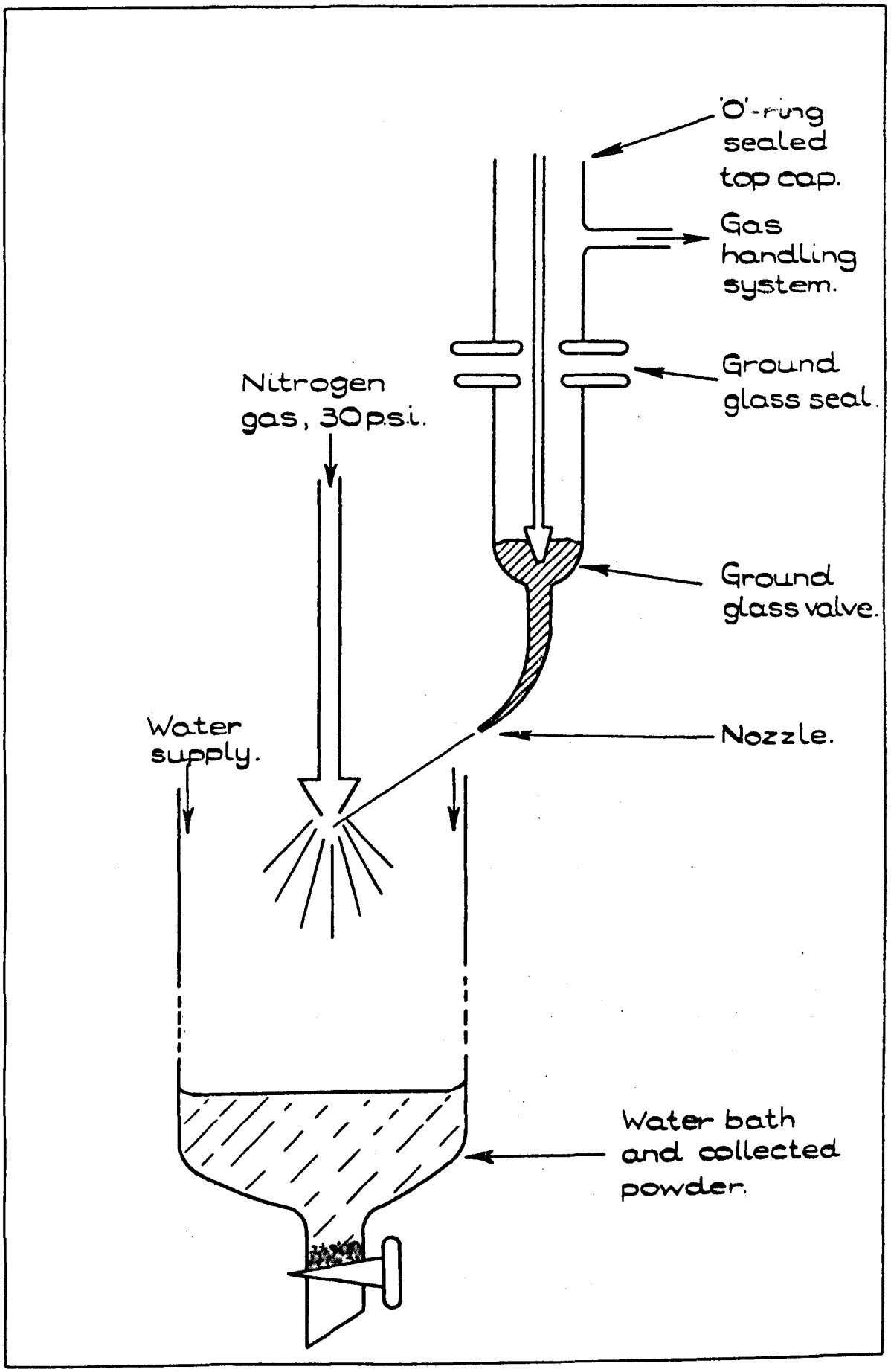

Figure 2.3. SCHEMATIC DIAGRAM OF AEROSOL TECHNIQUE.

(MEL 100 watt) was inserted into the oil. On tuning the drill the sample was violently agitated and, after a short time, was dispersed in the oil. This process was not easy to perform; the power must be concentrated onto the molten alloy (a round bottomed tube suffices) and it was found impossible to control the particle size. After washing with carbon tetrachloride and diethyl ether the powder was passed through a 50 μm sieve. Any not passing through was, if necessary, reprocessed. All the early lead alloys were prepared in this manner. The particles were spherical and about 5 μm diameter, comfortably less than the skin depth. To ensure electrical insulation at high temperatures, the powder was mixed with an equal volume of Polishing Alumina. In certain alloys a higher proportion of Alumina was required to ensure good liquid encapsulation, and thus good probe balancing.

(b) Aerosol technique. Again the ingot was cut, but all of it was placed into a glass crucible (see fig. 2.3). The crucible was evacuated, flushed with argon and the alloy melted. A small overpressure of argon was applied and, on opening the ground glass valve, the molten alloy was shot from a fine nozzle into a high pressure nitrogen gas stream. The jet of liquid alloy was immediately dispersed and condensed in the surrounding water bath. The resulting powder, after washing, was sieved. The particle size was a function of the nozzle diameter, nitrogen gas pressure and argon overpressure. For a nozzle diameter 0.2 mm, a nitrogen pressure of 30 p.s.i. and an argon overpressure of 6 cmHg, particles of approximately 40 μm diameter were produced. All the Pb-Bi alloys discussed in Chapter 6 were prepared in this way.

2.04 Measuring Technique

As a preliminary to any measurements the homogeneity and stability of the magnetic field were checked. A heavy water sample was used, and the width of the observed resonance taken as a measure of the homogeneity. Over the volume occupied by the sample the deuterium linewidth was 0.1×10^{-4} tesla, and this was taken as an upper limit of the line broadening, due to field inhomogeneity. The stability was checked by observing the deuterium resonance as a function of time. In all experimental measurements a period of two hours was allowed for the apparatus to reach a working equilibrium.

Because of the good homogeneity, the deuterium resonance was visible from the subsidiary probe, even when the metal sample was in the centre of the pole face. Since all measurements to be made were of relative changes in the resonance position, any fixed small difference between the measured field and the actual field is immaterial. There was, thus, no need to rack in the deuterium probe. When field dependence measurements were performed this no longer held, and the probes were placed successively in the centre of the poles.

The modulation amplitude, transmitter level, sweep range and sweep time were optimised, for any given nucleus, before detailed measurements were made. The modulation amplitude (p - p) was easily determined by noting the field shift required to move a deuterium resonance from edge to edge of the oscilloscope trace. The resonance was located, and the centre of the magnetic field sweep carefully set and determined, using the deuterium probe. The sweep was begun; at periods of

fifteen minutes it was stopped and the frequency, control field and probe balance carefully reset. When a satisfactory signal-to-noise ratio had been obtained on the CAT, the resonance was recorded. Using the deuterium probe, two subsidiary resonances were put onto the recorded trace and their frequencies carefully noted. From these the field axis of the trace was calibrated and the position and width of the line determined. The 'equal heights' construction of fig. 2.4 was used because the lines were in general Lorentzian in shape, and had long tails. To include the whole of these tails would have meant a large increase in sweep range, and a corresponding loss of intensity for a given number of sweeps.

All observations were repeated an equal number of times on the increase and decrease modes of the sweep. Mean values of position (and width where signal strength allowed) were determined for each mode. These means were significantly different (for the value of the position) due to a small delay caused by the output time constant. By taking a final average of the two means, the small systematic error involved was eliminated.

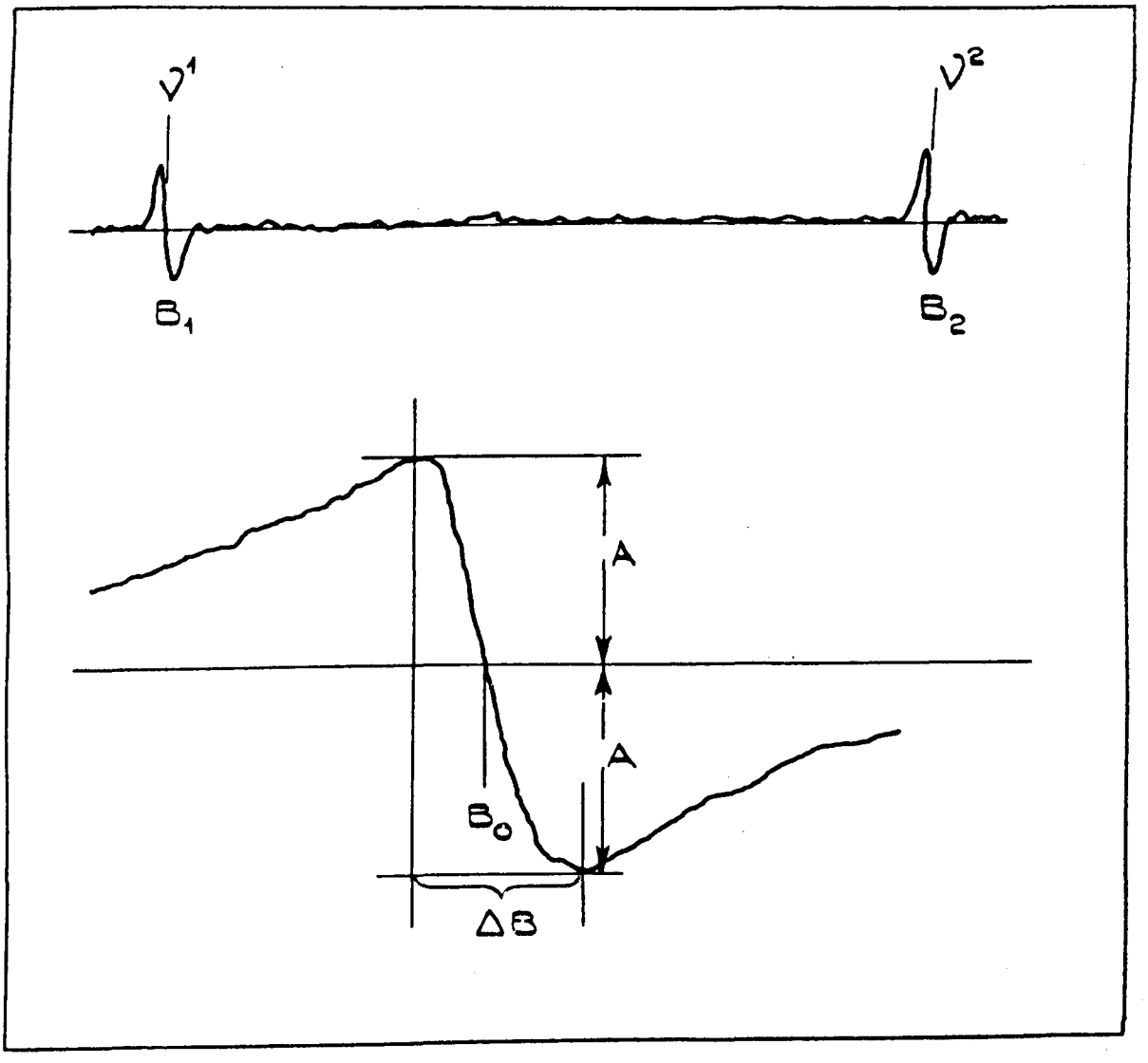

Figure 2.4. SCHEMATIC DIAGRAM OF THE MEASURING TECHNIQUE.

References

(1) Andrew E. R., Nuc. Mag. Resonance (C.U.P. 1958).

(2) Flynn C. P. and Seymour E. F. W., J. Sci. Instr., 39, (1962), 352.

(3) Smith G. W., J. Appl. Phys., 35, (1964), 1217.

(4) Buckmaster H. A. and Dering J. C., J. Appl. Phys., 39, (1968), 4486.

(5) Styles G. A., PhD. Thesis, Leeds, (1964).

(6) Schreiber D. S., Rev. Sci. Instr., 35, (1964), 1582.

(7) Anderson H. L., Phys. Rev., 76, (1949), 1460.

(8) Chapman A. C., Rhodes P. and Seymour E. F. W., Proc. Phys. Soc., B70, (1959), 345.

CHAPTER THREE

EXPERIMENTAL RESULTS

3.01 Introduction

To evaluate the Knight shift K, the ratio of the resonance field in the metal, and in one of its salts, may be measured for a constant radio-frequency.

$$K = \frac{\Delta B}{B} = \frac{B_r - B_m}{B_m} \qquad 3.1$$

where B_r is the field required for resonance in the reference compound, and B_m is the field required for resonance in the metal, at the same radio-frequency ν.

Thus K can be written

$$K = \frac{(B/\nu)_r - (B/\nu)_m}{(B/\nu)_m} \qquad 3.2$$

The measurement of K is complicated by the chemical shift; for instance in ^{207}Pb the experimental value of K varies from approximately 1.2% to 1.5% depending on the reference compound chosen[1]. The present investigation was concerned only with small relative changes in K, so that the choice of reference compound was not of great significance. In fact, K was calculated from eqn. 3.2 using a value of $(B/\nu)_r$ taken from published data[2]. Values of K in the alloys were calculated similarly, and compared with the value for pure lead, at the same temperature and magnetic field, to obtain the relative

change $\delta K/K$.

$$\frac{\delta K}{K} = \frac{K_a - K_m}{K_m} = \frac{\left[(B/\nu)_r - (B/\nu)_a\right](B/\nu)_m}{\left[(B/\nu)_r - (B/\nu)_m\right](B/\nu)_a} - 1 \qquad 3.3$$

where the subscript 'a' denotes the alloy. In an anologous way, the change of K with temperature for an alloy was found from

$$\frac{\delta K}{K} = \frac{K_{a,T} - K_{a,0}}{K_{m,0}} \simeq \frac{(B/\nu)_{a,T} - (B/\nu)_{a,0}}{(B/\nu)_{r,0} - (B/\nu)_{m,0}} \qquad 3.4$$

where the denominator $\gg$ numerator.

The linewidths given are the separations ΔB of the peaks of the absorption derivatives, and have been corrected for broadening, due to a finite modulation amplitude, by the method of Smith[3], which is ideally suited to the Lorentzian lineshape, observed in almost all cases. An exception is the case of pure solid lead; a discussion of the lineshape observed in this case is left until Chapter 4.

In all cases the result quoted for the Knight shift or linewidth is the mean of at least three readings with increasing field sweep, and three with decreasing field sweep and the uncertainty is the mean deviation from the mean. All temperatures are given in kelvins and all concentrations in atomic percent.

3.02 Pure Lead

^{207}Pb, the only naturally occurring lead isotope with a magnetic moment, is 21% abundant and has spin $\frac{1}{2}$. The measurements in pure lead were taken as a preliminary to measurements on the liquid lead alloy systems. The temperature dependence

of both the Knight shift and linewidth of ^{207}Pb was observed in the solid and liquid phases. The results are shown in fig. 3.1 and fig. 3.2. The results for K(T) in the solid were a repeat of work performed by Moulson[4] but no previous results for K(T) in the liquid phase, or for $\Delta B(T)$ in the solid or liquid phases, exist. The value of $(B/\nu)_r$ used in eqn. 3.2 corresponds to a value of K at 293 K of 1.192(±.003)%. The accuracy of the data for ΔB in the liquid state is very poor because of the poor signals obtained, and no conclusions will be drawn for them. As is usual for pure metals in small particle form (Turnbull[5]), it was possible to supercool the liquid, in this case through 40 K, as was evident from the results for the relative change of the Knight shift in fig. 3.1.

All measurements were made at 12 MHz and approximately 1.4 tesla. The variation of the Knight shift with temperature is small and linear in both the solid and liquid phases. In the solid between 300 K and 600 K the measured temperature coefficient $(1/K)(dK/dT)$ is $6.3(\pm0.4) \times 10^{-5}K^{-1}$ which compares well with the value $7 \times 10^{-5}K^{-1}$ obtained by Snodgrass and Bennett[6] from measurements at 77 K and 300 K only. In the liquid phase the measured temperature coefficient is $-7.6(\pm0.9) \times 10^{-5}K^{-1}$.

3.03 Liquid Alloys

3.03.1 Concentration dependence of the Knight shift

The measurements on a given alloy series were all made at the same field (1.4 tesla), modulation amplitude (3.6×10^{-4} tesla) and, where possible, the same temperature (625 K). The exception to the last condition was the Pb - 5% Ag alloy where a temperature

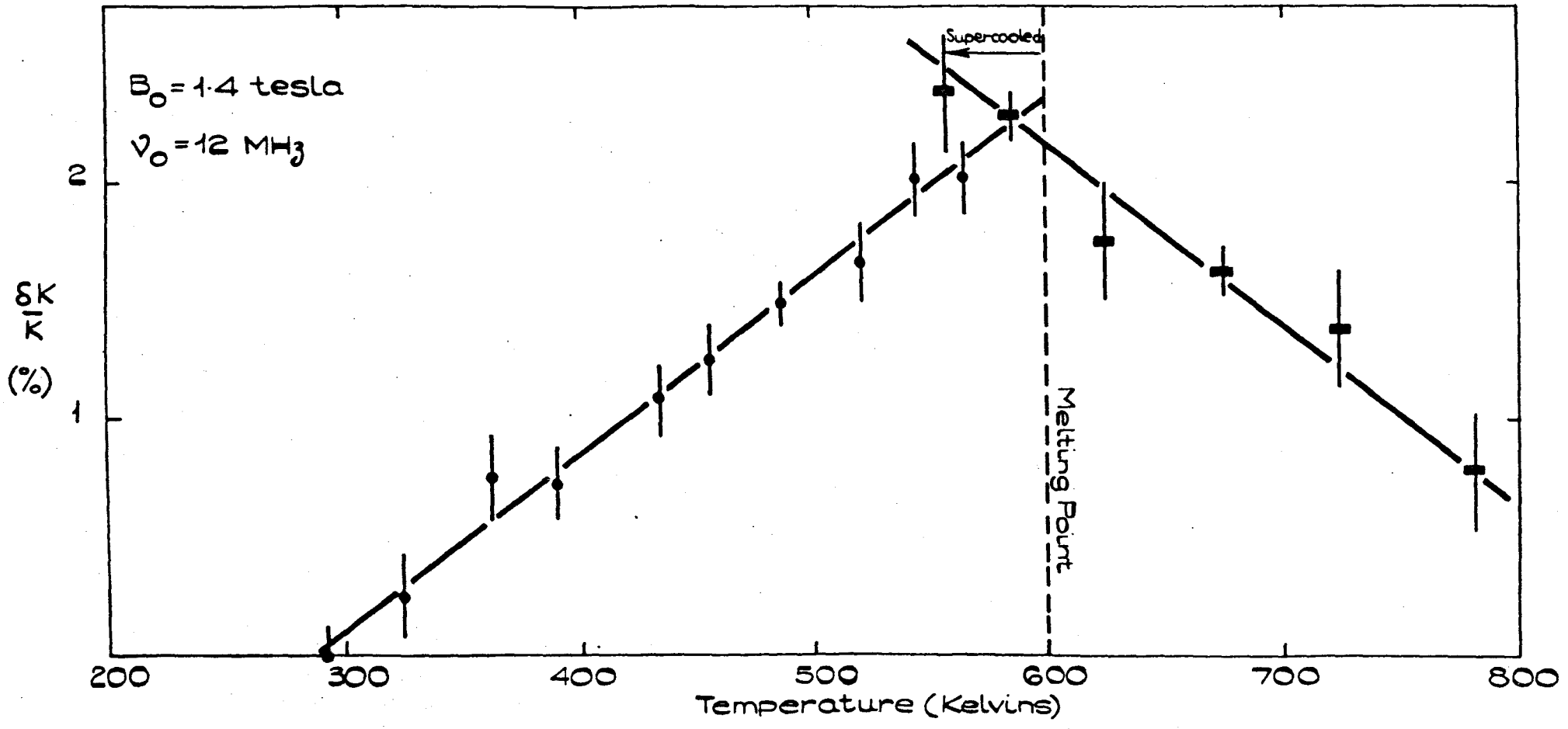

Figure 3.1. THE RELATIVE CHANGE OF THE KNIGHT SHIFT OF ^{207}Pb IN 100% Pb WITH TEMPERATURE.

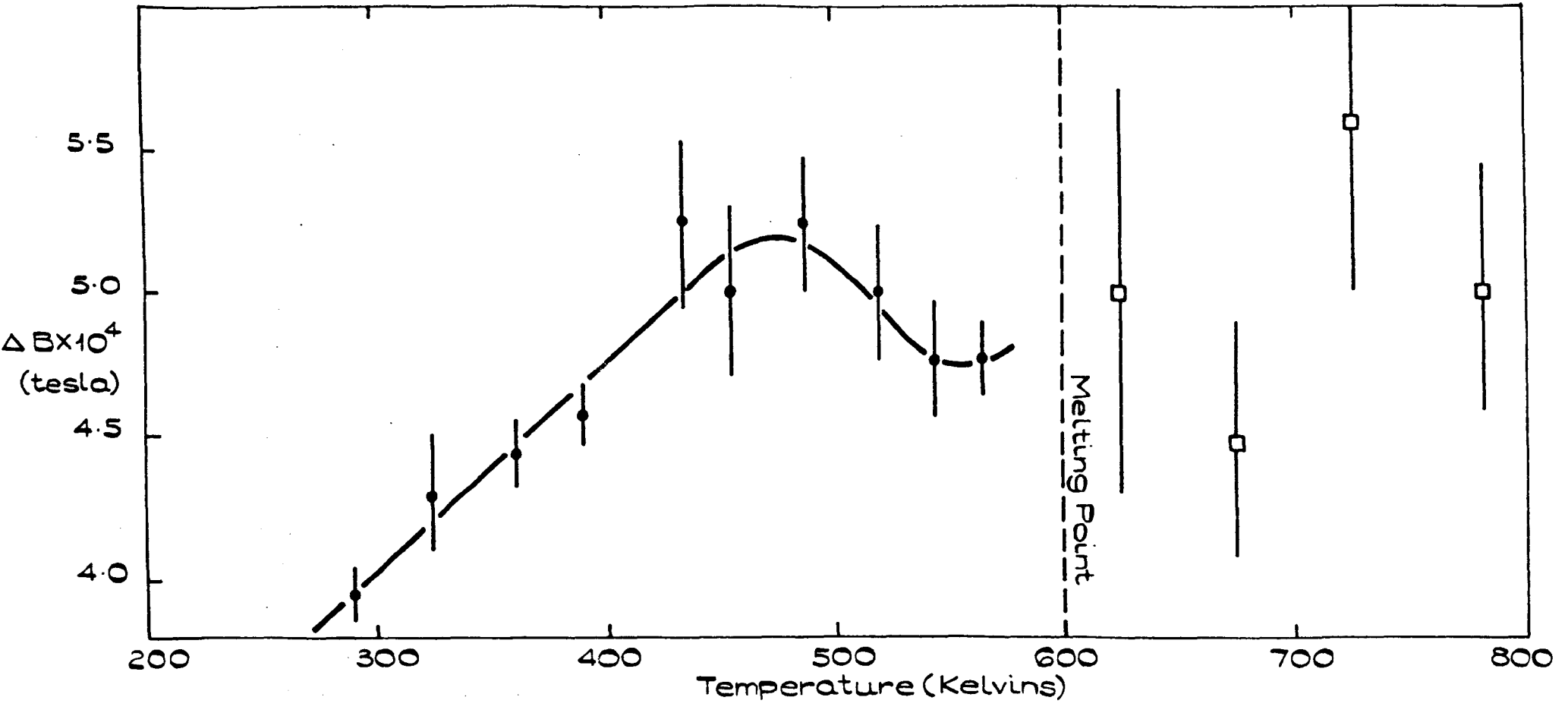

Figure 3.2. THE VARIATION OF THE ^{207}Pb LINE WIDTH IN 100% Pb WITH TEMPERATURE.

of ~673 K was needed to keep the alloy molten. Whenever possible (Cd, In, Sb, Bi) both solvent and solute resonances were recorded. This was not possible in many cases because of lack of signal strength, due to dilution. In the reported results the zero was taken as the value of the Knight shift of the pure metal at 625 K as recorded, all relative changes use this value as a reference; the case of antimony is exceptional because at 625 K it is still solid.

The data are summarised in fig. 3.3 - fig. 3.10 where the relative change of the Knight shift, with alloy concentration, is reported. The figures cover the eight alloy systems investigated; additionally all the ^{207}Pb data are collected in fig. 3.11 for comparison purposes. (The data for the Pb - Sn in fig. 3.11 are that of Moulson[7].) All Knight shift variations shown, are tabulated in Appendix I. Typically, the measurements shown involved 64 sweeps, lasting 30 seconds each sweep, with a response time of 0.3 seconds. The plotted uncertainties are mean deviations from the mean. For the samples Pb - 10% Cd, Pb - 28% Cd, Pb - 5% Hg and Pb - 10% Hg the compositions were checked by quantitative analysis for the minor constituent (Johnson and Matthey Ltd.). The comparison between nominal and actual atomic percent which provides an estimate of the x-axis uncertainty, is given in Table 3.1:

Table 3.1

Nominal	Analysis
10% Cd	9.2% Cd
28% Cd	26.4% Cd
5% Hg	8.3% Hg
10% Hg	13.0% Hg

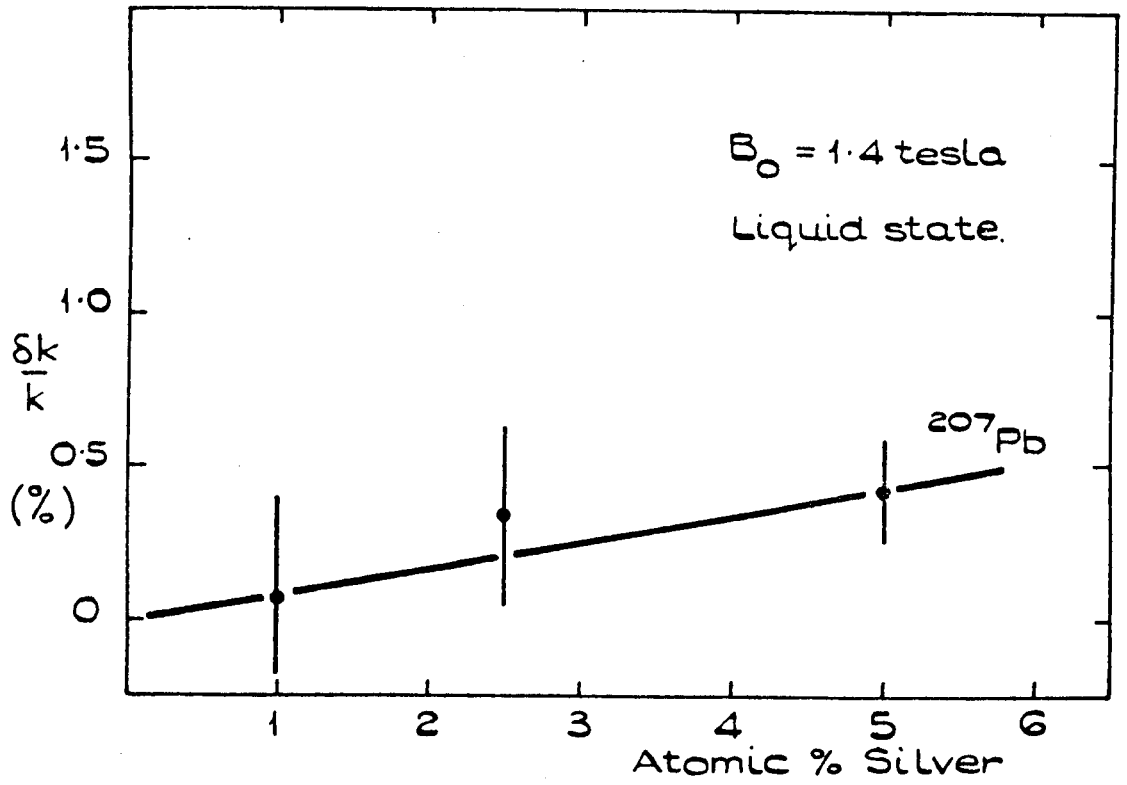

Figure 3.3. Pb-Ag ALLOYS

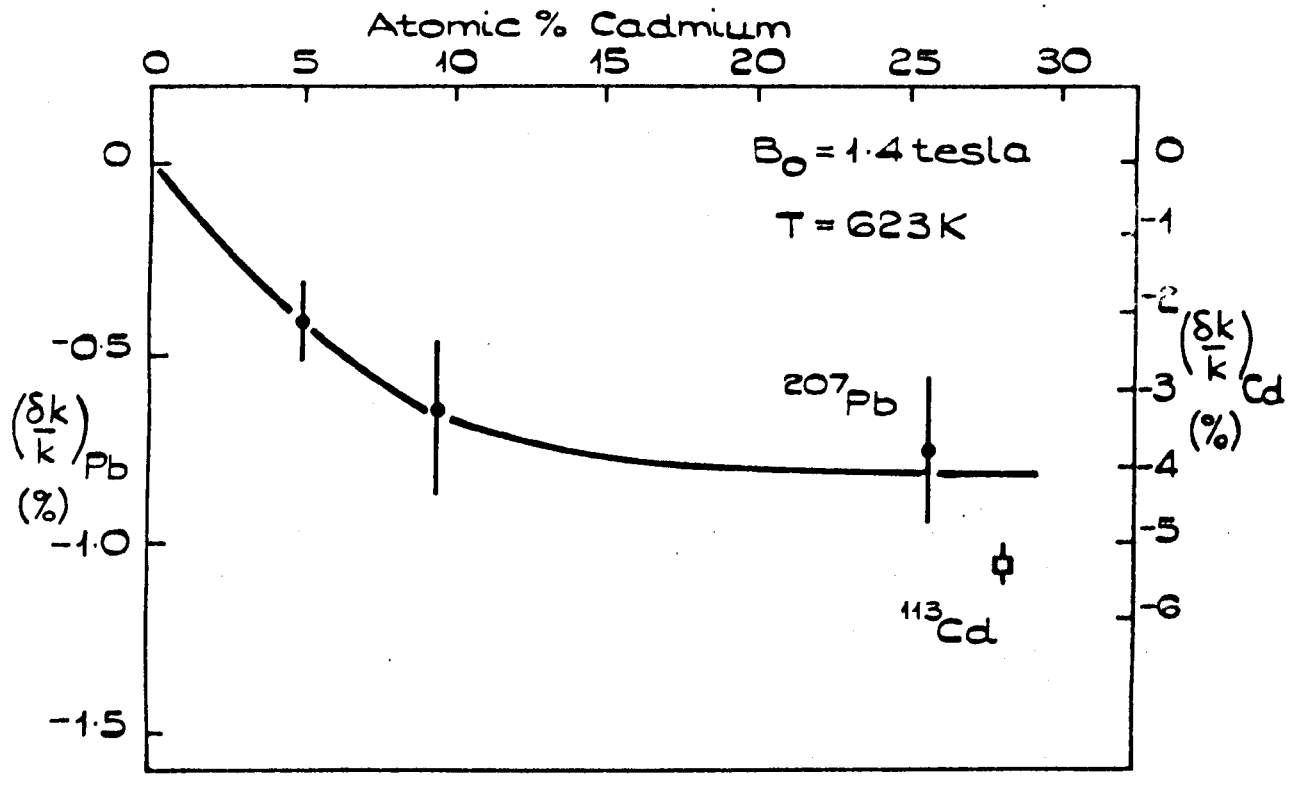

Figure 3.4. Pb-Cd ALLOYS

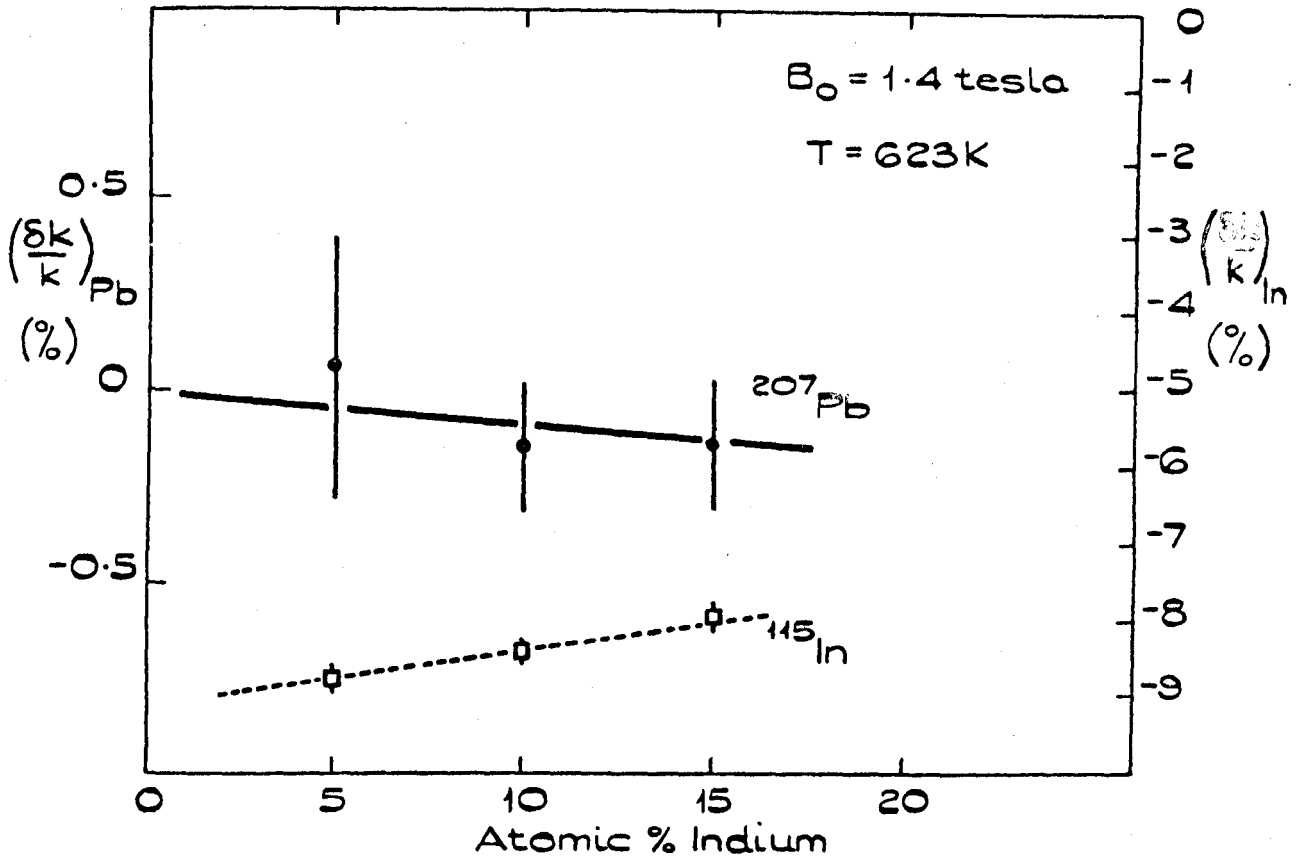

Figure 3.5. Pb - In ALLOYS

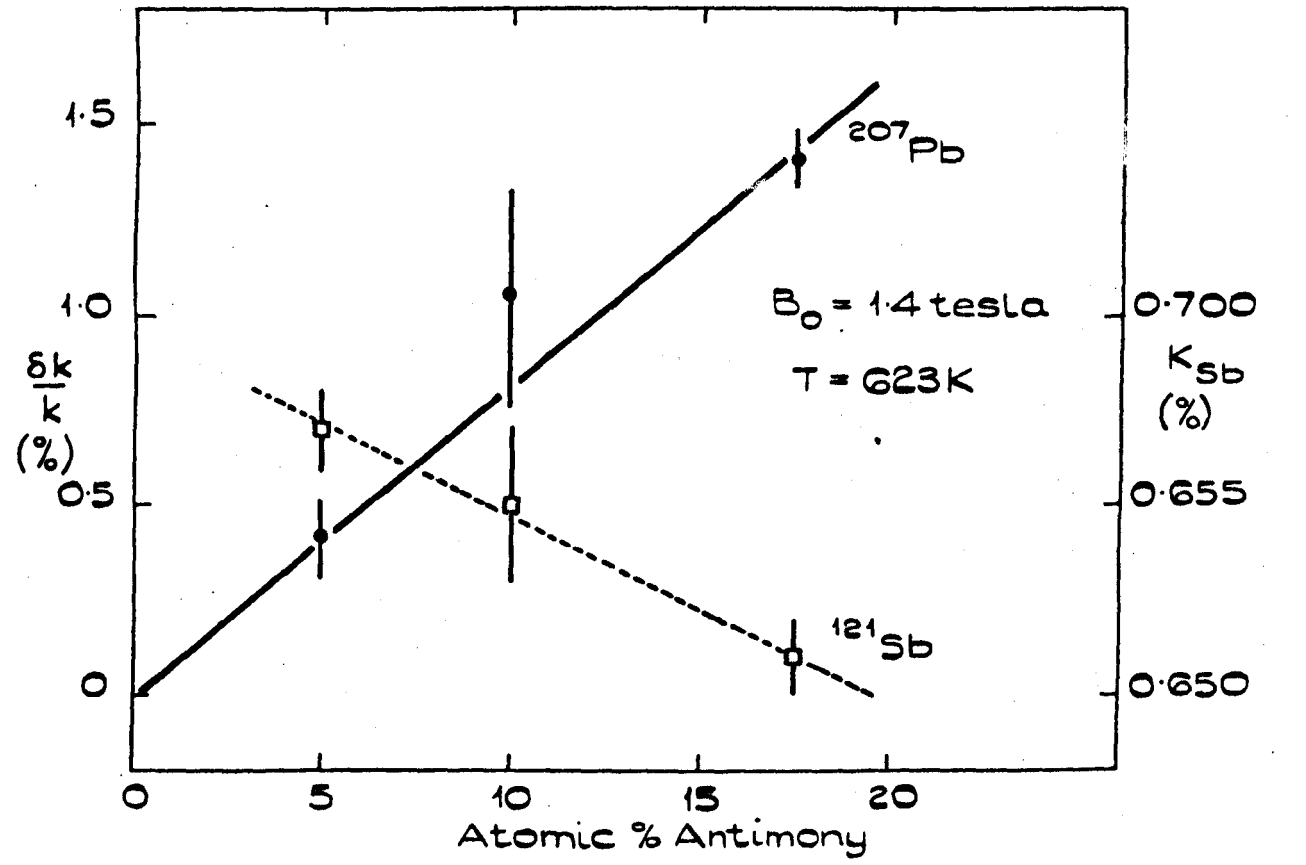

Figure 3.6. Pb - Sb ALLOYS

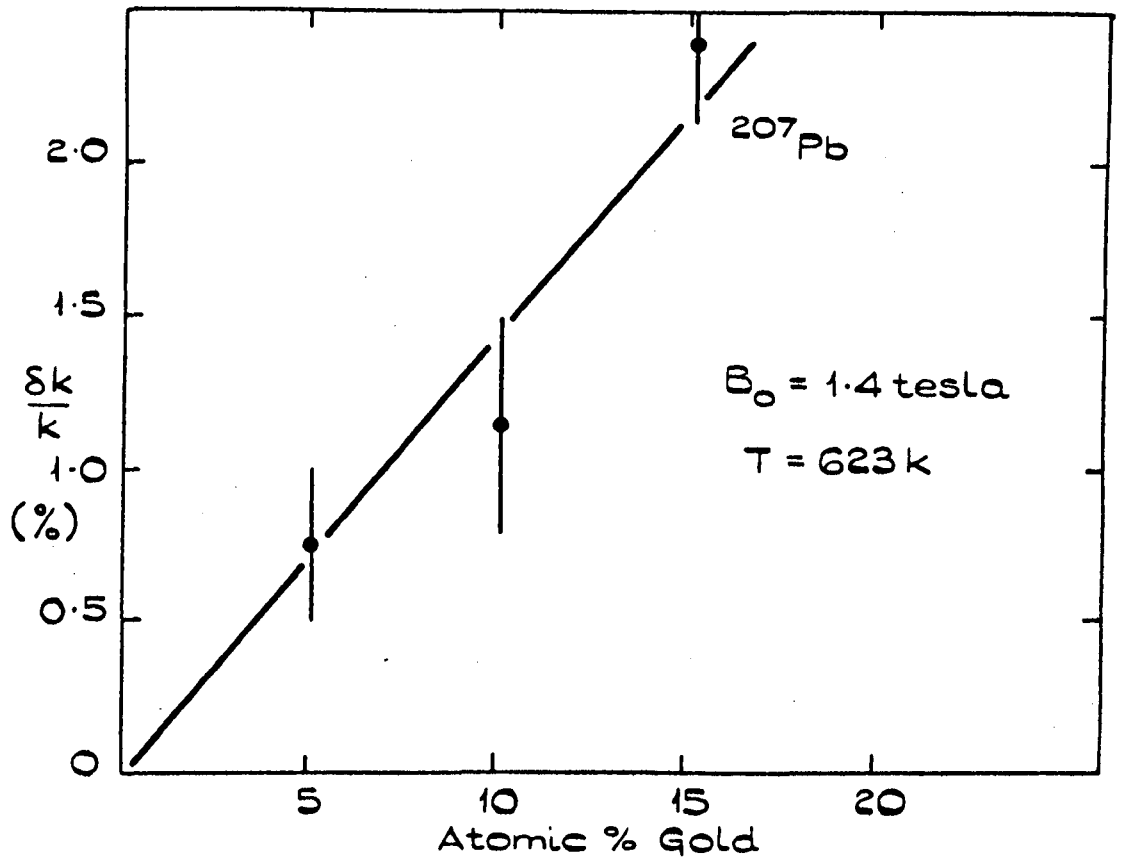

Figure 3.7 Pb – Au ALLOYS

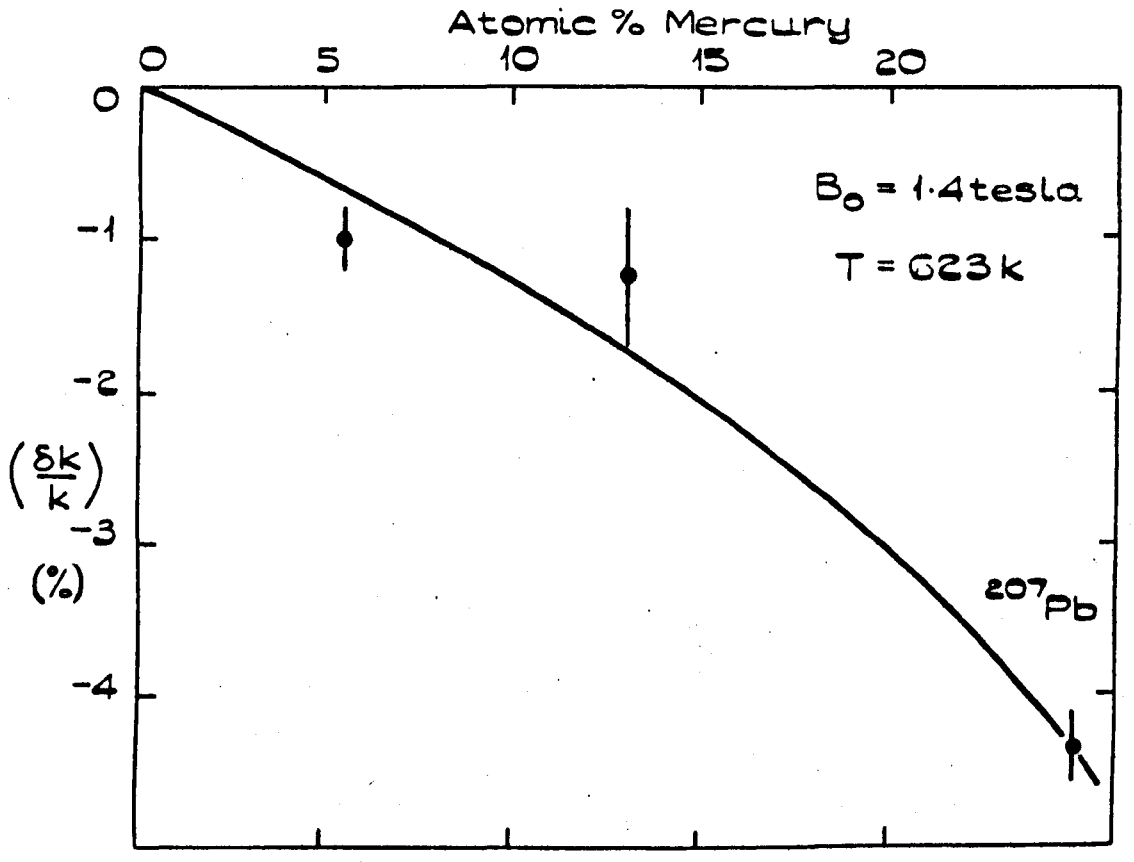

Figure 3.8 Pb – Hg ALLOYS.

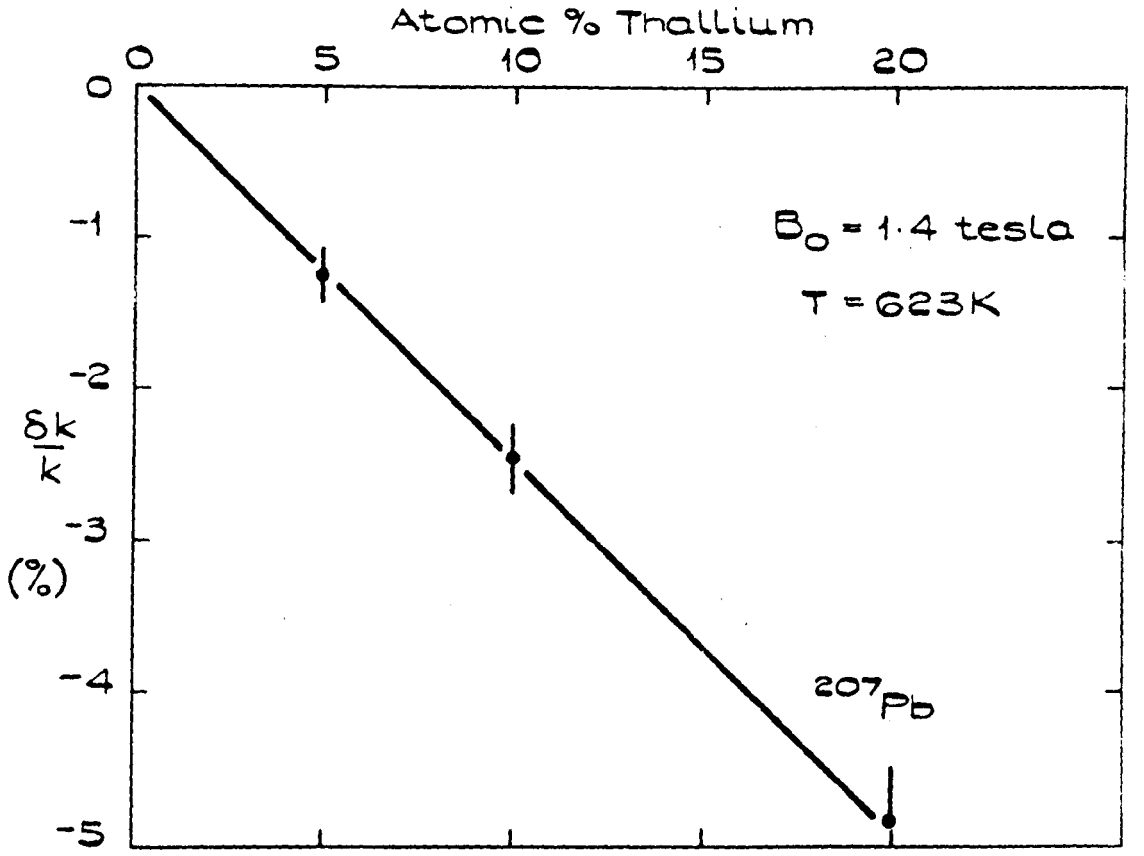

Figure 3.9. Pb - Tl ALLOYS

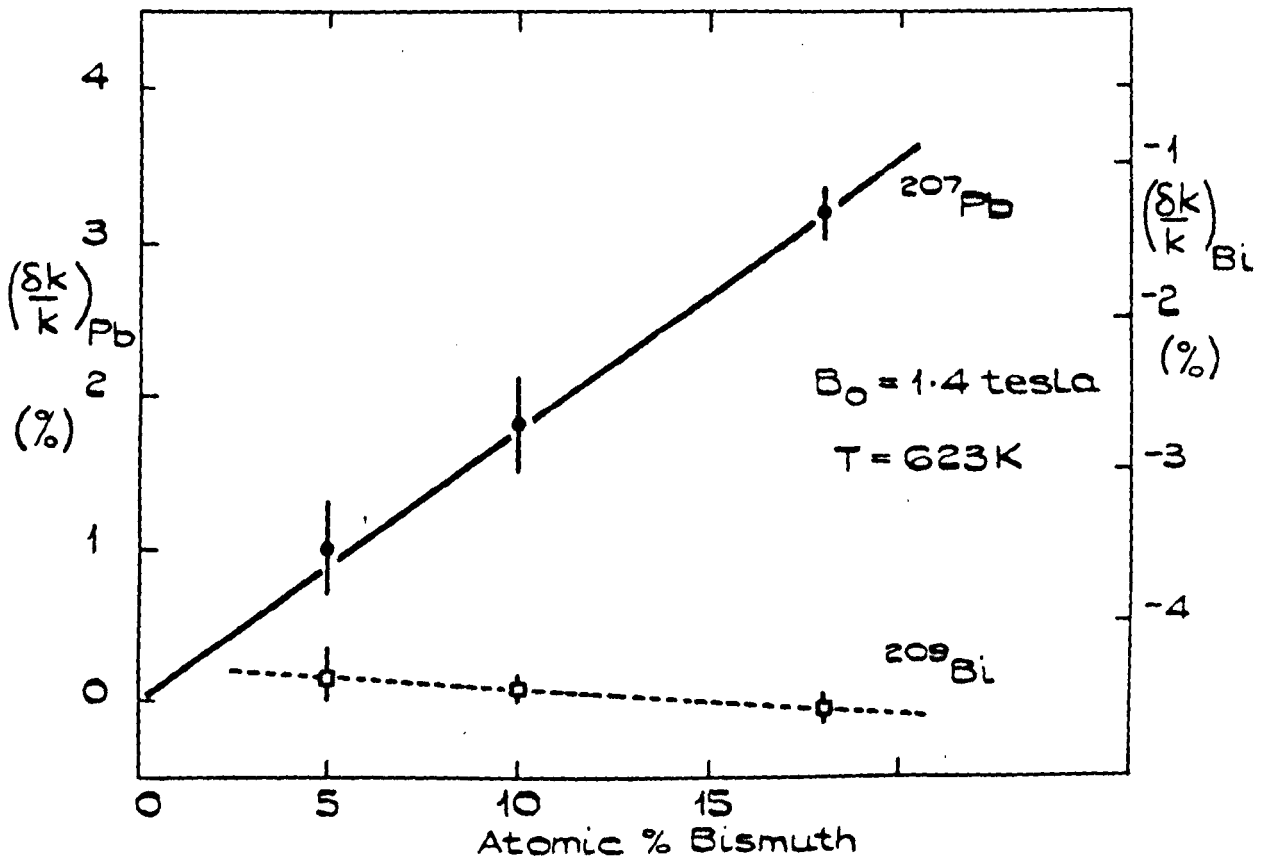

Figure 3.10. Pb - Bi ALLOYS

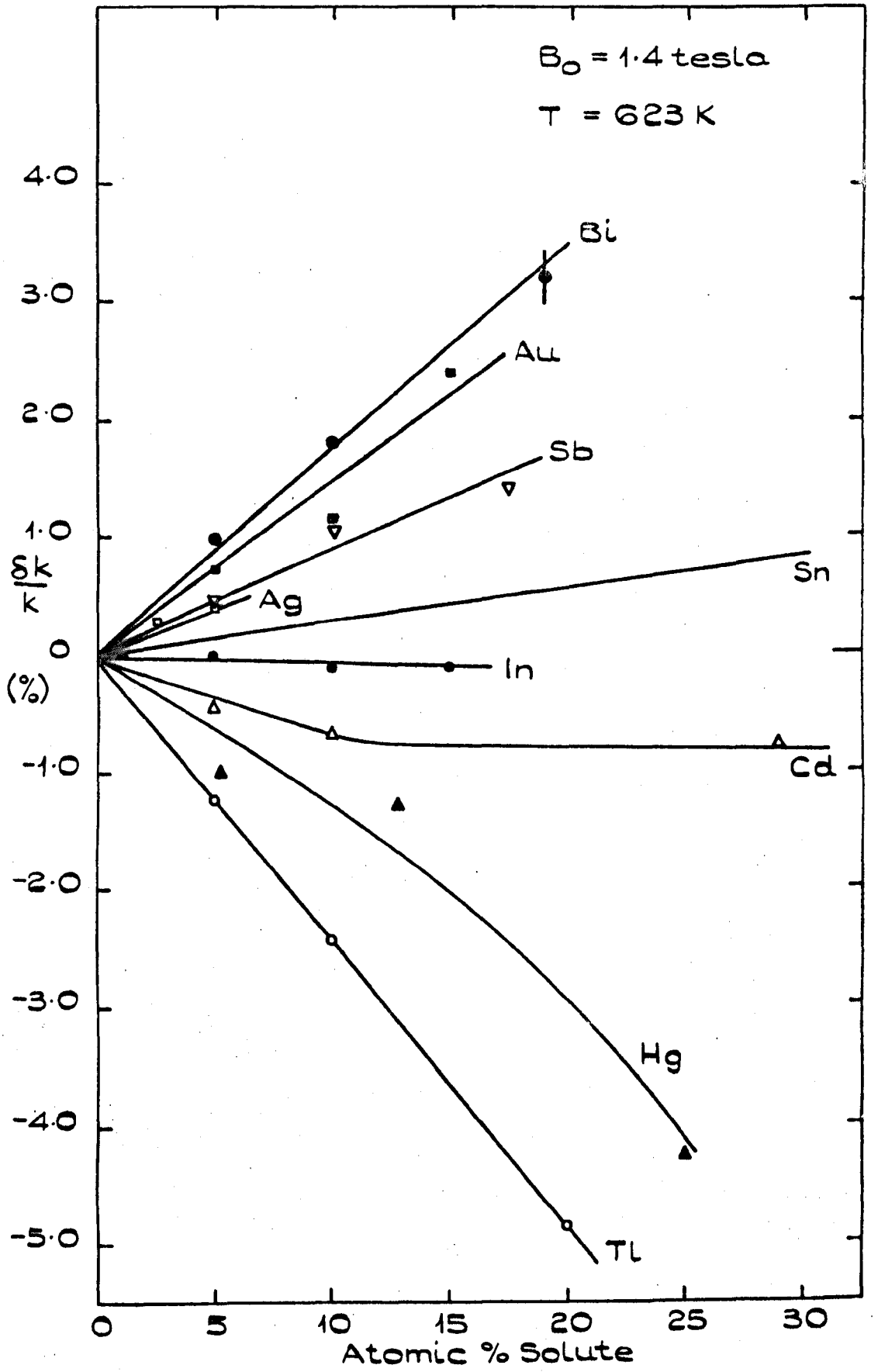

Figure 3.11. SUMMARY OF THE RELATIVE CHANGES OF THE ^{207}Pb KNIGHT SHIFT IN BINARY LIQUID ALLOYS.

3.03.2 Temperature dependence of the Knight shift

Room temperature measurements on several lead base solid solutions have been reported previously[6], and show radical differences from the results in the liquids reported in 3.03.1. For this reason the ^{207}Pb resonance has been followed through the melting temperature for two of the alloys. The two alloys, Pb - 18% Bi and Pb - 20% Tl, were chosen for two reasons; firstly they form solid solutions[8], and thus it is possible to make measurements in the solid phase as well as the liquid, and, secondly, they show the largest effect (positive and negative respectively) on the Knight shift in the liquid phase.

The ^{207}Pb Knight shift temperature dependences for Pb - 18% Bi and Pb - 20% Tl are shown in fig. 3.12 and 3.13 respectively. Figure 3.12 also contains the ^{209}Bi Knight shift results, in the liquid phase only because quadrupolar effects wash out the ^{209}Bi signal in the solid. Both fig. 3.12 and 3.13 give the temperature dependence of the ^{207}Pb shift in pure lead for comparison.

3.03.3 Temperature dependence of the ^{207}Pb linewidth

The ^{207}Pb width in pure lead (fig. 3.2) shows a small but definite decrease at approximately 500 K. The addition of the impurities bismuth and thallium has been shown[6], at room temperature, to increase the ^{207}Pb width dramatically. With this in mind, the ^{207}Pb linewidth temperature dependences were observed in the Pb - 18% Bi and Pb - 20% Tl alloys. The results are shown in fig. 3.14 and, as before, have been corrected for finite modulation amplitude, using the technique of Smith[3].

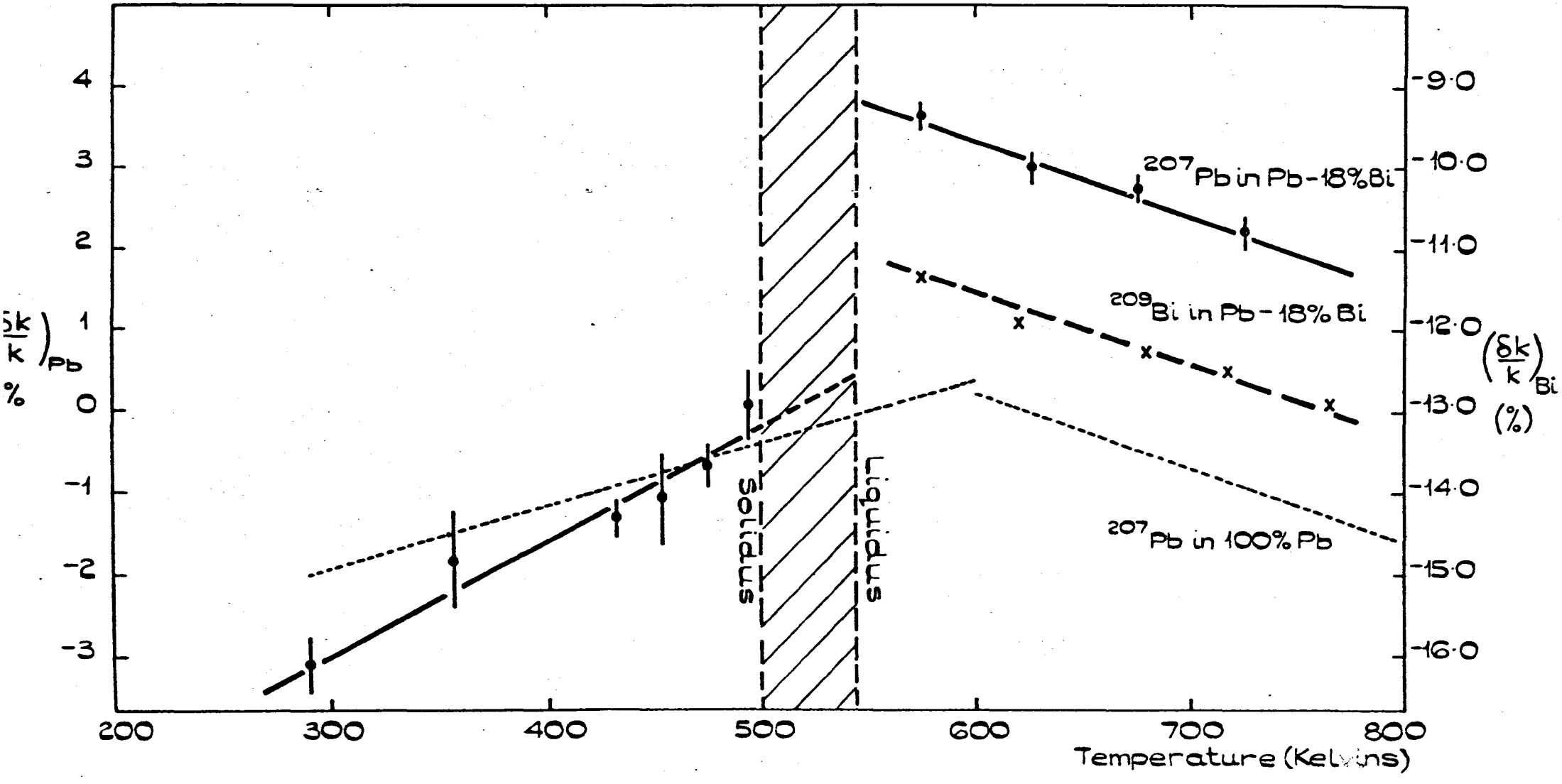

Figure 3.12. Pb – 18% Bi

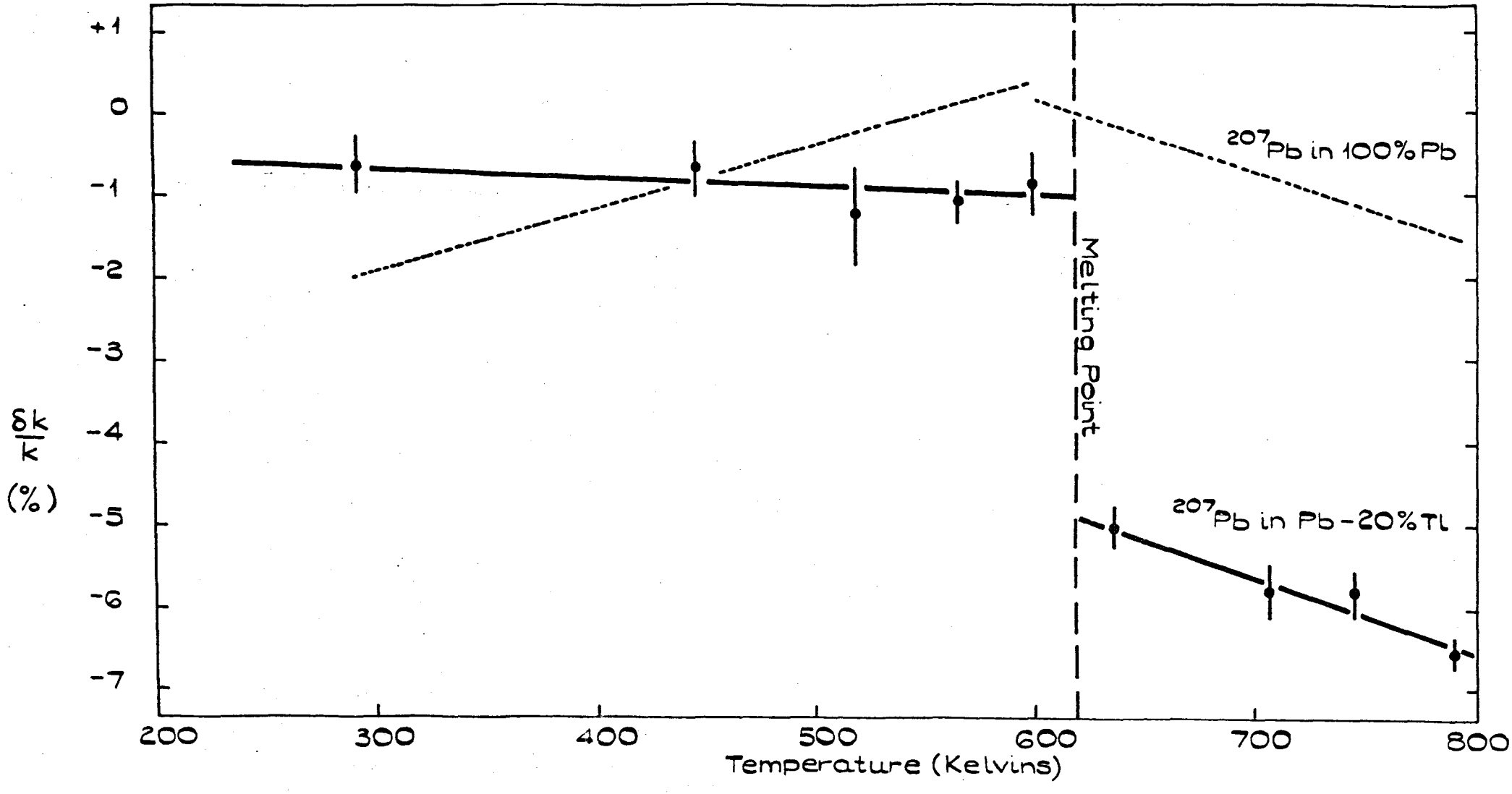

Figure 3.13. Pb - 20% Tl

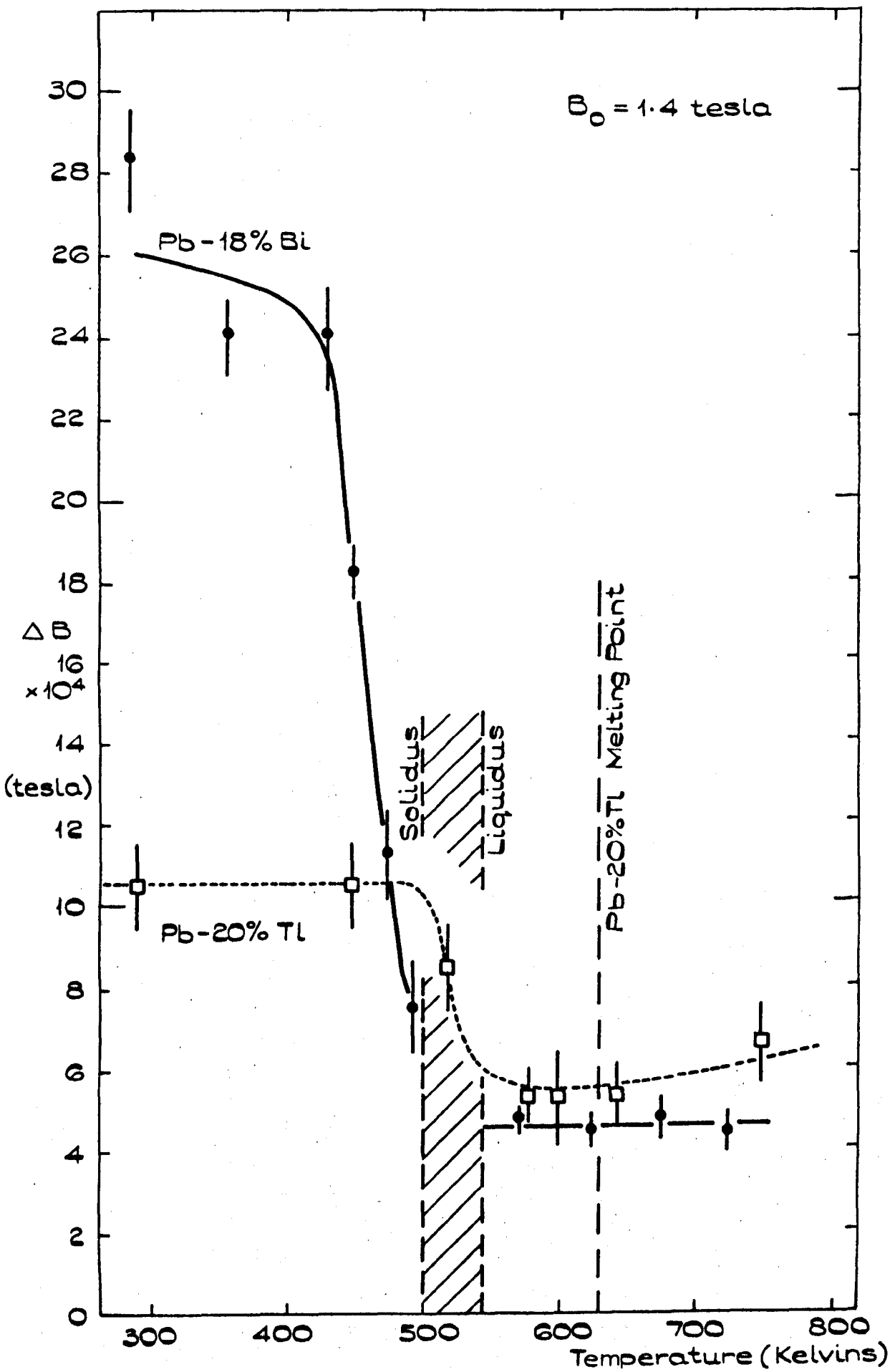

Figure 3.14. LINE WIDTHS IN ALLOYS.

References

(1) Snodgrass R. J. and Bennett L. H., Phys. Rev., 132, (1963), 1465.

(2) Varian Associates, N.M.R. Table, 5th Edition.

(3) Smith G. W., J. Appl. Phys., 35, (1964), 1218.

(4) Moulson D. J., Ph.D. Thesis, Leeds, (1966).

(5) Turnbull D., J. Appl. Phys., 21, (1950), 1022.

(6) Snodgrass R. J. and Bennett L. H., Phys. Rev., 134, (1964), 1294.

(7) Moulson D. J. and Seymour E. F. W., Adv. in Phys., 16, (1966), 449.

(8) Hansen M., Constitution of Binary Alloys, McGraw Hill (1958), 325 and 1115.

CHAPTER FOUR

DISCUSSION OF THE OBSERVATIONS FOR PURE METALS

4.01 Introduction

We have seen that the Knight shift may be written

$$K = \frac{8\pi}{3}\Omega\chi_p P_F \qquad 4.1$$

Most experimental investigations of n.m.r. in liquid metals have measured the Knight shift with the aim of evaluating P_F and of finding how it changes with changes in temperature and with the introduction of impurities. Because the electron theory of metals has been most tested on monovalent metals, and also because χ_p is only at all well known for the alkalis, most experimental observations have been made on the monovalent metals.

By contrast, this chapter considers Knight shifts for liquid metals of all valences. In section 4.03 K is evaluated from first principles by a method suggested by Holland[1]; this involves a zero-order pseudopotential technique. In section 4.04 the first-order pseudopotential method of Faber[2] is discussed, with particular reference to the evaluation of the temperature coefficient of K. Firstly, however, in section 4.02 the ^{207}Pb linewidth in pure lead is discussed.

4.02 ^{207}Pb Linewidth

In theory the lineshape of a n.m.r. absorption can be approximated (at any rate for cubic metals) by either a Gaussian, $\exp(-x^2)$, or a Lorentzian function, $1/(1 + x^2)$. These shapes

very seldom give an exact representation of experimental lineshapes which are in general an admixture of the two, being composed of contributions from different sources. However, at low enough temperatures many metals have Gaussian lineshapes (resulting from random orientations of neighbouring nuclear spins) whilst at high enough temperatures a Lorentzian shape is common (resulting from lifetime limiting processes). In the abscence of quadrupolar interactions the lineshape is largely composed of contributions from four sources: (a) Dipolar broadening (b) Spin-lattice relaxation time broadening (c) Pseudo-dipolar effects and (d) Pseudo-exchange effects. These will be briefly discussed.

(a) Dipolar broadening is caused by the variation from one lattice site to another, in local magnetic fields produced directly by other nuclei. Van Vleck[3] derived a rigorous expression for the second moment, $\overline{\Delta B^2}$, of an absorption line due to this effect. To evaluate the expression a knowledge of the crystal structure is required; if all nuclei are identical,

$$\overline{\Delta B^2} \equiv \int_0^\infty (B - B_0)^2 \, g(B) \, dB$$
$$= (3/5) \, I(I+1) \, \gamma_n^2 \, \hbar^2 \sum_j r_j^{-6} \qquad 4.2$$

where $g(B)$ is the lineshape function and the sum extends over all internuclear distances r_j. The relation between the second moment and the measured width naturally depends on the lineshape[4].

For light metals the dipolar interaction is often the only important contributor to the linewidth at room temperature and below. (For heavier metals the indirect interactions become important.) However, at higher temperatures the observed width is often much smaller than that calculated from eqn. 4.2.

This discrepancy is caused by 'motional narrowing'. Atomic movements, such as diffusion, may cause the local field to be averaged to zero, so that the dipolar broadening is removed and the residual width is that due (in general) to spin-lattice relaxation. Narrowing requires that the atomic correlation time τ_c, which is the average time that an interaction between spins proceeds before being disturbed by a lattice jump, shall be smaller than a critical value given by

$$\frac{1}{\tau_c} \sim \gamma_n (\overline{\Delta B^2})^{\frac{1}{2}} \qquad 4.3$$

The time τ_c decreases as the temperature is increased and, since for a diffusion process $\tau_c = r^2/6D$ where r is the 'jump distance' and D the diffusion coefficient which can be written $D = D_0 \exp(-E/RT)$, it is possible to study diffusion over a limited temperature range through observation of the linewidth. Extensive measurements of line narrowing have been reported for a number of metals in the solid state[5].

(b) Spin-lattice relaxation in metals is, in general, almost entirely produced by the conduction electrons at the Fermi surface. This contribution increases with temperature (the fraction of electrons available to accept small amounts of energy from the spins is proportional to T) until ultimately all linewidths in the high temperature limit are determined by T_1 broadening. Since hyperfine interactions with the conduction electrons generally increase in magnitude with increasing atomic number, this T_1 broadening is greater in the heavier metals.

(c) and (d) The indirect interaction between nuclei via the conduction electrons includes both pseudo-dipolar and pseudo-exchange broadening. The nuclear magnetic moments are coupled

to each other because each in turn interacts with the conduction electrons i.e. the orientation of one nuclear spin affects the energy of another. The contact term is responsible for the indirect exchange interaction; the existence of a non-s part of the conduction electron wave functions gives rise to the pseudo-dipolar interaction, which owes its name to the fact that the coupling is similar in form to that between free dipoles. The second moment of a line including both pseudo- and classical dipolar contributions becomes (again for identical nuclei)

$$\overline{\Delta B^2} = \frac{3}{5}\frac{I(I+1)}{(\gamma_n \hbar)^2}\sum_j\left[\tilde{B}_j + \gamma_n^2 \hbar^2 r_j^{-3}\right]^2 \qquad 4.4$$

where $\tilde{B}_j$ is the interaction constant between the j'th nucleus and that at the origin. For identical nuclei the exchange interaction does not affect the second moment.

Turning now to the specific case of lead, the second moment due to the direct dipolar interaction amounts to $\sim 0.3_5 \times 10^{-4}$ tesla. Froidevaux[6] has investigated the pseudo-dipolar coupling in lead using a technique involving spin echoes formed by 90° - 180° pulse sequences at helium temperatures. From an analysis of the echo profile in a series of lead solid solutions, together with the continuous-wave linewidth results, he derived a value of $\tilde{B}/h = 2.2$ kHz for nearest neighbours. This corresponds to a second moment of $\sim 17.4\,(\text{kHz})^2$ or, in terms of magnetic field, a linewidth of $\sim 4.5 \times 10^{-4}$ tesla. This is to be compared with an estimate of $\sim 3 \times 10^{-4}$ tesla by Snodgrass and Bennett[7] from the measured total linewidth for pure lead at room temperature. Like the classical dipolar interaction, the pseudo-dipolar contribution to the width

produces a Gaussian shape and since T_1 broadening produces a Lorentzian shape, a change in shape occurs in 'motional narrowing'. This considerably complicates the detailed description of the narrowing process; however for ^{207}Pb the experimental uncertainty does not warrant the use of the more detailed theory.

The narrowing observed in the ^{207}Pb linewidth - temperature curve at 500 K, fig. 3.2, is attributed to self diffusion acting to remove the classical and pseudo-dipolar contributions to the width. The width of a Gaussian line that would have had to be removed by the motion to give the observed initial and final lines was found to be $\sim 3 \times 10^{-4}$ tesla. That removal of a combined contribution of $\sim 3 \times 10^{-4}$ tesla fits the observed narrowing was checked by numerically computing the result of broadening a Lorentzian line of width 4.9×10^{-4} tesla (observed at 550 K see fig. 3.2) with a Gaussian line of width 3×10^{-4} tesla. The composite line had a width of 6.0×10^{-4} tesla, quite consistent with the width expected at 550 K had narrowing not occurred. The two effects taken together suggest a value of $\sim 2.9 \times 10^{-4}$ tesla for the pseudo-dipolar contribution which is in good agreement with that of Snodgrass but is smaller than the value given by Froidevaux above. It is also in reasonable agreement with that predicted on the basis of the low temperature (77 K) T_1 results of Asayama and Itoh[8]. In fact, using the Korringa relation, $T_1 TK^2 =$ constant, the predicted linewidth at 550 K is $4.1(\pm 0.3) \times 10^{-4}$ tesla, the observed value being $4.9(\pm 0.3) \times 10^{-4}$ tesla.

From the narrowing condition, eqn. 4.3, the correlation time for diffusive motion is $\sim 9 \times 10^{-5}$s at 500 K. Since the observations do not show accurately the detailed way in which

the narrowing proceeds, and in any case the relevant measurements are confined to a very narrow temperature range, it is not possible to deduce values of τ_c at other temperatures, and it is not therefore possible to find values of D_0 and E. However the value of the self-diffusion coefficient D itself at the one temperature 500 K is accessible and (using $r = 3.49 \times 10^{-10}$m) is $2.2 \times 10^{-16}\ m^2 s^{-1}$. This is in very good agreement with the radiotracer measurements of Nachtrieb et al.[9] who found precisely this value at 479 K.

It is concluded that the narrowing observed at 500 K is quite consistent with that expected from a joint narrowing of the classical- and pseudo-dipolar contributions to the width. The residual width is solely relaxation time broadening and has been shown to be consistent with that expected on the basis of the available pulsed n.m.r. results.

4.03 Knight shifts in liquid metals

4.03.1 Introduction Little theoretical effort has been applied to the problem of the evaluation of the Knight shift for individual liquid metals. It is safe to say that the reason for this has been the uncertainty in the value of χ_p and therefore the inability to test theoretical values against experiment. More effort has been applied to the evaluation of the effect of alloying and of changes in temperature upon K and two similar, yet distinct, approaches have been developed. Partial wave analysis has been used by Friedel et al.[10], and the pseudopotential method used by Faber[2], to discuss the problem of electron distributions in alloys. These methods will be

considered in more detail in Chapter 5; the derivation of a temperature dependence using the pseudopotential approach[2,11] will be discussed in section 4.04 of this chapter.

The pseudopotential technique, where the real potential inside the ion core is replaced by a much weaker pseudo-potential, would not seem, at first sight, to be suitable for the evaluation of a wavefunction at the nuclear site. With this in mind, Holland[1] set out to test the general applicability of the technique to the evaluation of P_F for metals. In essence his argument is that, if the pseudopotential is small enough so that first-order perturbation theory will be valid, then a calculation to zero-order in the pseudopotential ought to give a result for K not more than, say, 20% different from the observed value. He performed this calculation, based on an orthogonalised plane wave (O.P.W.) and his agreement with experiment in a number of test cases was good. It therefore seemed that the use of a pseudo-potential, as a first-order perturbation, might improve this agreement.

Watson and Freeman[12], in the course of a discussion of Knight shifts in alloys, pointed out that the emphasis in the current explanations of solvent shift changes on the effects of screening charge clouds round solute ions, might be misplaced. They showed that a change in the Fermi wavevector (in their case due to alloying and evaluated on the basis of a rigid band model) could produce a significant change in P_F even in a zero-order calculation. This effect was due to the change in the degree of constancy of the conduction electron wavefunction over an ion core. They calculated the concentration dependence of K in the alloys Ag - Cd and Cu - Zn and showed that in these alloys the

effect was of considerable importance.

With these ideas in mind a simple extension, suggested by Holland, to the zero-order pseudopotential calculation has been performed with a view to (i) testing the accuracy of the zero-order calculation in heavy polyvalent metals, and (ii) assessing the importance of lack of complete constancy to the absolute value of K, and to its change with temperature, on melting and upon alloying.

4.03.2 The Theory of Holland The derivation of Holland will be discussed in some detail because the extension to include a correction for the variation of the conduction electron wavefunction over the ion core follows this derivation in a straightforward fashion.

The wavefunction of a conduction electron may be written (in the spirit of an O.P.W. formulation)

$$\Psi(\underline{r}) = C\left\{\varphi(\underline{r}) - \sum_{in}\left(\left[\int d^3\underline{r}\,\Psi^*_{in}(\underline{r})\,\varphi(\underline{r})\right]\,\Psi_{in}(\underline{r})\right)\right\} \qquad 4.5$$

where $\Psi(\underline{r})$ is the true wavefunction,

$\varphi(\underline{r})$ the pseudowavefunction,

$\Psi_{in}(\underline{r})$ the n'th core state of the i'th ion, and C normalises $\Psi(\underline{r})$ in the volume of the specimen, V. If the pseudofunction varies only slowly over an ion core, the overlap integral can be written

$$I \simeq \varphi(\underline{R}_i)\int d^3\underline{r}\,\Psi^*_{in}(\underline{r}) \qquad 4.6$$

where the integral is only non-zero for even functions. If a typical Fermi wave vector is considered the effect of this assumption can be estimated. In sodium $k_F \sim 0.5(\text{A.U.})^{-1}$;

thus $\lambda_F \sim 10$ A.U. which suggests that something like a 10% error might be incurred by neglecting any variation over an ion core radius of ~ 1 A.U.

Evaluating $\Psi(\underline{r})$ at a nuclear site gives

$$\Psi(\underline{R}_i) = C\,\varphi(\underline{R}_i)\left[1 - \sum_n b_n \Psi_{in}(\underline{R}_i)\right] \qquad 4.7$$

where $b_n \equiv \int d^3\underline{r}\, \Psi^*_{in}(\underline{r})$. This can be further compacted by writing $\alpha_n = \Psi_{in}(\underline{R}_i)$ and $\gamma = 1 - \sum_n b_n \alpha_n$. The quantity γ depends only on the type of ion being considered. Then

$$\Psi(\underline{R}_i) = C\gamma\varphi(\underline{R}_i)$$

and

$$\Psi^*(\underline{R}_i)\Psi(\underline{R}_i) = |C|^2 |\gamma|^2 \varphi^*(\underline{R}_i)\varphi(\underline{R}_i). \qquad 4.8$$

In this expression a value $|C|^2$ is required; the following derivation will use the more compact Dirac notation.

$$1 = |C|^2\left[\langle\varphi|\varphi\rangle - \sum_{in}\langle in|\varphi\rangle\langle\varphi|in\rangle\right] \qquad 4.9$$

where $\langle in|\varphi\rangle \equiv b_n\varphi(\underline{R}_i)$. Thus

$$\sum_{in}\langle in|\varphi\rangle\langle\varphi|in\rangle = \sum_{in} b_n^* b_n \varphi^*(\underline{R}_i)\varphi(\underline{R}_i). \quad \text{Now}$$

$$\sum_i \varphi^*(\underline{R}_i)\varphi(\underline{R}_i) = \int d^3\underline{r}\, \rho(\underline{R}_i)\varphi^*(\underline{r})\varphi(\underline{r}) \quad \text{where}$$

$\rho(\underline{R}_i)$ is the number density and thus the summation can be written

$$\frac{N}{V}\langle\varphi|\varphi\rangle \quad \text{or} \quad \Omega^{-1}\langle\varphi|\varphi\rangle$$

where N is the number of ions in volume V and Ω the atomic volume. Hence

$$|C|^{-2} = \langle\varphi|\varphi\rangle\left[1 - \Omega^{-1}\sum_n b_n^* b_n\right].$$

Substituting into eqn. 4.8

$$\Psi^*(\underline{R}_i)\Psi(\underline{R}_i) = \frac{|\gamma|^2}{(1 - \Omega^{-1}\sum_n b_n^* b_n)} \varphi^*(\underline{R}_i)\varphi(\underline{R}_i) \qquad 4.10$$

if φ is normalised to unity in volume V. This is the expression obtained by Holland; it can readily be extended to include terms to first order in the pseudopotential, as follows.

By writing $|\varphi\rangle = |\varphi^{(0)}\rangle + |\varphi^{(1)}\rangle$ and substituting into eqn. 4.9

$$|C|^{-2} = \langle\varphi^{(0)}|\varphi^{(0)}\rangle + 2\mathrm{Re}\{\langle\varphi^{(0)}|\varphi^{(1)}\rangle\} - \sum_{in}\{\langle in|\varphi^{(0)}\rangle\langle\varphi^{(0)}|in\rangle + 2\mathrm{Re}\,\langle in|\varphi^{(0)}\rangle\langle\varphi^{(1)}|in\rangle\}$$

$$\text{or } |C|^2 = \frac{1}{A^{(0)} + A^{(1)}} = \frac{1}{A^{(0)}}\left[1 - \frac{A^{(1)}}{A^{(0)}}\right]$$

$$\text{with } A^{(0)} = 1 - \sum_{in}\langle in|\varphi^{(0)}\rangle\langle\varphi^{(0)}|in\rangle$$

$$\text{and } A^{(1)} = -2\mathrm{Re}\left\{\sum_{in}\langle in|\varphi^{(0)}\rangle\langle\varphi^{(1)}|in\rangle\right\}$$

which are the zero- and first-order terms respectively, and $A^{(1)} \ll A^{(0)}$. Substituting into eqn. 4.8 the result becomes, after some rearrangement

$$\Psi^*(\underline{R}_i)\Psi(\underline{R}_i) = \frac{|\gamma|^2|\varphi^{(0)}(\underline{R}_i)|^2}{(1 - \Omega^{-1}\sum_n b_n^* b_n)}\left[1 + 2\mathrm{Re}\left\{\frac{\varphi^{(0)*}(\underline{R}_i)\,\varphi^{(1)}(\underline{R}_i)}{|\varphi^{(0)}(\underline{R}_i)|^2}\right\}\right.$$

$$\left. + \frac{2\sum_n (b_n^* b_n)\,\mathrm{Re}\left\{\sum_j \varphi^{(1)*}(\underline{R}_j)\,\varphi^{(0)}(\underline{R}_j)\right\}}{(1 - \Omega^{-1}\sum_n b_n^* b_n)}\right] \qquad 4.11$$

This expression, when averaged over all electrons at the Fermi surface, over all ions for a given configuration, and then ensemble averaged, provides an expression for P_F correct to first order in the pseudopotential. The second term in eqn. 4.11 is equivalent to the expression deduced by Watabe[11] and by Faber[2]. It will be shown in section 4.04 that, although the pseudopotentials currently available in the literature (for example, see reference[13]) are sufficiently small for first-order perturbation theory to be used, quantitative evaluation of the above scheme is not fully useful because of inaccuracies of the functions involved. The third term in eqn. 4.11, which has not been obtained previously, turns out to be much smaller than the second; as an example, for sodium its magnitude is only 6% of that of the second. It is not considered further.

From the first term of eqn. 4.11 it is not only possible to deduce a value of K for a given metal but also to obtain a temperature dependence through the change in the atomic volume . For all liquid metals that expand on heating this effect is such as to produce a small, negative temperature coefficient; for liquid sodium the value of this coefficient is $-1.9 \times 10^{-5}(\text{kelvins})^{-1}$.

4.03.3 Extension of the zero-order theory to take account of incomplete 'constancy'. As discussed earlier, the assumption that the zero-order wavefunction was constant over an ion core was used for convenience in Holland's work and was introduced in eqn. 4.6. Rewriting this

$$I = \int d^3\underline{r}\, \psi^*_{in}(\underline{r} - \underline{R}_i)\, \varphi(\underline{r})$$

and representing $\varphi(\underline{r})$ as a plane wave

$$\varphi(\underline{r}) = V^{-\frac{1}{2}} \exp(i\underline{k}.\underline{r})$$

$$I = V^{-\frac{1}{2}} \int d^3\underline{r}\, \psi^*_{in}(\underline{r} - \underline{R}_i)\exp(i\underline{k}.\underline{r})$$

which can be written by a simple change of variable

$$I = V^{-\frac{1}{2}} \int d^3\underline{x}\, \psi^*_{in}(\underline{x})\exp\{i\underline{k}.(\underline{r} + \underline{R}_i)\}$$

$$= V^{-\frac{1}{2}}\exp(i\underline{k}.\underline{R}_i) \int d^3\underline{x}\, \psi^*_{in}(\underline{x})\exp(i\underline{k}.\underline{x}) \ .$$

By expanding $\exp(i\underline{k}.\underline{x})$ as a power series, higher order corrections to the constancy approximation can be introduced.

$$I = V^{-\frac{1}{2}}\exp(i\underline{k}.\underline{R}_i) \int d^3\underline{x}\, \psi^*_{in}(\underline{x}) \left[1 + i\underline{k}.\underline{x} - \frac{(\underline{k}.\underline{x})^2}{2} + ...\right]$$

or $\langle in|\varphi\rangle = \varphi(\underline{R}_i)\left[b_n + \Theta^{(1)}_{nk} + \Theta^{(2)}_{nk}\right]$

where $b_n = \int d^3\underline{x}\, \psi^*_{in}(\underline{x})$

$$\Theta^{(1)}_{nk} = \int d^3\underline{x}\, \psi^*_{in}(\underline{x})\ i\underline{k}.\underline{x}$$

and $$\Theta^{(2)}_{nk} = \int d^3\underline{x}\, \psi^*_{in}(\underline{x})\ (-1/2)(\underline{k}.\underline{x})^2 \ .$$

The argument follows exactly as given in the previous section with $(b_n + \Theta^{(1)}_{nk} + \Theta^{(2)}_{nk})$ replacing b_n wherever it appeared. The resulting expression for $\psi^*\psi$ is

$$\psi^*(\underline{R}_i)\psi(\underline{R}_i) = \varphi^*(\underline{R}_i)\varphi(\underline{R}_i)\ \frac{|\gamma|^2}{\beta} - \frac{\varphi^*(\underline{R}_i)\varphi(\underline{R}_i)}{\beta}\left[T_k + \frac{|\gamma|^2 S_k}{\beta} - \frac{T_k S_k}{\beta} - \frac{|\gamma|^2\ S_k^{\ 2}}{\beta^2} + \frac{T_k |S_k|^2}{\beta^2}\right] \qquad 4.12$$

where $\beta = 1 - \frac{1}{\Omega}\sum_n b^*_n b_n$

$$S_k = -\frac{\langle\varphi|\varphi\rangle}{\Omega}\sum_n \left\{2\mathrm{Re}(b_n\Theta^{(1)}_{nk} + b_n\Theta^{(2)}_{nk} + \Theta^{(1)*}_{nk}\Theta^{(1)}_{nk}\right\}$$

and $T_k = 2\mathrm{Re}\left\{ \sum_n \left(\left[\Theta_{nk}^{(1)} + \Theta_{nk}^{(2)} \right] \alpha_n \right) - \right.$

$$\left. \sum_n \left\{ \left(\Theta_{nk}^{(1)} + \Theta_{nk}^{(2)} \right) \alpha_n \right\} \sum_n \left\{ \left(\Theta_{nk}^{(1)*} + \Theta_{nk}^{(2)*} \right) \alpha_n^* \right\} \right.$$

All expressions are correct to second-order throughout.

The expression 4.12 can be separated into zero-, first-, and second-order terms,

$$P_F^{(0)} = \frac{\varphi^*(\underline{R}_i)\varphi(\underline{R}_i)}{\beta} |\gamma|^2$$

$$P_F^{(1)} = \frac{-\varphi^*(\underline{R}_i)\varphi(\underline{R}_i)}{\beta} \left[2\left(\gamma \sum_n {}^{(1)}_{nk} \alpha_n \right) - \frac{\langle \varphi | \varphi \rangle}{\beta \Omega} |\gamma|^2 \sum_n 2\left(b_n \Theta_{nk}^{(1)} \right) \right]$$

$$P_F^{(2)} = \frac{-\varphi^*(\underline{R}_i)\varphi(\underline{R}_i)}{\beta} \left[2 \sum_n \Theta_{nk}^{(2)} \alpha_n - \sum_n |\alpha_n \Theta_{nk}^{(1)}|^2 \right. \qquad 4.13$$

$$- \frac{\langle \varphi | \varphi \rangle}{\beta \Omega} \left\{ |\gamma|^2 \sum_n \left(\Theta_{nk}^{(1)*} \Theta_{nk}^{(1)} + 2 b_n \Theta_{nk}^{(2)} \right) \right.$$

$$\left. \left. + 4\gamma \sum_n \left(\Theta_{nk}^{(1)} \alpha_n \right) \sum_n \left(\Theta_{nk}^{(1)} b_n \right) \right\} \right]$$

This very complicated expression is considerably simplified by the parity of the core wavefunctions. In fact, b_n is only non-zero for s- and d-states, $\Theta_{nk}^{(1)}$ is only non-zero for p-states and α_n is only non-zero for s-states. Hence

$$b_n \Theta_{nk}^{(1)} = 0$$

$$\alpha_n \Theta_{nk}^{(1)} = 0$$

Thus the equations 4.13 become

$$
\begin{aligned}
\rho_F^{(0)} &= \frac{\varphi^*(\underline{R}_i)\varphi(\underline{R}_i)}{\beta}\,|\gamma|^2 \\
\rho_F^{(1)} &= 0 \\
\rho_F^{(2)} &= -\frac{\varphi^*(\underline{R}_i)\varphi(\underline{R}_i)}{\beta}\,|\gamma|^2\left[\frac{2}{\gamma}\sum_n(\Theta_{nk}^{(2)}\alpha_n)\right. \\
&\quad \left. -\frac{\langle\varphi|\varphi\rangle}{\beta\Omega}\sum_n(\Theta_{nk}^{(1)*}\Theta_{nk}^{(1)} + 2b_n\Theta_{nk}^{(2)})\right]
\end{aligned}
\qquad 4.14
$$

As can be seen, eqn. 4.14 contains contributions from the p-state wavefunctions through the terms $\Theta_{nk}^{(1)}$ which involve an angular dependence. Because for a spherical Fermi surface all directions for $\underline{k}$ are equally represented then, on averaging over the Fermi surface, the angular functions average to simple numerical factors. Equation 4.14 reduces to the form

$$
\Omega\rho_F = \frac{|\gamma|^2}{1 - a\Omega^{-1}}\left[1 - \frac{bk_F^2}{\Omega - a} - ck_F^2\right] \qquad 4.15
$$

The quantities $|\gamma|^2$, a, b and c depend on the values of α_n, b_n, $\Theta_{nk}^{(1)}$ and $\Theta_{nk}^{(2)}$. The evaluation of eqn. 4.15 to obtain the absolute magnitude of K and its temperature dependence will now be discussed.

4.03.4 Calculation of Knight shifts correct to second-order in the displacements. The simplest metal on which to perform a meaningful test of the zero-order pseudopotential calculation is sodium (lithium is unsuitable because there are no p-states in the core and there can be no p-cancellation in the pseudopotential). Holland[1] performed this calculation and obtained good agreement with experiment, using analytic wave-functions, for which the values of the parameters were taken from

Tubis[14]. The correction for 'non-constancy', given in the preceding section, should improve the estimate and also allow the determination of a contribution to the temperature coefficient of K additional to that given at the end of section 4.03.2. This calculation was reported at the XV Colloque Ampere[15]. The agreement with the observed value of K is slightly improved by the 20% correction obtained.

With this encouragement it was decided to undertake similar computations for a representative selection of metals: further alkalis and two series of group B metals. To facilitate the mechanics of calculating $|\gamma|^2$, a, b and c an ALGOL 60 computer program was written (for details see Appendix II) which evaluated the overlap integrals involved. The core state wavefunctions were taken from Herman and Skillman[16]. The values of the quantities $|\gamma|^2$, a, b and c for the 13 metals selected are given in table 4.1 and the resulting Knight shifts in table 4.2. The atomic volumes, and k_F values are given for the liquids at their melting points. The term δ represents the correction introduced by p_F[2]. All values are given in terms of atomic units because these are the units most often used when discussing wavefunctions. To obtain K from the calculated value of P_F, eqn. 4.1 was used. The value of χ_p was taken from Silverstein[17], where values of the Pauli spin susceptibility for an interacting electron gas are given in c.g.s. volume units. The final column of table 4.2 gives experimental values of K for comparison purposes. Wherever possible these refer to a temperature just above the melting point; for Ag and Au the values are for the solid, but, because the temperature dependence of K is most unlikely to be at all large, the temperature difference will not invalidate the comparison.

Table 4.1

Details of $|\gamma|^2$, a, b and c calculated for 13 elements.

Metal	$\|\gamma\|^2$	a	b	c	Ω
*Na	134	2.4_5	0.11_4	0.26_6	270.6
Rb	993.6	83.1_4	$-75._0$	0.62_0	684.5
Ag	653.3	19.4_5	-3.6_5	0.26_5	136.9
Cd	667.8	18.6_3	-2.7_0	0.23_8	165.4
In	599.3	16.6_0	-1.9_7	0.22_8	192.9
Sn	623.4	14.8_2	-1.5_8	0.21_1	201.5
Sb	600.3	13.1_4	-1.2_2	0.18_8	220.8
Cs	1620.0	138.2_0	-148.0	0.88_0	852.9
Au	1259.6	25.2_6	-5.1_3	0.27_4	134.0
Hg	1236.3	22.9_4	-4.0_4	0.25_5	174.8
Tl	1168.0	20.8_8	-3.3_0	0.24_2	213.8
Pb	1125.2	19.1_0	-2.9_8	0.22_8	204.9
Bi	1100.0	17.5_4	-2.1_6	0.21_6	245.3

* Atomic units were not used for sodium because the analytic form of the wavefunctions was used in this calculation.

Table 4.2

Knight shifts calculated to second-order in the displacements

Metal	Valence	k_F	M.P.(K)	$\delta(\%)$	$\chi_{silv.}$	$K_{calc.}\%$	$K_{exp.}\%$
Na	1	0.4_7	370.6	-22	0.8_5	0.10_5	0.11_6 (a)
Rb	1	0.3_5	312.0	-6	0.5_8	0.5_2	0.6_6 (a)
Ag	1	0.6_0	1233.0	-8	1.1_0	0.6_3	0.5_3 (d)
Cd	2	0.7_1	594.0	-3	1.2_7	0.7_8	0.7_9 (c)
In	3	0.7_7	428.0	-7	1.3_5	0.7_3	0.8_0 (a)
Sn	4	0.8_4	505.0	-14	1.4_7	0.7_1	0.7_3 (a)
Sb	5	0.8_8	903.5	-14	1.5_3	0.7_0	0.7_2 (e)
Cs	1	0.3_3	303.0	-7	0.6 or 1.1_5	0.9 or 1.7	1.4_4 (a)
Au	1	0.6_0	1336.0	-4	1.0_8	1.3_6	1.6_4 (f)
Hg	2	0.7_0	233.0	-5	1.2_4	1.4_4	2.4_5 (a)
Tl	3	0.7_5	576.0	-14	1.3_2	1.6_4	1.4_8 (b)
Pb	4	0.8_3	600.0	-14	1.4_6	1.3_0	1.4_9 (b)
Bi	5	0.7_8	544.0	-14	1.3_8	1.5_7	1.4_1 (a)

(a) Knight, Berger and Heine, Ann. Phys., 8, (1959), 173.

(b) Moulson and Seymour, Adv. Phys., 16, (1967), 449.

(c) Seymour and Styles, Phys. Letts., 10, (1964), 269.

(d) Brun, Oeser, Staub and Telschow, Phys. Rev., 93, (1954), 172 (SOLID).

(e) Odle and Flynn, J. Phys. Chem. Solids, 26, (1965), 1685, (SOLID).

(f) Narath, Phys. Rev., 163, (1967), 232.

4.03.5 Discussion The calculated results are generally in excellent agreement with the measured values of K. As the calculation is based on a free-electron picture with a pseudo-potential that is zero, the agreement obtained is felt to be additional evidence that liquid metals are free-electron like. Further, it was shown by Holland[1] that the same expression for P_F is obtained when the zero-order pseudofunction is chosen either as a single O.P.W. or as a linear combination of plane waves. This shows that P_F will be insensitive to melting, for instance, and substantiates the discussion of Chapter 1 regarding the constancy of $\rho(E_F)$ across the melting transition. Nevertheless. it must be added that the excellence of the agreement between experiment and theory may be fortuitous.

Firstly, no account has been taken of contributions to the measured Knight shift other than from the straightforward s-electron density at the nuclear site. There may well be orbital or core-polarisation terms which can be either negative or positive. In fact, for the alkali metals Mahanti[18] has calculated the core-polarisation contributions and obtains +23%, +24% and +25% of K_s for Cs, Rb and Na respectively. Inspection of table 4.2 shows that, if anything, these corrections improve the agreement. The Knight shift of ^{209}Bi is discussed in detail in Chapter 6 and it is concluded there that the contact Knight shift $K_s \sim 2.0\%$ as opposed to the observed 1.4% i.e. there is another contribution of $-0.3_3 K_s$. A similar conclusion is reached for Pb from the T_1 results of Dickson (private communication, reference[19]) which suggest that there is a substantial ($\sim 25\%$ K_s) negative core-polarisation contribution to the ^{207}Pb Knight shift. There seems little doubt, then, that the good agreement for the Cs row of the

Periodic table is, to a certain extent, fortuitous although the results are definitely of the right order.

The effect of negative core-polarisation contributions in upsetting the agreement may, to a certain degree, be offset by a further effect; the core functions of Herman and Skillman are non-relativistic. This is undoubtedly important for the heavy elements; Tterlikkis et al.[20] have estimated the effect of relativistic corrections for Cs and Rb for which the effect is to increase K by $\sim 30\%$ and $\sim 7\%$ respectively. For the Rb row this effect can most certainly be neglected, but it must be included in a rigorous calculation for metals in the Cs row. Thus, it seems that the results in table 4.2 for the Rb row may be fairly reliable ($\pm 20\%$) whereas the agreement obtained for the Cs row seems to be the result of a happy accident in the balance of core-polarisation and relativistic effects.

A third source of uncertainty is introduced by the use of Silverstein susceptibilities. Alternative values for the susceptibility of an interacting electron gas are available (Rice[21]) but the differences are not significant for the present purpose. Throughout the calculations the values taken from Silverstein[17] have been used consistently, since it is thought that any differences between these and the true values will be similar for metals of all valences.

The essential conclusions remain, however, and the calculated results for the lighter elements show good agreement with the observed Knight shifts. It will be shown later (table 4.5) that the second term of eqn. 4.11 contributes only a small correction to the absolute value of K; at least for the heavier

metals considered. It is concluded that the free-electron theory seems to be adequate to explain the magnitudes of Knight shifts in metals.

4.04 The temperature dependence of Knight shifts in liquid metals

4.04.1 General considerations Measurements of the temperature coefficient of the Knight shift have been reported for a number of liquid metals (though no results are yet available for liquid transition metals). The results lie in the range $+2 \times 10^{-4}$ to -2×10^{-4} $(\text{kelvin})^{-1}$. After the initial investigations of the temperature dependence of K in alkali metals it was reasonably supposed that the change in K was entirely due to the effects of volume expansion; on $\rho(E_F)$ and thus χ_p through k_F, and on P_F through renormalisation. The effects on $\Omega\chi_p$ and on P_F were thought to act in opposite ways, $\Omega\chi_p$ increasing, and P_F decreasing as the metal expands. However, measurements on the pressure dependence of K (Benedek and Kushida[22]) showed an intrinsic temperature effect for solids that was comparable with the expansion effect.

They subsequently proposed[23] a model in which the intrinsic temperature dependence arose from the effect of lattice vibrations on P_F. They suggested that as the lattice vibrates, the electron wavefunction at each point adjusts instantaneously to the local strain i.e. P_F is a time varying function. In second order the average value of P_F varies linearly with the mean square local strain, the coefficient of the linear term being dependent on the form of the variation of P_F with volume. Moulson[24] evaluated this effect assuming P_F to be inversely proportional to volume for various polyvalent metals and found

no correlation with experiment whatsoever, for either the solid or liquid phases. It will be seen later that the alternative method of allowing for the effect of the vibrational motion of atoms on P_F, through the change in the structure factor with temperature, is more successful in accounting for observed temperature coefficients in the liquid phase.

It is easy to show that the intrinsic temperature dependence of χ_p is not important. Mott and Jones[25] show that χ_p at constant volume may be written as

$$\chi_p = \frac{3}{2} \frac{N_e \mu_B^2}{kT_F} \left[1 - \frac{\pi^2}{12} \left\{ \frac{T}{T_F} \right\}^2 \ldots\ldots \right]$$

where μ_B is the Bohr magneton, N_e the number of electrons per unit volume and T_F the Fermi temperature. As $T_F \sim 10^5$ kelvins for many of the metals being considered, this contribution to the temperature dependence of K is of order -0.6×10^{-7} (kelvin)$^{-1}$ at 600 kelvins. This figure is clearly negligible compared to the experimental values and need not be considered further. Similarly, the temperature dependence of χ_p arising from volume changes can be evaluated for a free-electron case.

$$\rho(E_F) \propto \left\{ \frac{1}{\Omega} \right\}^{\frac{1}{3}}$$

from which

$$\frac{1}{\rho} \frac{d\rho}{dT} = \frac{-1}{3} \frac{1}{\Omega} \frac{d\Omega}{dT}$$

This term has been evaluated for the 13 metals discussed previously and its effect is shown in table 4.3. Attention will now be concentrated on more recent methods of evaluating the temperature dependence of P_F.

4.04.2 <u>The temperature coefficient, and the change on melting, from the zero-order pseudopotential expression</u> Equation 4.14 of section 4.03.3 gave an expression

$$P_F = P_F^{(0)} + P_F^{(2)}$$

where the superscripts denote the zero-order and second-order terms in the displacements. Evaluation of this expression gave

$$\Omega P_F = \frac{|\gamma|^2}{1 - a\Omega^{-1}} \left[1 - \frac{bk_F^2}{\Omega - a} - ck_F^2 \right] \qquad 4.15$$

A temperature dependence of P_F will therefore occur both from the change in atomic volume, and from the subsequent change in the Fermi wave vector. The latter is related to the atomic volume through

$$k_F^2 = f\Omega^{-2/3}$$

where f is a constant. Thus

$$\frac{1}{\Omega P_F} \frac{d(\Omega P_F)}{d\Omega} = - \frac{(d/d\Omega)\{bf\Omega^{-2/3}(\Omega - a)^{-1} + cf\Omega^{-2/3}\}}{\{1 - bf\Omega^{-2/3}(\Omega - a)^{-1} - cf\Omega^{-2/3}\}}$$

$$- \frac{(d/d\Omega)\{1 - a\Omega^{-1}\}}{1 - a\Omega^{-1}} \qquad 4.16$$

and

$$\frac{1}{\Omega P_F} \frac{d(\Omega P_F)}{dT} = \frac{1}{\Omega} \frac{d\Omega}{dT} \left[\frac{(1/3)bk_F^2(5\Omega - 2a)(\Omega - a)^{-2} + (2/3)ck_F^2}{1 - bk_F^2(\Omega - a)^{-1} - ck_F^2} \right.$$

$$\left. - a(\Omega - a)^{-1} \right] \qquad 4.17$$

The contribution to the temperature coefficient of K from this expression has been calculated for the 13 liquid metals listed in table 4.2. The values of $(1/\Omega)(d\Omega/dT)$ which

are the volume expansion coefficients, were mostly taken from Smithells[26] (but for Au see Wise[27], and for Rb see Hackspill [28]). The results, together with the contribution from the volume dependence of χ_p, are given in table 4.3, which also includes a comparison with the observed temperature dependence.

It is clear from table 4.3 that the dominant effect is that due to the volume dependence of χ_p. This term is always negative (because the metals chosen expand on heating) and thus the predicted temperature coefficient is always negative. The calculated results have the wrong sign for Na, Rb and Cd. It is concluded that the zero-order pseudopotential term does not provide an important contribution to the temperature coefficient, and that the first-order pseudopotential term must provide an important effect.

From eqn. 4.16 it is possible to deduce the fractional change of (ΩP_F) on melting, and hence, adding a term for the change in χ_p with volume, to estimate the change of K. The results are contained in table 4.4. Again the dominant effect is the change of the spin susceptibility with volume. The agreement with the observed changes is not good - for In, Sn, Cs and Pb the wrong sign is obtained - and once more it is suggested that the contribution from the term to first-order in the pseudopotential is important. This term, however, has not been evaluated in the present work. The anomalously large observed changes in Cd and Bi have been discussed in the introduction. It is concluded there, that free-electron based spin susceptibilities are not an adequate description of these metals in the solid phase.

Table 4.3

The temperature coefficient of the Knight shift to zero-order in the pseudopotential *

Metal	$\frac{1}{\Omega P_F}\frac{d(\Omega P_F)}{dT}$ §	$\frac{1}{\chi_p}\frac{d\chi_p}{dT}$	$\frac{1}{K}\left(\frac{dK}{dT}\right)_{calc.}$	$\frac{1}{K}\left(\frac{dK}{dT}\right)_{obs.}$
Na	+0.35	-1.06	-0.71	+1.60 (b)
Rb	-0.37	-1.10	-1.47	+1.74 (b)
Ag	-0.11	-0.32	-0.43	-
Cd	-0.10	-0.50	-0.60	+0.50 (c)
In	-0.02	-0.37	-0.39	-1.03 (e)
Sn	+0.02	-0.33	-0.31	-0.10 (a)
Sb	+0.38	-0.31	+0.07	+0.70 (a)
Cs	-0.93	-1.80	-2.73	-3.10 (b)
Au	-0.21	-0.34	-0.55	-
Hg	-0.17	-0.62	-0.79	-1.45 (a)
Tl	-0.03	-0.44	-0.47	-1.70 (a)
Pb	-0.01	-0.40	-0.41	-0.67 (d)
Bi	+0.03	-0.44	-0.41	-0.90 (a)

* All values are given x 10^4 (kelvin)$^{-1}$.

(a) Moulson[24].

(b) Gutowsky and McGarvey, J. Chem. Phys., 21, (1953), 2114.

(c) Styles (private communication).

(d) Present work.

(e) Styles[c]. The value given by Flynn et al., Proc. Phys. Soc., 76, (1960), 301 appears to be incorrect.

Table 4.4

The change in the Knight shift on melting

Metal	$\frac{\Delta(\Omega P_F)}{\Omega P_F}(\%)$ §	$\frac{\Delta \chi_p}{\chi_p}(\%)$ §	$\left\{\frac{\Delta K}{K}\right\}_{calc.}(\%)$ §	$\left\{\frac{\Delta K}{K}\right\}_{obs.}(\%)$ *
Na	+0.3	+1.2	+1.5	+2.2
Rb	+0.4	+1.2	+1.6	+1.2
Ag	+1.1	+3.0	+4.1	(c)
Cd	0.0	+2.3	+2.3	+33(+1)
In	0.0	+0.1	+0.1	-4(±6)
Sn	-0.1	+1.4	+1.53	-2.7
Sb	-0.1	+0.7	+0.86	(a)
Cs	+0.2	+0.45	+0.65	-2.1
Au	$+0.20\frac{\Delta\Omega}{\Omega}$	$+0.33\frac{\Delta\Omega}{\Omega}$	$+0.53\frac{\Delta\Omega}{\Omega}$	(c)
Hg	$+0.09\frac{\Delta\Omega}{\Omega}$	$+0.33\frac{\Delta\Omega}{\Omega}$	$+0.42\frac{\Delta\Omega}{\Omega}$	-1(±2)
Tl	+0.1	+1.35	+1.45	0(±1)
Pb	0.0	+1.5	+1.5	-0.7(±0.4)
Bi	+0.3	-1.0	-0.7	-210 (b)

* Values taken from Drain, Met. Rev. 119, (1967).

(a) No shift measurements are available for the solid.

(b) Knight shift in the solid is small and negative.

(c) No shift measurements are available for the liquid.

§ The signs of quantities in these columns should be changed.

4.04.3 The temperature coefficient from the first-order pseudopotential term So far, attention has been concentrated on the first term of eqn. 4.11 for P_F (and its modification when the plane wave representing the conduction electron is not constant over the ion core). The effect of the second term will now be discussed. The explicit form of this term, involving the introduction of the pseudopotential to first order, was deduced by Watabe and Tanaka[11] and Faber[2]. The derivation will be sketched.

From first-order perturbation theory the wavefunction can be written[29]

$$\varphi_N = \varphi_N^0 + \sum_r{}' \left[\frac{V_{rN}}{E_N^0 - E_r^0} \varphi_r^0 \right]$$

where the prime means $r \neq N$ (to avoid a singularity) and $V_{rN} = \langle r|V|N\rangle$. The matrix element of the perturbing potential in this case can be written[30]

$$\langle k|u|k'\rangle = u(\underline{K})\rho(\underline{K})$$

where $\underline{K} = \underline{k} - \underline{k}'$ and thus

$$\varphi_{\underline{k}}^1 = \frac{\Omega}{(2\pi)^3} \int d\underline{K} \, \frac{u(\underline{K})\rho(\underline{K})}{(E_{\underline{k}} - E_{\underline{k}-\underline{K}})} \varphi_{\underline{k}-\underline{K}}^0$$

By substituting a single plane wave for the zero-order wavefunction the ratio $\varphi_{k_F}^1(\underline{R}_i)/\varphi_{k_F}^0(R_i)$ is obtained as

$$\frac{\varphi_{k_F}^1(\underline{R}_i)}{\varphi_{k_F}^0(\underline{R}_i)} = \frac{\Omega}{(2\pi)^3} \int d\underline{K} \, \frac{u(\underline{K})\rho(\underline{K})}{(E_{\underline{k}} - E_{\underline{k}-\underline{K}})} \exp\left[-i(\underline{K}.\underline{R}_i)\right]$$

and the ratio $P_F^{(1)}/P_F^{(0)}$ can be determined. The final expression is deduced by taking the principal value of the integral (to avoid

the singularity) over a spherical Fermi surface. The resulting expression after ensemble averaging is

$$\frac{P_F^{(1)}}{P_F^{(0)}} = \left\{\frac{-6m}{\hbar^2 k_F^2}\right\}\int_0^\infty d\left(\frac{K}{2k_F}\right)\frac{K}{2k_F}\ln\left|\frac{K+2k_F}{K-2k_F}\right| u(K)\ N.a(K)$$

and $P_F = P_F^{(0)}\left(1 + \frac{P_F^{(1)}}{P_F^{(0)}}\right)$ which in the formalism of Faber can be written

$$\Omega P_F \propto \left(1 + 2Z\int_0^\infty \left[a(K) - 1\right] h(K)\ \frac{K}{2k_F}\ln\left|\frac{K+2k_F}{K-2k_F}\right| d\left(\frac{K}{2k_F}\right)\right) \quad 4.17$$

where $h(K) = u(K)/u(0)$, $u(K)$ and $a(K)$ the Fourier transforms of the pseudopotential of an ion and of the atomic pair distribution function respectively, and Z the valence. The derivation has, of course, been carried through assuming that the electron wave-function is constant over an ion core. As discussed above, this involves an error of approximately 10% in $P_F^{(0)}$, omits a small temperature dependence of $P_F^{(0)}$ and also introduces a small error into $P_F^{(1)}$. The derivation of the exact form of $P_F^{(1)}$ has not been performed because the accuracy of the functions $a(K)$ and $u(K)$ does not warrant it.

Equation 4.17 gives

$$\frac{\Delta(\Omega P_F)}{\Omega P_F} = \frac{\Delta K}{K} = \frac{\Delta\epsilon}{1+\epsilon} \quad \text{say,}$$

where $$\epsilon = 2Z\int d\left(\frac{K}{2k_F}\right) h(K)\left[a(K) - 1\right]\frac{K}{2k_F}\ln\left|\frac{K+2k_F}{K-2k_F}\right| \quad 4.18$$

For first-order perturbation theory to be valid $\epsilon \ll 1$ 4.19

and thus

$$\frac{1}{K}\frac{dK}{dT} = \frac{d\epsilon}{dT} \quad 4.20$$

The eqn. 4.20 has been evaluated for a number of

liquid metals. (Since the labour involved is considerably greater than in evaluation of the zero-order expression, the number of metals is less than in table 4.2. However at least one metal of each valence from 1 → 5 is included.) In all cases the pseudopotential used was the model potential of Heine et al.[13]; the damped form being preferred. For structure factors there is a choice between experimental values (in some cases) and those calculated from the model of Ashcroft and Lekner[31]; both were in fact used. In order that any effect of changing valence (operating through k_F) might be displayed, calculations were performed for Na, Cd, In, Sn and Bi using structure factors obtained in a consistent fashion from the model. By way of illustration, the calculation of the temperature coefficient for liquid indium will be detailed; the results in this case are more complete.

For indium the structure factor is available experimentally[32] at 443 K and 923 K and eqn. 4.20 has been evaluated for these temperatures. In addition to a structure factor change, the pseudopotential was allowed to be temperature dependent through the change in scale caused by the change in k_F, and this change was also included in the logarithmic factor. Numerical integration, using Simpson's rule yielded a value of $-2.6_0 \times 10^{-4}$ $(\text{kelvin})^{-1}$. This calculation was repeated using two Ashcroft-Lekner structure factors at 443 K and 923 K. To do this packing densities of 0.45 and 0.38, and hard sphere diameters (calculated on the basis of the observed nearest neighbour distances[32]) of 2.86×10^{-10} m and 2.75×10^{-10} m respectively, were used. Again the change in k_F was incorporated and a value of $-1.4_0 \times 10^{-4}$ $(\text{kelvin})^{-1}$ was obtained. These results give an estimate of the uncertainty in the temperature coefficient due to lack of precise

knowledge of a(K) and both compare reasonably with the observed value of $-1.0_3 \times 10^{-4}$ (kelvin)$^{-1}$. These estimates assumed that eqn. 4.19 was obeyed, and this assumption was carefully checked for all the calculated temperature coefficients.

Table 4.5 contains the results for all the calculations and comparison with experiments made. A number of points can be deduced: firstly, the value of ϵ is always less than unity and for In, Sn, Pb and Bi considerably so. Secondly the calculated temperature coefficients are now of the right order, and generally the right sign, to explain the experimental results. It is interesting to note that although this first-order pseudopotential term represents only a small part of the Knight shift, at any rate for metals of higher valence, it is responsible for the greater part of the temperature coefficient. Thirdly, only in the case of bismuth is the discrepancy between theory and experiment really marked. That the magnitude of ϵ is still small in this case suggests that the fault may lie with the structure factor. Fourthly, from column 3 of table 4.5, a systematic variation of $(1/\Omega P_F)\ (d\Omega P_F/dT)$ with valence seems to occur. This may well be due to the variation of the point $h(K) = 0$ with valence but with the present uncertainties in both u(K) and a(K) it is not possible to quantitatively account for this trend. Finally, the two results for indium emphasise how important the structure factor is to this calculation and suggest that, at present, agreement within a factor of two is perhaps all that can be expected.

The expression 4.17 has been extended by Faber to include a term that depends on the lifetime of an electron in a free-electron travelling wave state. This means that the term

Table 4.5

The temperature coefficient of the Knight shift § to first-order in the pseudopotential

Metal	ϵ	$\frac{1}{\Omega P_F}\frac{d(\Omega P_F)}{dT}$	$\frac{1}{\chi_p}\frac{d\chi_p}{dT}$	$\frac{1}{K}\left(\frac{dK}{dT}\right)_{calc.}$	$\frac{1}{K}\left(\frac{dK}{dT}\right)_{obs.}$
Na	$-0.47^{\dagger}$	$+3.3_0$	-1.0_6	$+2.2_4$	$+1.6_0$
Cd	$-0.45^{\dagger}$	$+1.4_0$	-0.4_5	$+0.9_5$	$+0.5_5$
In	-0.12^{*}	-2.6_0	-0.3_7	-2.9_7	-1.0_3
In	$-0.17^{\dagger}$	-1.4_0	-0.3_7	-1.7_7	-1.0_3
Sn	$-0.16^{\dagger}$	$+0.1_7$	-0.3_3	-0.1_6	-0.1_8
Pb	-0.03^{*}	$+0.1_9$	-0.4_0	-0.2_1	-0.6_7
Bi	$-0.09^{\dagger}$	$+1.0_5$	-0.4_4	$+0.6_7$	-0.9_0

† Calculated using Ashcroft - Lekner a(K).

* Calculated using the observed a(K).

§ All values quoted are x 10^4 (kelvin)$^{-1}$.

$\ln \left| \frac{K + 2k_F}{K - 2k_F} \right|$ should be replaced by

$$\tfrac{1}{2}\ln \left| \frac{(K + 2k_F)^2 + m^2/4h^2\tau^2 K^2}{(K - 2k_F)^2 + m^2/4h^2\tau^2 K^2} \right|$$

where τ is the lifetime. This sophistication is not warranted with the presently available structure factors.

4.05 Conclusions

The linewidth of ^{207}Pb exhibits a narrowing at ~ 500 K which has been explained by motional narrowing of the pseudo- and classical dipolar contributions to the width. The magnitude of the pseudo-dipolar contribution has been shown to be consistent with that reported in the literature.

It has been established that the Knight shift of both liquid and solid metals can be calculated by a single O.P.W. method with a pseudopotential that is zero. The results agree, within the uncertainty of the spin susceptibility and core - polarisation Knight shift, with the observed values for light elements. For heavier elements, relativistic effects are important and good correlation between theory and experiment is only to be expected when relativistic core functions become available. The temperature coefficients calculated from this zero-order pseudopotential method show no agreement with the observed results both as regards sign and magnitude.

The term to first-order in the pseudopotential has been shown (at least for the heavier elements) to produce only a small correction to the absolute value of K but a large contribution to

the temperature dependence. An exact calculation of the temperature coefficient of K awaits more precise radial distribution functions for the liquid state, when first-order calculations should provide a good description of the experimental results.

References

(1) Holland B. W., Phys. Stat. Solidi, 28, (1968), 121.

(2) Faber T. E., Adv. in Phys., 16, (1967), 637.

(3) Van Vleck J. H., Phys. Rev., 74, (1948), 1168.

(4) Andrew E. R., Nuc. Mag. Res., (1958), 105.

(5) Rowland T. J., Prog. in Mat. Sci., 9, (1961), 45.

(6) Froidevaux C. and Alloul H., Phys. Rev., 163, (1967), 324.

(7) Snodgrass R. J. and Bennett L. H., Phys. Rev., 132, (1963), 1465.

(8) Asayama K. and Itoh J., J. Phys. Soc. Japan, 17, (1962), 1065.

(9) Nachtrieb N. H., J. Chem. Phys., 20, (1952), 1185.

(10) Blandin A., Daniel E., and Friedel J., Phil. Mag., 4, (1959), 180.

(11) Watabe M. and Tanaka W., Phil. Mag., 12, (1965), 347.

(12) Watson R. E., Freeman A. J. and Bennett L. H., Phys. Rev. Letts., 20, (1968), 653.

(13) Heine V. and Animalu A. O. E., Phil. Mag., 12, (1965), 1249.

(14) Tubis A., Phys. Rev., 102, (1956), 1049.

(15) Heighway J., Seymour E. F. W. and Styles G. A., XV Colloque Ampère, Grenoble, (1968).

(16) Herman F. and Skillman S., Atomic Structure Calc., (Prentice-Hall, 1963).

(17) Silverstein D., Phys. Rev., 130, (1963), 912.

(18) Mahanti S. D., Ph.D. Thesis, Riverside, (1968).

(19) Dickson E. M., Ph.D. Thesis, Berkeley, (1968).

(20) Tterlikkis L., Mahanti S. D. and Das T. P., (to be published).

(21) Rice T. M., Ann. Phys., 31, (1965), 100.

(22) Benedek C. B. and Kushida T., J. Phys. Chem., 21, (1953), 2114.

(23) Benedek C. B. and Kushida T., J. Phys. Chem. Sol., 5, (1958), 241.

(24) Moulson D., Ph.D. Thesis, Leeds, (1966).

(25) Mott N. F. and Jones H., Theory of the properties of metals and alloys, (C.U.P., 1936), 186.

(26) Smithells C. J., Met. Ref. Book, (Butterworths, 1967), 688.

(27) Wise E. M., Gold, (Van Nostrand, 1964), 74.

(28) Hackspill L., C.R.D. l'Acad. des Sciences, 152, (1911), 259.

(29) Mandl F., Quantum Mechanics, (Butterworths, 1957), 133

(30) Ziman J. M., Phil. Mag., 6, (1961), 1017.

(31) Ashcroft N. W. and Lekner J., Phys. Rev., 145, (1966), 83.

(32) Ocken H. and Wagner C. N. J., Phys. Rev., 149, (1966), 122.

CHAPTER FIVE

DISCUSSION OF THE OBSERVATIONS FOR LIQUID ALLOYS

5.01 Introduction

This discussion of the results for liquid alloys concerns, mainly, the variation of the ^{207}Pb Knight shift with solute concentration in a series of dilute binary liquid alloys. Firstly, however, the subsidiary topic of the ^{207}Pb linewidth in two distinct alloys —Pb - 18% Bi and Pb - 20% Tl — will be briefly considered. Discussion of the temperature dependence of the ^{207}Pb Knight shift in these alloys (in both the solid and liquid phases) is left until section 5.05, and the far more detailed investigation of the complete Pb - Bi system is deferred until Chapter 6.

There are a number of contributions to the change in the Knight shift on alloying which must be combined to give a complete description. In the past, different authors have considered different contributions to be the dominant one. For instance, Young[1] has discussed the variation of K in liquid alkali-alkali alloys solely in terms of changes in P_F. His agreement with experiment was very good. On the other hand, Kaeck[2] and Holcomb (private communication) obtain as good agreement with experiment in these systems by neglecting changes in P_F and considering only changes in $\rho(E_F)$, through volume effects. A true explanation ought only to be possible by considering both effects but, when this is done, poor agreement with experiment is obtained. The situation is not at all clear and in the present work both effects have been included. In Chapter 1,

the free-electron model was shown to be reasonably successful in describing the physical properties of many pure metals. This was further substantiated in Chapter 4, and it seems sensible to begin a full discussion of Knight shifts in liquid alloys using the free-electron approach - section 5.03.1 contains this discussion. The Holland[3] scheme, extended to second-order in the displacements (section 4.03.3), is discussed in section 5.03.2. Up to this point the calculation assumes an homogeneous effect on alloying, hereafter the local redistribution of charge is considered as screening the perturbing potential. Thus, the applicability of the nearly-free-electron theory of Faber[4], the first-order pseudopotential model, is considered in section 5.03.3 and in section 5.03.4 the analogous scattering theory of Friedel et al.[5, 6, 7] is discussed. For the purposes of these discussions the Knight shift will everywhere be considered to be that due solely to the hyperfine contact interaction; it is not possible to make quantitative estimates of the variation of other contributions on alloying. In view of the fact that the core-polarisation contribution to K can contain counterbalancing parts (see section 1.04.2) it is clear that the alloy dependence of this component will not simply follow that of the s-state contact part. Since the orbital contribution contains a summation over all filled and unfilled states in the band it is much less likely to be sensitive to small changes in the Fermi level.

5.02 ^{207}Pb linewidth in Pb - 18% Bi and Pb - 20% Tl

The observations considered in this section were made in conjunction with the Knight shift temperature dependence and will be discussed only briefly. Snodgrass and Bennett[8] have

reported a marked increase in the ^{207}Pb linewidth with increasing solute concentration for lead solid solutions at room temperature. The present observations (fig. 3.14) confirm this effect. No explanation of this increase in width was given by Snodgrass and a qualitative explanation only is offered. An estimate, from the observed (1/K)(dK/dc), of inhomogeneous Knight shift broadening (following Blandin and Daniel[6]) shows that this contribution should be quite negligible; for the solute bismuth this contribution is only 0.1×10^{-4} tesla. It is suggested that the addition of impurities (particularly heavy impurities) introduces a large pseudo-exchange and pseudo-dipolar interaction. As the temperature is increased motional narrowing of these interactions occurs since both depend on the magnitude of the internuclear vector. The observed width in the liquid is consistent, within experimental uncertainty, with that expected on the basis of spin-lattice relaxation deduced from the Korringa relation (see table 5.1).

Table 5.1

Comparison of the ^{207}Pb linewidths at 625 K

	100% Pb	Pb - 18% Bi	Pb - 20% Tl
$\Delta B_{obs.}$	5.0(±0.6)	4.7(±0.3)	5.3(±0.5)
$\Delta B^{*}_{calc.}$	4.7	4.9	4.4

* Evaluated from the Korringa relation using the observed values of K for the alloys. All values are x 10^{4} (tesla).

5.03 The variation of the ^{207}Pb Knight shift with solute concentration

5.03.1 Volume and electron/atom ratio effects In the free-electron model the potential is everywhere considered to be constant and the well known quadratic E-k relation applies. The density of states is then related to the Fermi energy through

$$\rho(E_F) = \frac{3}{2}\frac{\bar{Z}}{\Omega E_F} \qquad 5.1$$

where $\bar{Z}$ is the mean number of electrons per atomic volume Ω. The Fermi energy is given by

$$E_F = \frac{\hbar^2}{2m}\left\{\frac{3\pi^2\bar{Z}}{\Omega}\right\}^{2/3} \qquad 5.2$$

In this approach to alloy theory it is assumed that each atom gives all its valence electrons to the free-electron gas and that the only effect of adding an impurity is to alter the volume of the metal and the number of electrons per atomic volume; i.e. as the concentration changes the electron/atom ratio alters linearly (except when solute and solvent valences are the same).

It was stated earlier that the Knight shift due to the contact hyperfine interaction can be written

$$K \propto \Omega P_F \rho(E_F). \qquad 5.3$$

Since P_F is normalised within Ω the predicted change in K arises only from the change in $\rho(E_F)$ and from eqn. 5.1

$$K \propto \left\{\frac{\bar{Z}}{\Omega}\right\}^{1/3}$$

Thus

$$\frac{1}{K}\frac{dK}{dc} = \frac{1}{3}\frac{1}{\bar{Z}}\frac{d\bar{Z}}{dc} - \frac{1}{3}\frac{1}{\Omega}\frac{d\Omega}{dc} \qquad 5.4$$

where c is the solute concentration.

Using $Z = Z_0(1 - c) + Z_1 c$ this reduces to

$$\frac{1}{K}\frac{dK}{dc} = \frac{1}{3}\left\{\frac{Z_1 - Z_0}{Z_0}\right\} - \frac{1}{3}\frac{1}{\Omega}\frac{d\Omega}{dc} \qquad 5.5$$

where Z indicates the valence and the subscripts '0' and '1' refer to solvent and solute respectively.

Equation 5.5 has been evaluated for ^{207}Pb with various solutes and the results are given in table 5.2. To do this it is necessary to evaluate the expression $(1/\Omega)(d\Omega/dc)$, and as this has only been determined for a limited number of liquid alloys[9] a consistent way of calculating it has been used instead. The calculated result is based on the validity of Vegards law (see, for example, reference[9]) which relates the density of a binary alloy to the densities of its pure components:

$$d_{alloy} = d_0(1 - c) + d_1 c$$

where d_0 and d_1 are the densities of the solvent and solute respectively. Observations of liquid alloy densities show only small deviations from this law. The calculated results are compared with experiment in table 5.6, column 1. What is calculated here is an effect that changes K at each and every nucleus by the same amount. No intrinsic change in P_F has been considered at this point and this must be done before any comparison with experiment can be made.

5.03.2 Changes in P_F — to zero-order in the pseudopotential

A further effect of alloying, that is uniform over the whole of the sample, arises from the change in k_F due to changes in volume and electron/atom ratio. These, in turn, affect the values of the overlap integrals discussed in 4.03.3. Using eqn. 4.15.

Table 5.2

Γ calculated from the free-electron model

Solute	Z_1	$\frac{1}{3}\frac{(Z_1 - Z_0)}{Z_0}$	$-\frac{1}{3}\frac{1}{\Omega}\frac{d\Omega}{dc}$	Total
Ag	1	-0.25_0	$+0.12_0$	-0.13_0
Cd	2	-0.16_7	$+0.07_1$	-0.09_6
In	3	-0.08_3	$+0.03_7$	-0.04_6
Sn	4	0.00_0	$+0.03_1$	$+0.03_1$
Sb	5	$+0.08_3$	$+0.00_7$	$+0.09_0$
Au	1	-0.25_0	$+0.22_0$	-0.03_0
Hg	2	-0.16_7	$+0.10_2$	-0.06_5
Tl	3	-0.08_3	$+0.02_7$	-0.05_6
Bi	5	$+0.08_3$	-0.01_5	$+0.06_8$

$$\Omega P_F = \frac{|\gamma|^2}{(1 - a\Omega^{-1})}\left[1 - \frac{bk_F^2}{\Omega - a} - ck_F^2\right]$$

$$= \frac{|\gamma|^2}{(1 - a\Omega^{-1})}\{\Lambda\}$$

it is possible to derive an expression for the change in ΩP_F on alloying, if a spherical Fermi surface is assumed. By writing

$$\frac{1}{\Omega P_F}\frac{\partial(\Omega P_F)}{\partial c} = \frac{1}{\Omega P_F}\frac{\partial(\Omega P_F)}{\partial \bar{Z}}\cdot\frac{\partial \bar{Z}}{\partial c} + \frac{1}{\Omega P_F}\frac{\partial(\Omega P_F)}{\partial \Omega}\cdot\frac{\partial \Omega}{\partial c}$$

the variation of P_F with alloying can be derived directly from

eqn. 4.15. Hence

$$\frac{1}{\Omega P_F}\frac{\partial(\Omega P_F)}{\partial \bar{Z}} = -\frac{2}{3}\frac{k_F^2}{Z_0}\left[\frac{b}{\Omega - a} + c\right]\Big/\{\Lambda\}$$

$$\equiv \frac{1}{Z_0} A$$

and

$$\frac{1}{\Omega P_F}\frac{\partial(\Omega P_F)}{\partial \Omega} = \frac{1}{3}\frac{k_F^2}{\Omega}\left[\frac{b(5\Omega - 2a)}{(\Omega - a)^2} + 2c\right]\Big/\{\Lambda\} - \frac{1}{\Omega}\frac{a}{(\Omega - a)}$$

$$\equiv \frac{1}{\Omega} B$$

Thus

$$\frac{1}{\Omega P_F}\frac{\partial(\Omega P_F)}{\partial c} = \frac{1}{Z_0}\frac{\partial \bar{Z}}{\partial c}.A + \frac{1}{\Omega}\frac{\partial \Omega}{\partial c}.B \qquad 5.6$$

This expression has been evaluated for ^{207}Pb with the same solutes as in section 5.03.1 and the results are given in table 5.3. Again the total calculated results appear in table 5.6, column 2, for comparison with experiment.

5.03.3 Changes in P_F — to first-order in the pseudopotential

In addition to the homogeneous effects discussed so far, must be added the effects of local changes in the electron density due to screening of solute ions. In view of the reasonable success obtained in explaining the temperature dependence of K in liquid metals using the pseudopotential as a first-order perturbation, it is attractive, and logical, to apply this theory to alloying.

Indeed, Faber[4] has shown how this scheme can be extended to a discussion of liquid alloys. The problems involved in a complete, generally applicable theory are severe, and the original model was only valid for "substitutional" alloys —

Table 5.3

Γ calculated to second-order in the displacements

Solute	Z_1	A	B	$\frac{1}{Z_0}\frac{\partial \bar{Z}}{\partial c}.A$	$\frac{1}{\Omega}\frac{\partial \Omega}{\partial c}.B$	Total
Ag	1	-0.06	-0.12	$+0.04_5$	$+0.04_3$	$+0.08_8$
Cd	2	-0.08	-0.06	$+0.04_0$	$+0.01_3$	$+0.05_3$
In	3	-0.09	-0.01	$+0.02_3$	$+0.00_1$	$+0.02_4$
Sn	4	-0.11	+0.02	0.00_0	-0.00_2	-0.00_2
Sb	5	-0.11	+0.04	-0.02_8	-0.00_1	-0.02_9
Au	1	-0.06	-0.20	$+0.04_5$	$+0.13_2$	$+0.17_7$
Hg	2	-0.08	-0.07	$+0.04_0$	$+0.02_2$	$+0.06_2$
Tl	3	-0.10	-0.02	$+0.02_5$	$+0.00_2$	$+0.02_7$
Bi	5	-0.10	+0.01	-0.02_5	0.00_0	-0.02_5

equi-valent and with atomic volume independent of concentration. For most liquid alloys (even if equi-valent) the mean atomic volume is not independent of concentration (see last section) and the substitutional model is not valid. However, small dilatations have been treated; initially for a discussion of the resistivity[10] but extension to the Knight shift was relatively straightforward. Equation 4.17 gave the result of the Faber treatment of K for a pure metal.

$$K \propto 1 + 2Z\left\{\frac{M}{M^*}\right\}\int_0^\infty \left[a(K) - 1\right]\frac{U(K)}{U(0)}.\frac{K}{2k_F}.\ln\left|\frac{K + 2k_F}{K - 2k_F}\right| d\left(\frac{K}{2k_F}\right).$$

For a substitutional alloy the expression for the change of solvent Knight shift on alloying is

$$\Gamma = \frac{2Z_0(M/M^*)}{(1 + 2\epsilon)} \int_0^\infty [a(K) - 1] \left[\frac{U_1(K) - U_0(K)}{U_0(0)}\right] \frac{K}{2k_F} \ln\left|\frac{K + 2k_F}{K - 2k_F}\right| d\left(\frac{K}{2k_F}\right)$$

where changes in wavefunction only have been included. 5.7

This expression is valid for equi-valent alloys where the atomic volume and the structure factor are independent of solute concentration c. The subscripts '0' and '1' again refer to solvent and solute respectively.

The extension of this scheme to include non-substitutional alloys has been discussed by Halder[11]. He derived an expression for Γ with dilatation effects included and obtained

$$\Gamma = \frac{2(M/M^*)}{(1 + 2\epsilon)} \int_0^\infty [a'(K) - 1] \left[Z_1 \frac{U_1'(K)}{U_1(0)} - Z_0 \frac{U_0(K)}{U_0(0)}\right] \times \frac{K}{2k_F} \ln\left|\frac{K + 2k_F}{K - 2k_F}\right| d\left(\frac{K}{2k_F}\right) \quad 5.8$$

where $a'(K) = a(K) - \delta F(K)$ and $U_1'(K) = U_1(K) - U_0(K)\delta F(K)$. The function $F(K)$ was discussed by Faber[10] and is unity at $K = 0$ falling rapidly to zero near to $K = 2k_F$ with small oscillations about the zero. The factor δ represents the dilatation produced and is defined as $(V' - V)/V$ where V' is the alloy volume with one solute atom replacing one solvent atom, and V is the volume of the pure solvent.

This attempt to generalise the Faber approach is not entirely satisfactory. A full generalisation would involve the introduction of partial structure factors (rather than merely using a dilatation correction) together with energy dependent

pseudopotentials. After all, $U_1(K)$ ought to be associated with a different structure factor than $U_0(K)$. In general, however, measured partial structure factors are not available and results based on the calculations of Ashcroft and Langreth[12] would have to be used. Since the only features of the atoms that can be incorporated are the hard sphere diameters, the model may not be sufficiently refined, and in view of the importance of the function $a(K)$ to the value of the integral (see Chapter 4) any calculations of Γ based on approximations such as eqn. 5.8 must be viewed with scepticism.

In addition, the pseudopotentials available in the literature (Animalu and Heine[13]) have been shown by Heine et al.[14] to be uncertain by up to 30% in the range $k_F < K < 2k_F$. This is doubly unfortunate for the equi-valent systems because firstly, this region is important to the integral and secondly, the process of subtraction of the solute and solvent pseudopotentials magnifies the resulting uncertainty. For hetero-valent systems the further complication of the energy dependence of the derived potentials is introduced. This difficulty may again be magnified by the process of subtraction.

The calculations in alloys are thus very complicated in comparison to those of pure metals, and the bases from which they start are considerably less certain. In fact, equations 5.7 and 5.8 have been used to discuss liquid alloy Knight shifts, but at present the uncertainty in the results makes the efforts involved in computation (on the basis of such a refined theory) of little value. This is illustrated quite markedly by the general lack of quantitative agreement between observed results and those calculated using this approach. An apparent exception

is the case of sodium alloys. Kellington and Titman[15] have interpreted their results for ^{23}Na in dilute alloys with Cs, Hg, Cd, Tl and Pb using this method. The agreement is qualitatively excellent in that Γ changes sign on going from Cs to Hg and Cd alloys, but quantitatively the discrepancy is of order 3/2. They conclude that this is very reasonable agreement in view of the approximations involved. Two points arise: firstly, no account was taken in the structure factor for deviations from substitutional behaviour and secondly, no account was taken of changes in χ_p. Inclusion of this latter effect might act to considerably worsen the overall agreement with experiment. Despite these omissions, the agreement obtained for these monovalent base liquid alloys is considerably better than that obtained by Halder[11] and Moulson[16] on polyvalent base systems. For the systems In - Tl, Pb - Sn, Hg - In and Ga - In, Halder obtained predictions that were always of the same sign as the observed variations but quantitatively the agreement was very poor. In In - Tl the estimated changes were an order of magnitude too small whilst in Ga - In theory predicted a result five times too large. In no case was the observed curvature reproduced. Moulson used eqn. 5.7 to discuss a whole series of equi-valent alloys and again obtained qualitatively correct variations but, also again, quantitative agreement was poor. He illustrated very well the uncertainty involved in the use of total structure factors; by taking a(K) from two different sources he obtained results that differed appreciably from one another, even to the extent of a sign change. It must be concluded that for Knight shift calculations (at least for equi-valent systems) the structure factor is not sufficiently well known at the present time.

For hetero-valent systems the most important contribution to the integral of eqn. 5.8 comes from the low K region. This means that the predicted value of Γ is rather less sensitive, than is the case for equi-valent systems, to the detail of either U(K) or a(K). Inspection of eqn. 5.8 shows that if the value of the integrand is negligibly small except for K = 0 the expression tends to a value

$$Z_0 \frac{U_0(K)}{U_0(0)} - Z_1 \frac{U_1'(K)}{U_1(0)}$$

i.e. $\Gamma \propto (Z_0 - Z_1)$

In effect, this suggests that the core structures are not strong enough to break down the valence dependence, and any period effect (from different rows of the periodic table) is therefore expected to be slight. Further, because the low K region describes the effect of the outer core region, it suggests that both the pseudopotential approach and the scattering approach (see section 5.03.4) ought to give similar results. We have seen above that all that might be expected from the pseudopotential approach (at the present time) is qualitative agreement with experiment, and for this reason the admittedly coarser theory of Friedel et al.[5, 6,7] will be used to discuss the Knight shift variation in liquid lead base alloys.

5.03.4 Changes in P_F - the Friedel model This approach again uses a nearly-free-electron model to investigate the screening of impurities and has been used by a number of authors to discuss the change in P_F on alloying, particularly for monovalent solvents. Only a brief résumé of the theory will be given here.

Friedel et al.[5,6,7] proposed that an impurity atom in an alloy could be represented by a spherically symmetric square potential well which acts to scatter conduction electrons. They showed that the conduction electron gas around an impurity becomes distorted; the distortion being in the form of oscillations of electron density. Although the majority of the screening charge is contained in the solute cell these oscillations extend to long range and affect the Knight shift of the surrounding nuclei. The effect of this screening of the impurity is such that the initial assumption of a square well perturbing potential is not as unreasonable as it may at first seem.

By analysing the incident and scattered wavefunctions into spherical components (introducing the phase shift η_l of the partial wave of angular momentum l) they were able to obtain an expression for the relative variation of the charge density associated with an electron of wave number k at a point $\underline{r}$, due to a single scatterer at the origin

$$\frac{\Delta\rho(\underline{r})}{\rho(\underline{r})} = \sum_l (2l + 1)\Big\{ \left[n_l^2(kr) - j_l^2(kr)\right] \sin^2\eta_l - j_l(kr)n_l(kr)\sin 2\eta_l \Big\} \qquad 5.9$$

where n_l and j_l are spherical Neumann and Bessel functions respectively. This is an oscillating function which at large values of r decreases as $1/r^2$.

It is readily shown that the change in shift of the j'th host nucleus (at $\underline{r} = \underline{R}_j$) is given by

$$\frac{\Delta K_j}{K} = \frac{\Delta\rho(\underline{R}_j)}{\rho} \qquad 5.10$$

evaluated for $k = k_F$. To obtain the average shift for all

solvent nuclei in an alloy (eqn. 5.10 represents a range of values) three assumptions are made:

(i) The alloy must be perfectly disordered.

(ii) Multiple scattering of Fermi surface electrons is completely neglected.

(iii) The excess electron density produced at any point by different solute ions can be added (this is valid for small concentrations of impurities).

Under these assumptions, the average change in shift is obtained by integrating over all possible values of $\underline{R}_j$:

$$\frac{\overline{\Delta K}}{K} = c \int \frac{\Delta\rho(\underline{r})}{\rho} P(r)\, d^3\underline{r} \qquad 5.11$$

Here $P(r)$ is the pair distribution function of the liquid defined so that the probability of finding a solvent atom between r and r + dr from a solute atom is $4\pi r^2 P(r)\, dr$.

Hence

$$\Gamma = \frac{1}{K}\frac{\overline{dK}}{dc} = \sum_{l=0}^{\infty} \{A_l \sin^2\eta_l + B_l \sin 2\eta_l\} \qquad 5.12$$

where $A_l = (2l + 1) \int [n_l^2(kr) - j_l^2(kr)]\, P(r)\, d^3\underline{r}$

and $B_l = -(2l + 1) \int n_l(kr)\, j_l(kr) P(r)\, d^3\underline{r}$.

Equation 5.12 has been used by many authors; it appears that phase shifts derived from a spherically symmetric square potential well, suitably adjusted to satisfy the Friedel sum rule[17],

$$Z_l - Z_0 = \sum_{l=0}^{\infty} Z_l = \frac{2}{\pi} \sum_{l=0}^{\infty} (2l + 1)\eta_l \qquad 5.13$$

are adequate to reproduce the general dependence of K on c for monovalent solvents. This agreement has been improved for

alkali-alkali alloys by Thornton and Young[1] who consider a more realistic potential.

Styles[18] attempted to use square well potentials to represent solutes in polyvalent solvents. To do this he utilised a Friedel sum rule that was modified for volume changes by the method of Blatt[19]. The effective charge of the impurity is then written

$$Z' = Z_1 - Z_0 \frac{\Omega_1}{\Omega_0}$$

which assumes that the atoms retain their normal volumes when in solution. He was not successful in obtaining agreement with experiment. However, an alternative choice of phase shifts has been suggested by Flynn[20,21], based on the argument that the s-wave content of the screening charge cannot be such as to make the total s-electron content within a solute cell exceed 2; this is equivalent to 'saturation' of η_0 at $\pi/2$ for monovalent solvents. Similarly, for a 4-valent solvent for instance, $\eta_0 = 0$ and $\eta_1 = (\pi/6) \times (Z_1 - Z_0)$ for solutes of valence 2 to 6 if volume effects are not considered and if d- and higher order scattering are neglected. This relatively simple idea has led to a qualitative understanding of the dependence of Γ on solute - solvent valence difference, for alloys based on solvents of valence 1, 3 and 5. To obtain quantitative agreement in these cases Flynn called upon a scaling factor, of order 0.25 to 1 which was attributed to electron-electron interactions. The major quantitative discrepancy in this scheme occurred in the case of solid lead alloys, where theoretical prediction is of opposite sign to, and of much larger magnitude than the observations of Snodgrass and Bennett[8]; the scaling factor required here was -0.08. It will be shown below that such a factor is not required for liquid lead alloys.

Because of the lack of success when using square well potentials to represent solutes in polyvalent solvents no attempt has been made here to derive phase shifts from an assumed potential. Instead, the choice of phase shifts based on the chemical properties of the atoms, suggested by Flynn, has been used; that is, p-wave scattering only for solutes of valence 2 → 6 and for valence 1 a value $\eta_0 = -\pi/2$ (equivalent to the repulsion of one s-electron) plus the p-wave contribution. If it is assumed that the phase shifts are not affected by differing core structures (except for volume effects) the predictions are similar for each row of the periodic table. It is also necessary to calculate the constants A_1 and B_1 of eqn. 5.12 and this requires a knowledge of the radial distribution function (r.d.f.). Rather than use Flynn's crude approximation to the r.d.f. the values of A_1 and B_1 have been calculated from the experimental r.d.f. of Kaplow et al.[22]. The values obtained are shown in table 5.4 together with the values for the f.c.c. lattice (Snodgrass, quoted by Flynn[20]).

Table 5.4

	A_0	B_0	A_1	B_1	A_2	B_2
f.c.c.	0.04	-0.24	-0.67	0.70	2.29	-0.73
liquid	-0.04	-0.20	-0.23	0.50	1.69	-0.70

The results for Γ for the liquid are given in table 5.5, together with the phase shifts used, and comparison is made with the observed values. A graph of Γ versus the valence of the impurity, for the liquid is given in fig. 5.1

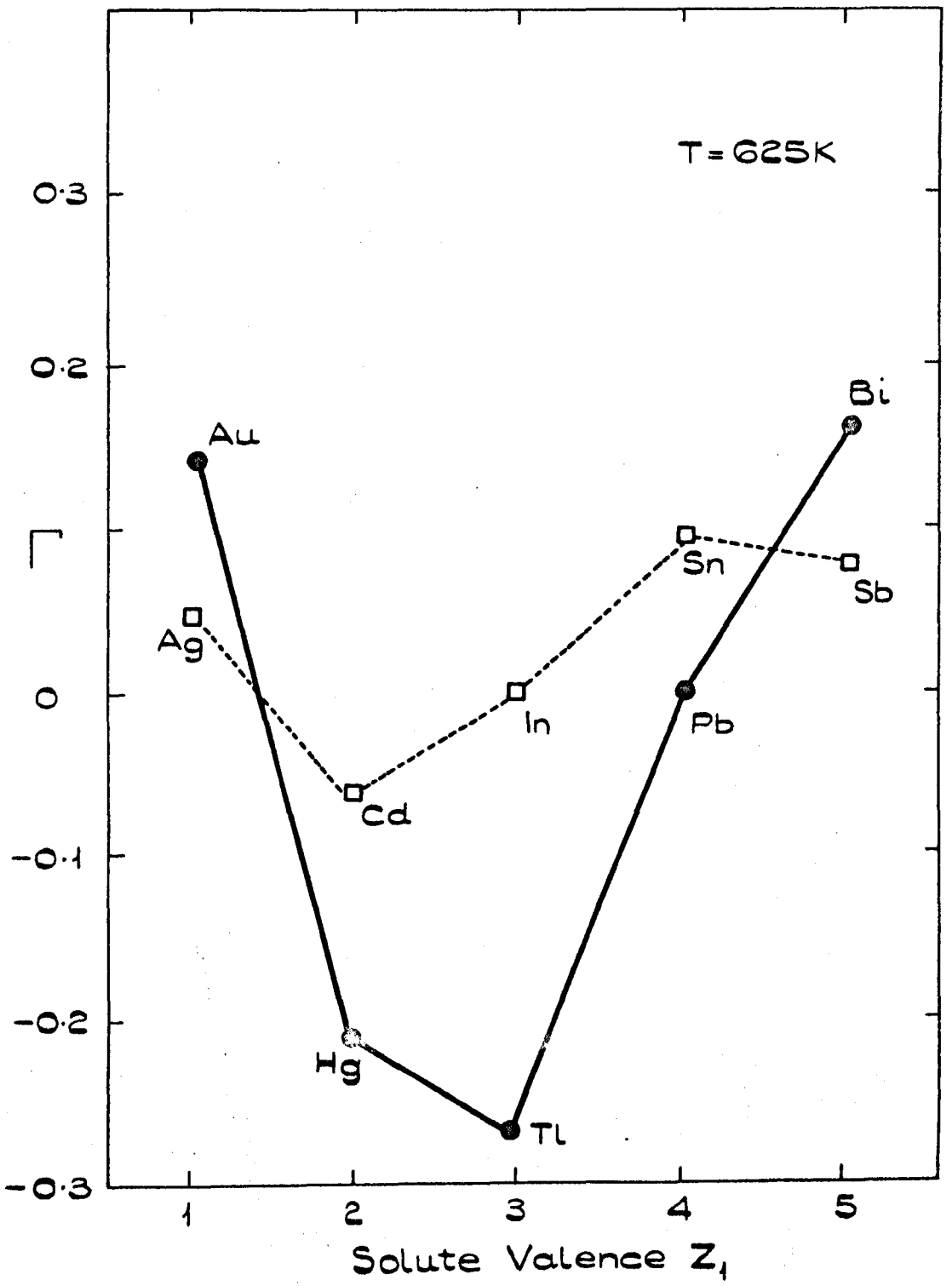

Figure 5.1. VARIATION OF (1/K) (dK/dc) WITH SOLUTE VALENCE FOR A NUMBER OF LIQUID LEAD-BASE ALLOYS.

Table 5.5

Solute	Z_1	Z'	η_1	$\Gamma_{calc.}$	$\Gamma_{obs.}$
Ag	1	-1.67	-0.03	-0.01	+0.06
Cd	2	-1.23	-0.64	-0.56	-0.06
In	3	-0.76	-0.40	-0.39	0.00
Sn	4	-0.07	-0.04	-0.04	+0.09
Sb	5	+0.69	+0.36	+0.31	+0.08
Au	1	-1.61	-0.01	-0.02	+0.14
Hg	2	-1.41	-0.74	-0.60	-0.21
Tl	3	-1.16	-0.61	-0.54	-0.27
Bi	5	+0.22	+0.12	+0.12	+0.16

For comparison purposes only, the equivalent solid results, with theoretical prediction in parenthesis, are Hg: +0.10 (-1.10), Tl: +0.06 (-0.77), and Bi: -0.05 (+0.43).

The conclusions that can be drawn from this comparison are, firstly, for the Pb row of the table the agreement between experiment and theory is much better for the liquid than for the solid. It should be pointed out that effects of changes in χ_p have not been included for this immediate comparison, and the discrepancy in the solid phase suggests that this is a far more important effect than in the liquid. Secondly, the change in r.d.f. on melting is insufficient to explain the drastic observed differences; the failure of the model in the solid must be attributed to specifically 'solid' band structure effects.

It is tempting to refine the model for the liquid, for instance by including a term in η_2; owing to the large numerical

values of A_2 and B_2 rather small values of η_{12} can have appreciable effects. However there seems little virtue in introducing arbitrarily adjustable constants and no progress has been made in understanding the differences in the effects of solutes from different rows of the periodic table. The method that immediately suggests itself is that of adjusting the phase shifts in the Pb - Sn system to reproduce the experimental result and applying this modification to all solutes in the tin row. This is possible in two ways: (i) Allowing a contribution from l = 2 or, (ii) Introducing a contribution from l = 0. Neither method, if applied consistently, can explain the experimental results; both merely introduce a constant difference between the rows of the table, across the valence range.

The values for $(1/\Omega P_F).(d\Omega P_F/dc)$ from this model are again recorded in table 5.6, column 3, and full comparison with experiment is made. It should be pointed out that this approach is only concerned with screening effects. The way in which the effects of non-constancy of the wavefunction over the ion core (section 5.03.2), and these screening effects could be combined is not clear. The results in table 5.6 suggest that improved agreement may be obtained if the two approaches can be mated but this has not been performed and the following section will discuss only the Friedel theory.

5.04 General discussion

A comparison of the observed values and those derived from the Friedel theory is given in fig. 5.2. It is apparent that the overall correlation between experiment and theory is

Table 5.6

Values of $(1/K)(dK/dc)$ for ^{207}Pb in a number of liquid alloys

Solute	p e/a effects	$p_F^{(0)}$ 'non-constancy'	$p_F^{(1)}$ Friedel	Total(1+2)	Total(1+3)	Expt.
Ag	-0.13_0	$+0.08_8$	-0.01	-0.04	-0.14	+0.06
Cd	-0.09_6	$+0.05_3$	-0.56	-0.04	-0.66	-0.06
In	-0.04_6	$+0.02_4$	-0.39	-0.02	-0.44	0.00
Sn	$+0.03_1$	-0.00_2	-0.04	+0.03	-0.01	+0.09
Sb	$+0.09_0$	-0.02_9	+0.31	+0.06	+0.40	+0.08
Au	-0.03_0	$+0.17_7$	-0.02	+0.15	-0.05	+0.14
Hg	-0.06_5	$+0.06_2$	-0.60	-0.00	-0.67	-0.21
Tl	-0.05_6	$+0.02_7$	-0.54	-0.03	-0.60	-0.27
Bi	$+0.06_8$	-0.02_5	+0.12	+0.04	+0.19	+0.16

Column 1 Column 2 Column 3

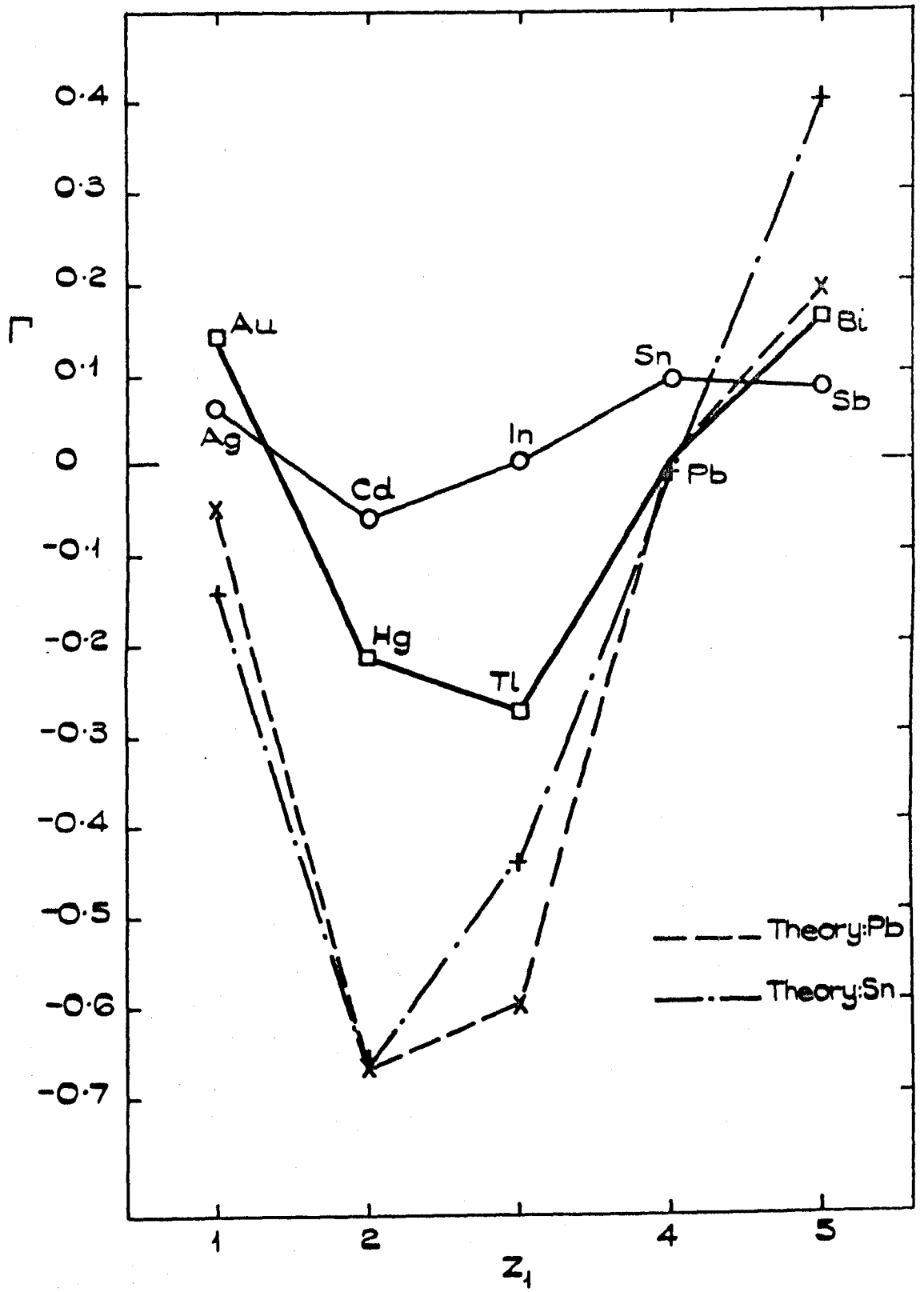

Figure 5.2 Comparison of experimental and theorectical values of Γ for liquid lead alloys.

very reasonable. The most gratifying part of this agreement is that obtained for the solutes Bi, Tl and Hg. The predicted values differ from the experimental values only by a factor of approximately 2. In addition, the general shape of the theoretically predicted curve is in good agreement with that of the observed curve. It should be pointed out, however, that the minimum in the predicted results is only produced if a contribution from η_0 is included for the monovalent solutes. With $\eta_0 = -\pi/2$, the value of η_1 required by the volume-modified Friedel sum rule is very small and the predicted value of Γ is then determined solely by the value of A_0.

From general considerations of the Friedel theory it is difficult to see how such a minimum can occur; the normal predicted dependence would seem to be a proportionality with $Z_1 - Z_0$. In fact liquid polyvalent base alloys do not produce such linear variations of Γ[21] and it has only been possible to obtain even qualitative agreement by using the Flynn approach. The results of the comparison for these liquid lead base alloys supports this general picture and suggests that, at present, phase shifts derived by this 'chemical' technique offer the best description. No progress has been made on justifying this method from sound physical bases.

The similarities between the Friedel small angle scattering theory and the pseudopotential model for hetero-valent systems were discussed earlier. It was shown that the pseudopotential model also predicts a tendency for the variation of Γ from alloy to alloy to be determined by the valence difference. Without doing detailed calculations (which have been shown to be unreliable at present) it is not possible to say whether the minimum in the

valence dependence could be reproduced by this approach. In view of the similarities between the two approaches however, there is reason to believe that the advent of more accurate potentials, and partial structure factors, may lead to a better description of alloying effects on Knight shifts both through a pseudopotential model and through the derivation of a 'correct' set of phase shifts.

At the present time a serious problem in the interpretation of liquid alloy Knight shifts is the existence of core-polarisation and orbital contributions to the shift. We have seen that the estimated size of these effects for ^{207}Pb is $\sim$-25% K_s in pure lead. The concentration dependence of these contributions may be large enough to make theoretical prediction based on the hyperfine interaction completely at variance with experiment.

5.05 The variation of the ^{207}Pb Knight shift with temperature in Pb - 18% Bi and Pb - 20% Tl

Figures 3.12 and 3.13 contain the results of an investigation of how the striking differences between the alloy dependence of the ^{207}Pb shift in solid solutions[8] and in liquid alloys (present work) occurred. The ^{207}Pb shift was followed from room temperature, through the melting point, to 800 K. Two effects are immediately apparent: firstly, the change of sign of Γ is progressive, occurring partially as the temperature of the solid is increased and partially on melting. Secondly, in the liquid phase there is no further change in Γ. The observed temperature coefficients of the ^{207}Pb Knight shift for both phases of the two alloys are given in table 5.7. The liquid state, being the simpler, will be discussed first.

Table 5.7

Sample	$(1/K)(dK/dT)_s$ x $10^5(K)^{-1}$	$(1/K)(dK/dT)_l$ x $10^5(K)^{-1}$	$\Delta K/K$ on melting
Pb - 18% Bi	14(±2)	-9.2(±0.7)	+4%
Pb	6.3(±0.4)	-7.6(±0.9)	-0.2%
Pb - 20% Tl	-1.2(±1.0)	-9.5(±1.2)	-4%

From table 5.7 it is apparent that, within experimental uncertainty the temperature coefficients in the liquid are all the same. Inspection of fig. 3.12 shows that the temperature coefficient of the ^{209}Bi shift, in this alloy, is also in the same range. This means that whatever changes occur with temperature in the liquid must occur in the same way for all three samples and suggests that for the whole range of dilute alloys of lead it is likely that Γ is independent of temperature. The temperature coefficient of K for pure lead was discussed in Chapter 4 and it was concluded that the explanation could be obtained from a first-order pseudopotential expression with the dominant temperature dependence arising from the changes in the structure factor. Thus, for these alloys, the temperature dependence would still appear to be dominated by the change in structure factor. It can therefore be deduced that such changes cannot be significantly different from those occurring in the pure metal.

Considering table 5.7 again, the results for the solid phase show a remarkable spectrum; both the temperature coefficients and the changes on melting have opposite signs in the two alloys.

The results for pure lead lie between those for the alloys. We now see whether the different electron/atom ratios, in the presence of overlapping bands at the Fermi level, can affect χ_p and P_F sufficiently in these alloys to account for the observed results.

It is relevant to discuss first the unusually large temperature coefficient of K observed in solid Cd. Kasowski and Falicov[23] have discussed this and, with the band structure data and the non-local pseudopotential available, were able to explain the observed temperature dependence and change of melting of the shift. They modified the band structure and the pseudopotential for finite temperatures using a Debye-Waller factor, and showed that the major contribution to the temperature dependence of K arose from the washing out of the electronic structural affects which were produced at T = 0 by the strong pseudopotential. They evaluated χ_p from the free-electron value $\mu_B^2 \rho(E_F)$ and showed that the change in the band structure with temperature increased $\rho(E_F)$ from a very low value at T = 0 to the free-electron value in the liquid at the melting point. This required a step at T_m, just as observed[18]. The change in χ_p produced a large part of the total predicted change; a smaller contribution did arise from the change in the character of the conduction electrons with temperature.

For simplicity, and because the above discussion suggests that χ_p plays the dominant role, attention will here be concentrated on the spin susceptibility. It will be assumed that only small differential effects arise from P_F. This requires that, in Pb - 18% Bi the temperature coefficient of χ_p has a large positive value, in pure lead it has a small positive value and in Pb - 20% Tl

a small negative value. For pure lead, measurements of the temperature dependence of the total susceptibility are available[24]. Alexandrov et al. show that χ_{total} increases diamagnetically in a linear fashion with decreasing temperature. They write

$$\chi_{total}\,(T) \;=\; \chi_{ion} + \chi_{elec.}\,(T)$$

and in a discussion involving contributions to $\chi_{elec.}(T)$ from electron and hole groups they conclude that, although it is possible to suggest that increase of the total susceptibility with temperature is due to overlapping bands, detailed quantitave work is not possible with present knowledge.

The way in which alloying can affect the temperature change of the susceptibility has been considered by Elcock et al.[25]. Using rectangular, open-ended, overlapping bands, the total susceptibility was derived as

$$\chi_{total} = 2\mu_B^2 \left\{ a\left(\frac{M_a^*}{M}\right)\left[\frac{\chi}{\chi_0}\right]_a + b\left(\frac{M_b^*}{M}\right)\left[\frac{\chi}{\chi_0}\right]_b \right\}$$

$$- \frac{2}{3}\mu_B^2 \left\{ a\left(\frac{M}{M_a^*}\right)\left[\frac{\chi}{\chi_0}\right]_a + b\left(\frac{M}{M_b^*}\right)\left[\frac{\chi}{\chi_0}\right]_b \right\} \qquad 5.14$$

where M^* represents the effective mass, μ_B the Bohr magneton, χ_0 the value of the susceptibility at T = 0, a and b the heights of the lower and upper bands and the subscripts 'a' and 'b' refer to holes and electrons respectively. The temperature dependence of (χ/χ_0) is given for various overlaps. The suggestion here is that changing the electron/atom ratio, by the addition of Bi or Tl changes the position of the Fermi level in the area of overlap. As E_F moves in the area of overlap the transfer of electrons from one band to the next changes, and the temperature dependence of (χ/χ_0) is altered. By assuming a rigid band model it is possible

to obtain changes in the susceptibility of the correct sign to explain the Knight shift changes. It must be emphasised, however, that Elcock's theory relates to the total susceptibility and it is not possible to separate the paramagnetic first term of eqn. 5.14 from the total expression. In addition it should be noted that with present knowledge almost any temperature dependence of χ_p is possible for different alloys.

The problems involved in the use of susceptibility data can perhaps be illustrated for the case of pure lead. The temperature coefficient of K is $\sim 6.3 \times 10^{-5}$ (kelvin)$^{-1}$. Thus a change of 4% in K occurs on raising the temperature from 77 K to 600 K. The observed change in χ_{total} over this range is equivalent to $\sim 40\%$ of the free-electron χ_p. Therefore either χ_p is not the dominant source of the temperature dependence in the total susceptibility or P_F is decreasing with temperature. It could well be that the experimental χ_{total} results are due to a decrease in the second term of eqn. 5.14 (the diamagnetic part) with temperature. It is worth noting that even when the band structure, the non-local pseudopotential and effective masses are reasonably well known (e.g. Cd) the diamagnetic part of the susceptibility has not been properly evaluated.

What is needed is a thorough investigation of the susceptibility of these alloys, not only as a function of alloy concentration but also as a function of temperature. After all, it was assumed that all the temperature dependence arose from χ_p changes due to overlapping bands. If the two bands had different electron character a large effect from P_F may be expected. A full explanation of the effects in these alloys is not available but

the overlapping band picture does seem to be capable of reproducing the observed temperature dependences.

5.06 Conclusions

In this chapter an attempt has been made to assess how successful the nearly-free-electron theories are in explaining the Knight shift in liquid polyvalent base alloys, and in particular the alloys with lead as solvent. The correlation between experiment and theory was reasonable. The discrepancy in sign between the Friedel prediction and the experimental results on solid solutions has been removed now liquid state data are available.

For all the alloys except Pb - Hg and Pb - Cd the concentration dependence was linear. This linearity is in agreement with theory. The minimum in the $(1/K)(dK/dc)$ versus valency of the solute curve was explained (at least, qualitatively) by means of the repulsion of one s-type electron from a monovalent solute cell. The quantitative discrepancies that occur have been discussed, briefly, in terms of (i) Electron-electron interactions and, (ii) Core-polarisation and orbital contributions to the observed value of the Knight shift. For heavy elements these effects have been shown to amount to $\sim 30\%$ K_s and their concentration dependence is not understood. Within the uncertainty imposed by these ideas the free-electron, and nearly-free-electron theories seem to be adequate for a description of polyvalent base liquid alloys.

The investigation of the variation of K with temperature in two dilute alloys provided essentially two points. Firstly, it emphasised the relative simplicity of the liquid state.

Secondly, the much more difficult solid solutions were discussed and a description in terms of overlapping bands was considered. No definite conclusions are possible at this stage and there is a need for more detailed studies of n.m.r. and magnetic susceptibility in lead solid solutions. A combined study provides an interesting possibility for future work.

References

(1) Thornton D. E. and Young W. H., J. Phys. C, 1, (1968), 1097.

(2) Kaeck J. A., Ph.D. Thesis, Cornell, (1968).

(3) Holland B. W., Phys. Stat. Solidi, 28, (1968), 121.

(4) Faber T. E., Adv. in Phys., 16, (1967), 637.

(5) Blandin A., Daniel E. and Friedel J., Phil. Mag., 4, (1959), 180.

(6) Blandin A. and Daniel E., J. Phys. Chem. Sol., 10, (1959), 126.

(7) Daniel E., J. Phys. Rad., 20, (1959), 769 and 849.

(8) Snodgrass R. J. and Bennett L. H., Phys. Rev., 134, (1964), A1294.

(9) Wilson J. R., Met. Rev., 10, (1965), 381.

(10) Faber T. E. and Ziman J. M., Phil. Mag., 11, (1965), 153.

(11) Halder N. C., Phys. Rev., 177, (1969), 471.

(12) Ashcroft N. W. and Langreth D. C., Phys. Rev., 156, (1967), 685.

(13) Animalu A. O. E. and Heine V., Phil. Mag., 12, (1965), 1249.

(14) Heine V., Nozières P. and Wilkins J. W., Phil. Mag., 13, (1966), 741.

(15) Kellington S. H. and Titman J. M., Phil. Mag., 15, (1967), 1045.

(16) Moulson D. J., Ph.D. Thesis, Leeds, (1966).

(17) Friedel J., Adv. in Phys., 3, (1954), 446.

(18) Styles G. A., Ph.D. Thesis, Leeds, 1964.

(19) Blatt F. J., Phys. Rev., 108, (1957), 285.

(20) Flynn C. P. and Rigney D. A., Phil. Mag., 15, (1967), 1213

(21) Flynn C. P. and Odle R. L., Phil. Mag., 13, (1966), 699.

(22) Kaplow R. L., Strong S. L. and Averbach B. L., Phys. Rev., 138, (1965), A1336.

(23) Kasowski R. V. and Falicov L. M., Phys. Rev. Letts., 22, (1969), 1001.

(24) Alexandrov B. N., Verkin B. I. and Svechkarev I. V., Sov. Phys. JETP., 12, (1961), 25.

(25) Elcock E. W., Rhodes P. and Teviotdale A., Proc. Roy. Soc., 221A, (1953), 53.

CHAPTER SIX

THE LEAD - BISMUTH SYSTEM

6.01 Introduction

There has recently been some evidence[1,2] that n.m.r. in liquid metals is a useful tool for the observation of structural changes in that the Knight shift appears to be sensitive to the local atomic arrangement. Styles[1] reported complicated variations of the ^{115}In and ^{209}Bi Knight shifts and ^{209}Bi linewidths, with temperature and composition in the liquid In-Bi system, which he explained in terms of the persistence of intermetallic grouping in the liquid phase. This interpretation is strongly supported by X-ray and viscosity data[3] which indicate the persistence of the groupings InBi and In_2Bi into the liquid. Such 'structural effects' have also been reported in other systems, particularly in the noble metal - tin systems[4]; evidence comes not only from direct structural observations but also from measurements of heats of mixing, viscosity, diffusion and electrical resistivity. The evidence in these cases suggests that unusual effects can occur in the liquid state when an intermetallic compound exists in the solid up to the liquidus temperature.

The phase diagram of the Pb-Bi system is shown in fig. 6.1; there is no intermetallic compound in the solid. However, X-ray and neutron diffraction studies[5] have led to the conclusion that the number of nearest neighbours in the liquid phase appears to stay constant at 12 up to approximately

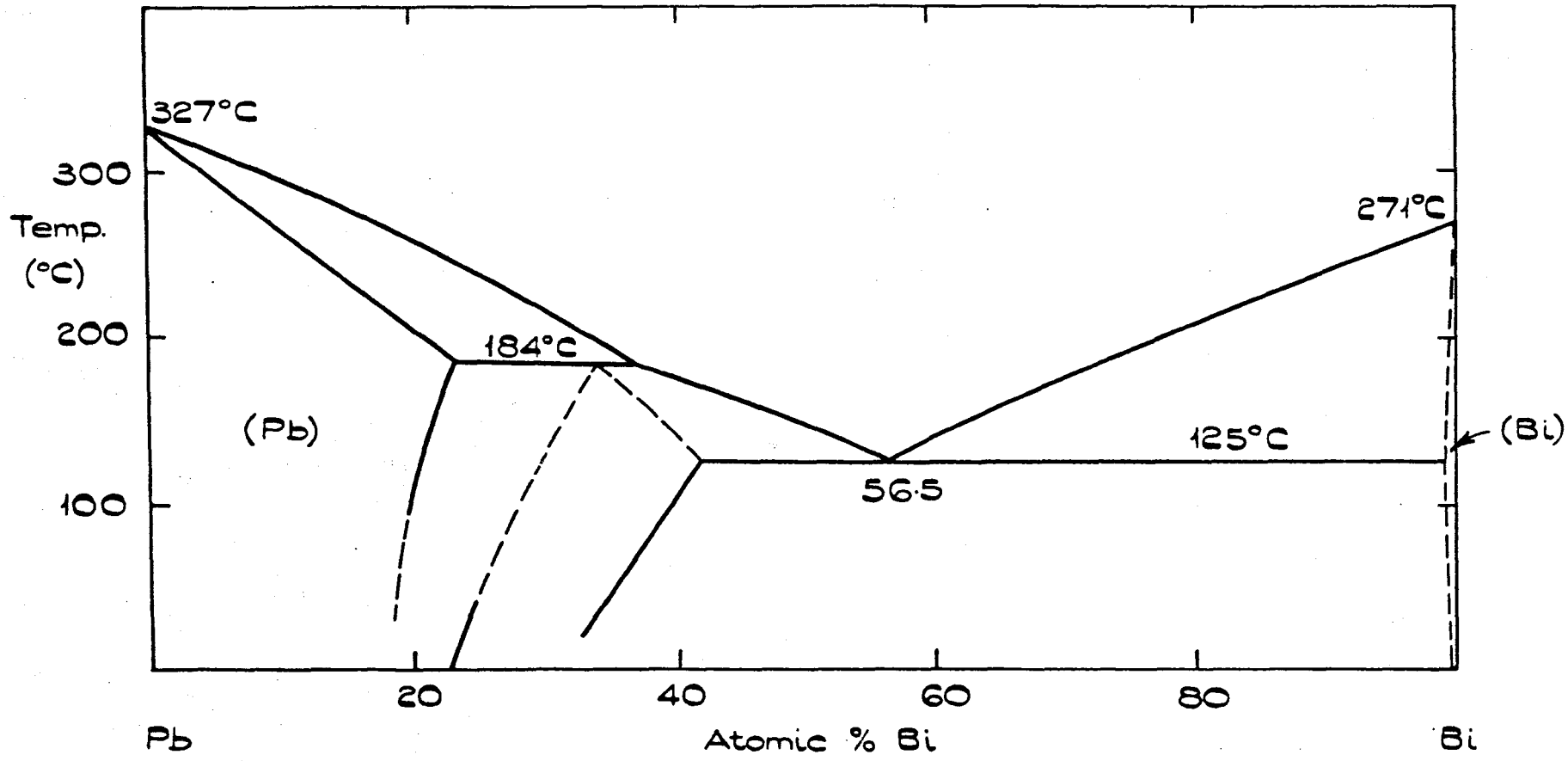

Figure 6.1. THE LEAD-BISMUTH PHASE DIAGRAM (ff. HANSEN)

60% Bi and then drop smoothly to about 8 in 100% Bi. This result prompted a n.m.r. investigation[6] of the liquid Pb-Bi system. The sensitivity of the apparatus then available was only sufficient to observe the variation of the ^{209}Bi Knight shift with concentration. The results were of a preliminary nature but they did seem to show good correlation with the nearest neighbour change. The observations were made at two temperatures 453 K and 733 K, with samples prepared using a grinding technique. The data showed two very unusual features: firstly, in the variation of the ^{209}Bi Knight shift with concentration a deviation from linearity occurred very sharply at 60% Bi and secondly, in this 60% Bi sample the temperature coefficient of the shift was unusually large and positive. At first sight these effects are not extraordinary but closer examination shows that the Knight shift cut off is too sharp to be accounted for by the observed nearest neighbour change. Also, the positive temperature coefficient observed for the 60% Bi sample is very unusual in that all other alloys of bismuth, and 100% Bi itself, show a small but negative temperature coefficient of the Knight shift in the liquid.

It would be expected that such a large change in local order would be reflected in other physical properties of the liquid system. However, measurements of heats of mixing[6], density[7], and viscosity[7] showed no anomalies and old measurements of the magnetic susceptibility[8] and resistivity[9] showed no deviations from linearity to the precision then available. Lambert (private communication) has recently remeasured the resistivity isotherm at 625 K. His results are very precise and show no unusual effects. This general lack of supporting

evidence, together with the difficulties involved in determining the number of nearest neighbours accurately from experimental distribution functions[10], casts some doubt on the authors' interpretations of both the X-ray and the n.m.r. data.

In the light of these considerations and of the availability of a spectrometer of increased sensitivity, a more complete investigation of n.m.r. in the liquid Pb-Bi system was undertaken.

6.02 Experimental Results

Samples of Pb-Bi alloys were prepared at approximately 10% intervals across the concentration range by the spraying technique described in Chapter 2. The results will be presented in two sections: firstly, the Knight shift observations and secondly, observations made on the ^{209}Bi linewidth. In the liquid phase, the signal strength of the ^{207}Pb resonance does not allow useful observations of its linewidth.

6.02.1 Knight shifts Observations were made on the ^{207}Pb and ^{209}Bi Knight shifts as a function of concentration at a fixed temperature of 625 K and also at a temperature 1.04 x T_m, where T_m is the liquidus temperature of the alloy under observation (fig. 6.2). In each case measurements were made both at fields of 1.4450 tesla and 0.5750 tesla. Further, the ^{209}Bi shift in 100% Bi and in Pb - 60% Bi was checked for any field dependence over an extended range from 0.30 to 1.45 tesla. Since no field dependence was in fact observed fig. 6.2 is equally applicable at any field in this range. In addition, for reasons discussed

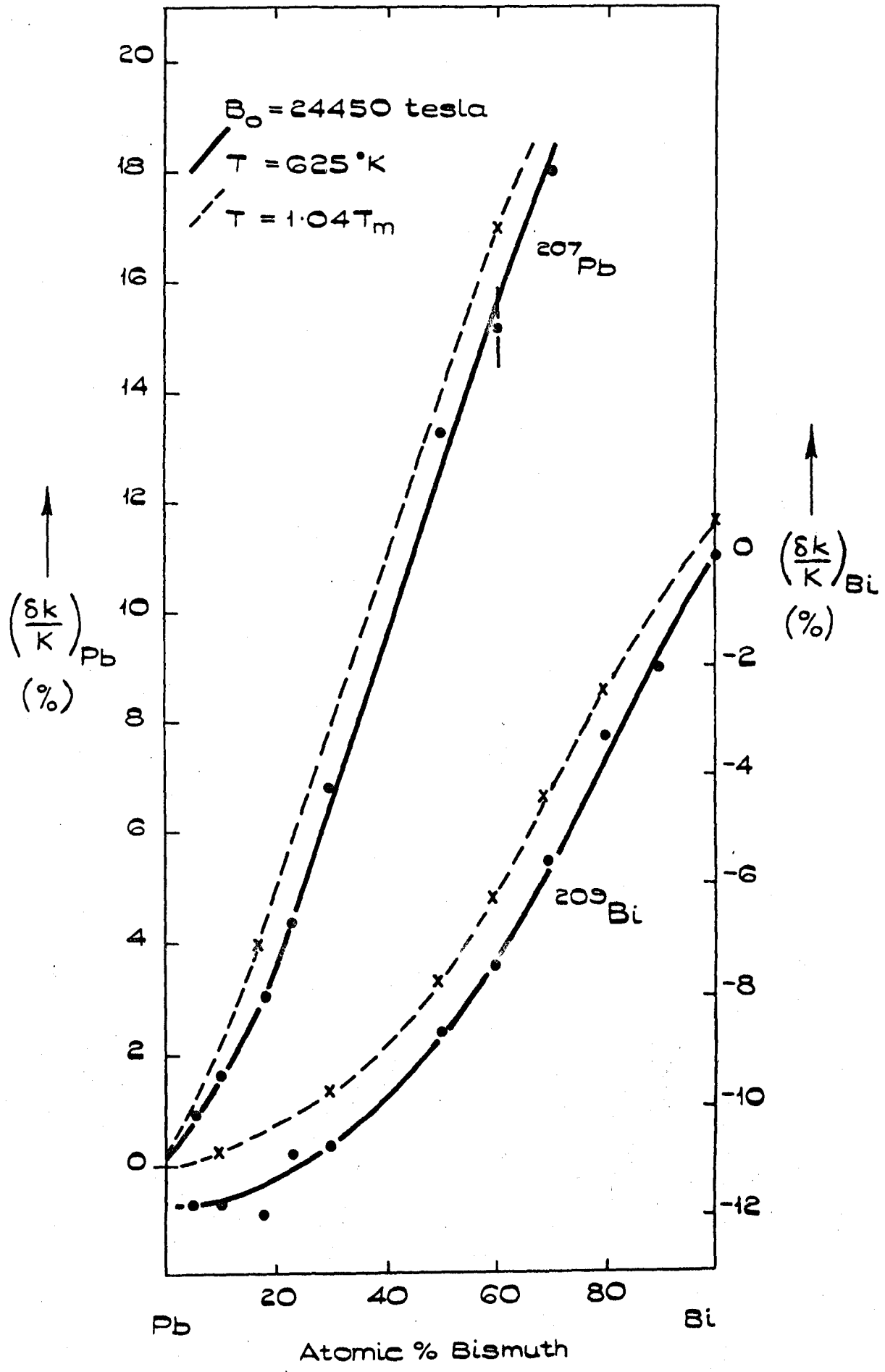

Figure .6.2. FRACTIONAL CHANGE OF THE KNIGHT SHIFTS OF ^{207}Pb AND ^{209}Bi WITH CONCENTRATION.

below, temperature dependences of the ^{209}Bi shift were observed in 100% Bi, Pb - 80% Bi, Pb - 60% Bi and, as reported in chapter 3, Pb - 18% Bi (fig. 6.3). The temperature dependence of the ^{207}Pb Knight shift in Pb - 60% Bi and Pb - 18% Bi is shown in fig. 6.4.

It is worth noting that there is no sudden fall of $(\delta K/K)_{Bi}$ or $(\delta K/K)_{Pb}$ at Pb - 60% Bi and likewise there is no anomalous temperature dependence of the ^{209}Bi shift in the Pb - 60% Bi alloy, in strong disagreement with the earlier results. It is found, in agreement with previous workers (see for instance Styles[6]), that supercooling was possible in 100% Bi, to approximately 80 K below T_m. It was also possible to supercool the Pb - 60% Bi alloy (a near eutectic composition) by about 50 K. Supercooling was however not observed for the Pb - 80% Bi alloy. The onset of freezing was readily deduced from a sudden break in the Knight shift - temperature curves (as shown in fig. 6.3), for alloys when the solidus and liquidus did not coincide, the break arising from a change in concentration of the remaining liquid phase.

6.02.2 Linewidth Because the linewidth is more difficult to measure than the Knight shift it was not possible to record the ^{207}Pb widths in the liquid alloys. The ^{209}Bi widths were recorded, however, all using the same modulation amplitude, response and sweep times and corrections for modulation broadening were again made using the method of Smith[12]. Measurements were made at two fields and at two temperatures.

The variation of the ^{209}Bi linewidth with concentration at two temperatures, 625 K and 1.04 T_m, is shown in fig. 6.5.

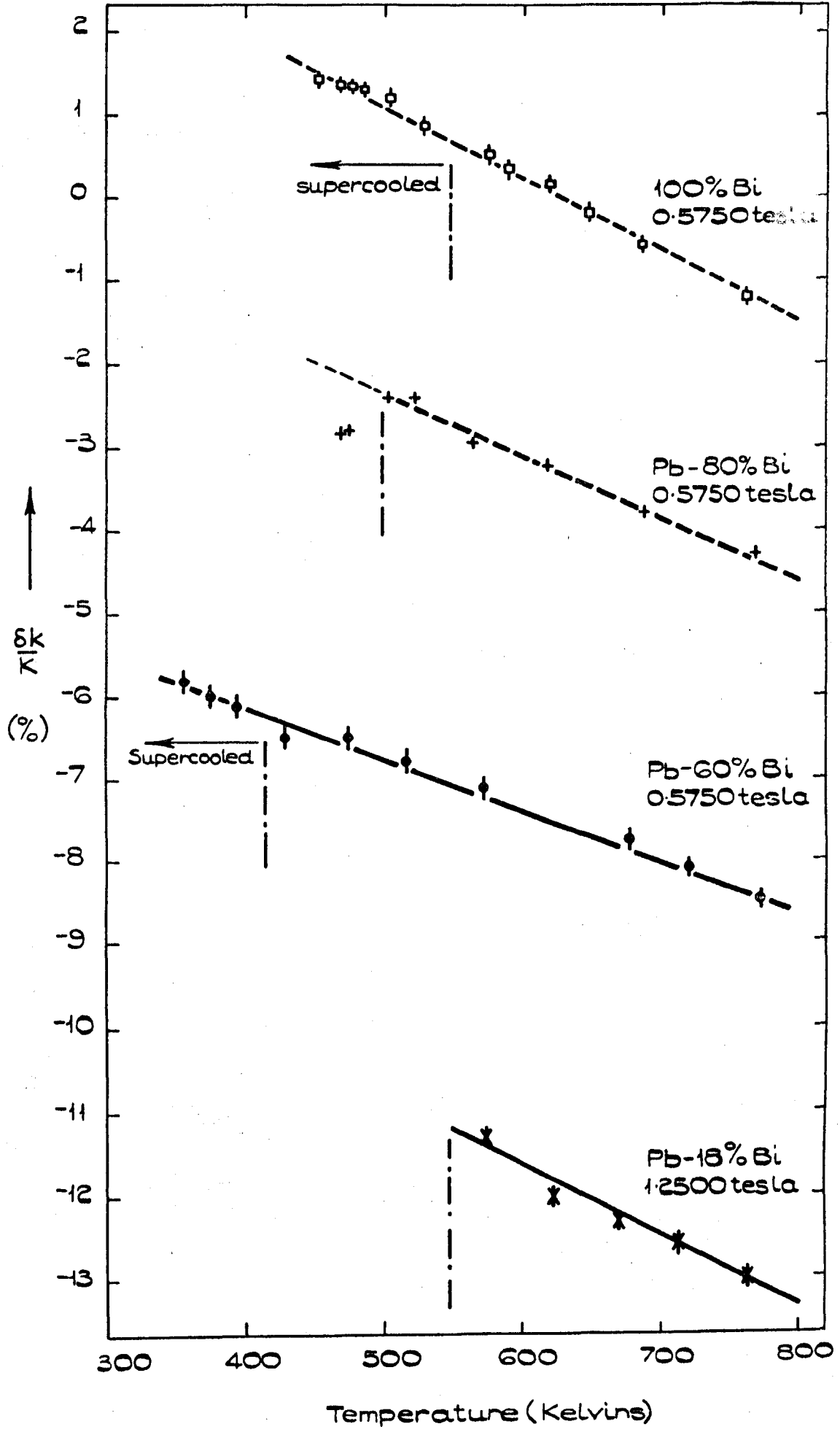

Figure 6.3. FRACTIONAL CHANGE IN KNIGHT SHIFT OF ^{209}Bi WITH TEMPERATURE IN A NUMBER OF Pb-Bi ALLOYS.

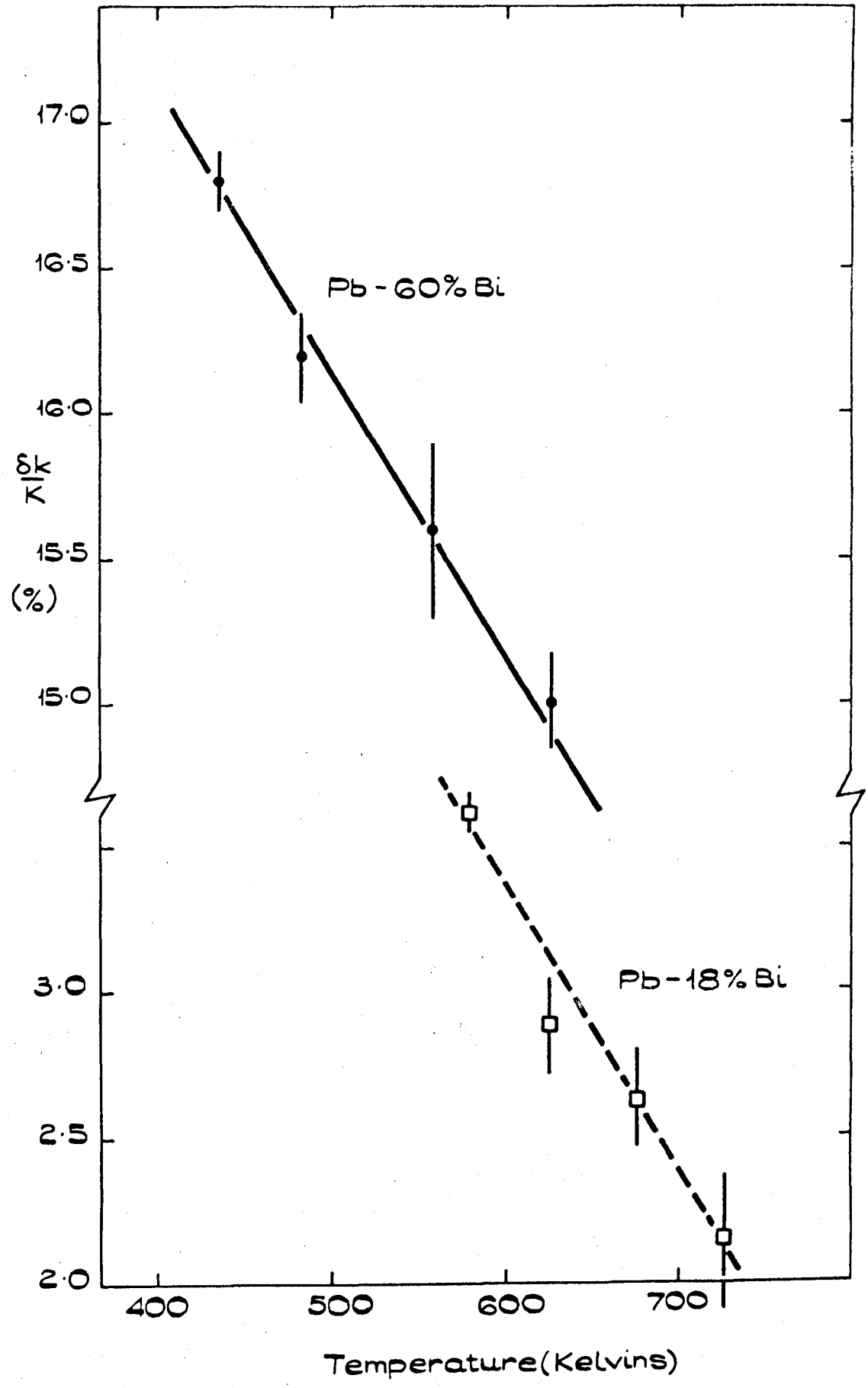

Figure 6.4. FRACTIONAL CHANGE IN ^{207}Pb KNIGHT SHIFT WITH TEMPERATURE IN SOME Pb-Bi ALLOYS.

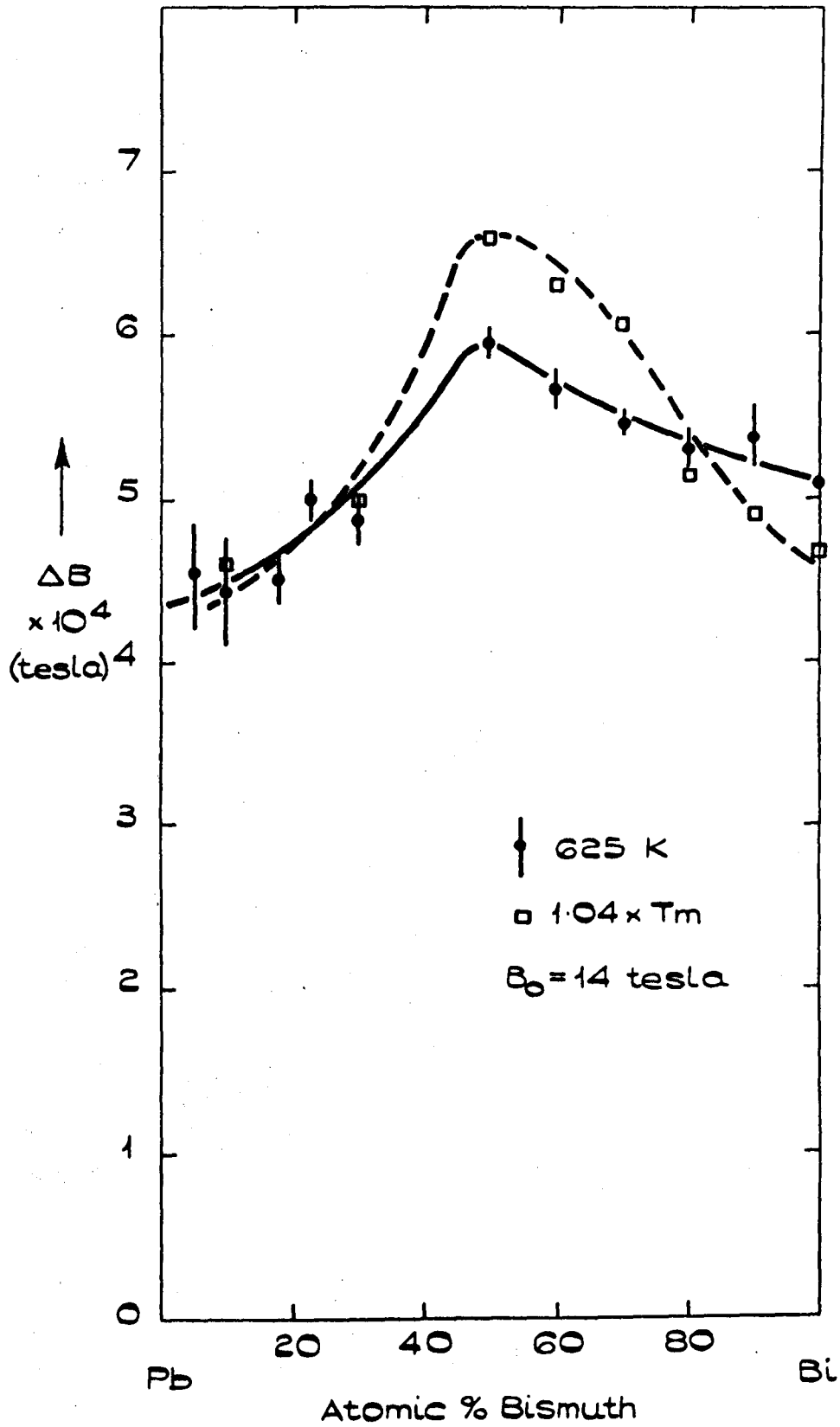

Figure 6.5. VARIATION OF THE LINE WIDTHS OF THE ^{209}Bi RESONANCE WITH CONCENTRATION FOR TWO TEMPERATURES.

At all concentrations 625 K is a higher temperature than 1.04 T_m, except for 100% Pb where the two are equal. Two features are of particular interest: first, there is a strong maximum at approximately 50% and second, around this maximum the linewidth increases with decreasing temperature. Figure 6.6 shows that there is no measurable field dependence of the linewidth.

Because of the unusual variation of the width with temperature around the maximum of fig. 6.5, more detailed observations of the ^{209}Bi resonance in 100% Bi, Pb - 80% Bi and Pb - 60% Bi were made. Figure 6.7 contains the additional data on the linewidths (the additional Knight shift data were given in fig. 6.3). It is apparent that the width in Pb - 60% Bi shows a very large temperature variation with a strong minimum at approximately 500 K. This feature is also definitely shown in the case of 100% Bi, but when supercooling was not possible (i.e. Pb - 80% Bi and Pb - 18% Bi) no firm conclusions on this point can be drawn. In view of these dramatic changes a careful field dependence study was performed. The width in Pb - 60% Bi and 100% Bi was observed at six fields between 0.30 and 1.45 tesla at constant temperature. No measurable field dependence was obtained; the results are not plotted but the data are given in Table 6.7(b) of Appendix I.

6.03 Knight shifts - comparison with earlier data

The earlier measurements[6] on this system were correlated with the change in local order reported by Sharrah et al.[4] but, as remarked in the introduction, careful examination shows that the correlation is not good and the results, particularly for Pb - 60% Bi, are disquieting. The present results of both

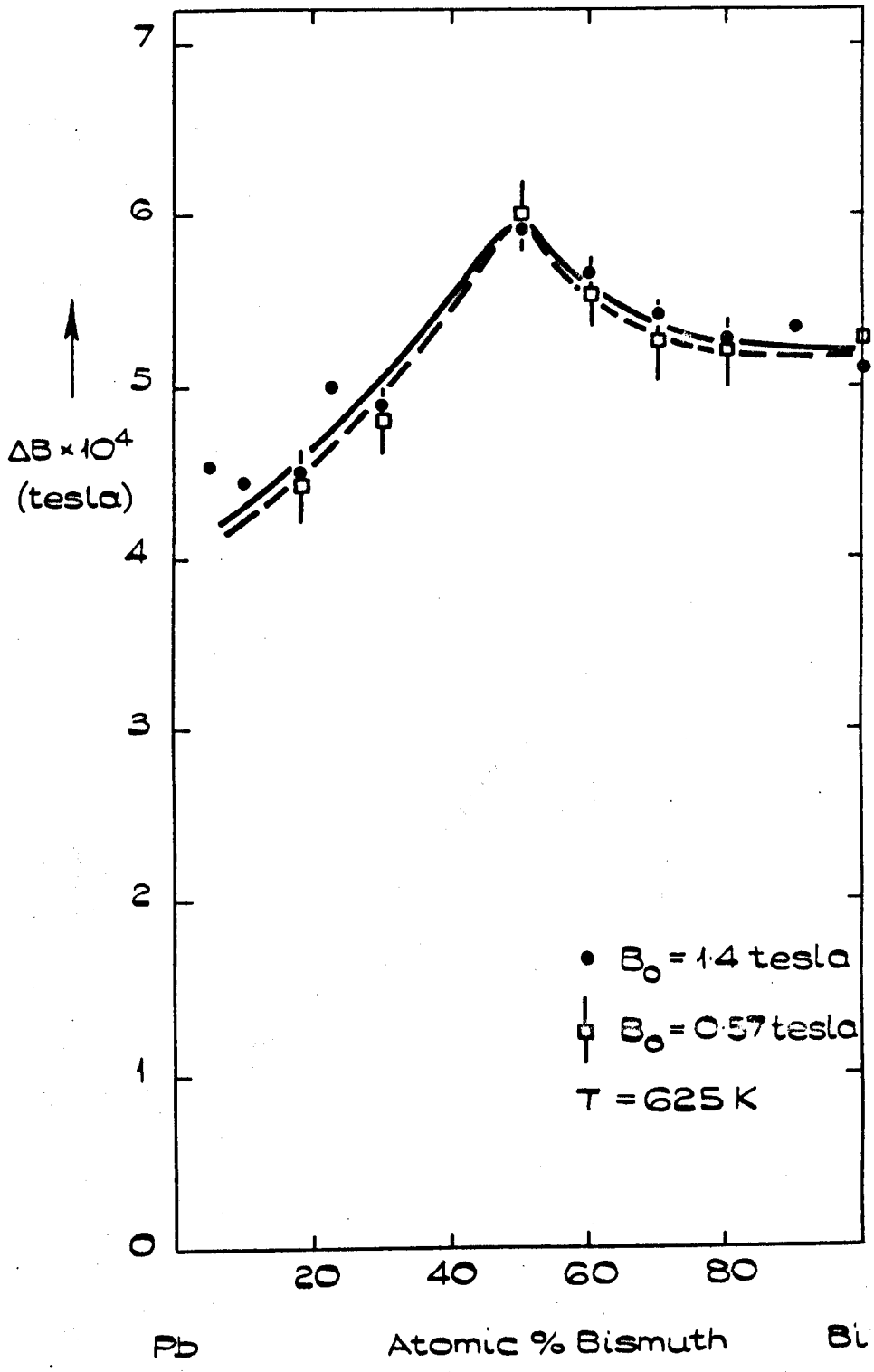

Figure 6.6. VARIATIONS OF THE LINE WIDTHS OF THE ^{209}Bi RESONANCE WITH CONCENTRATION FOR TWO FIELDS.

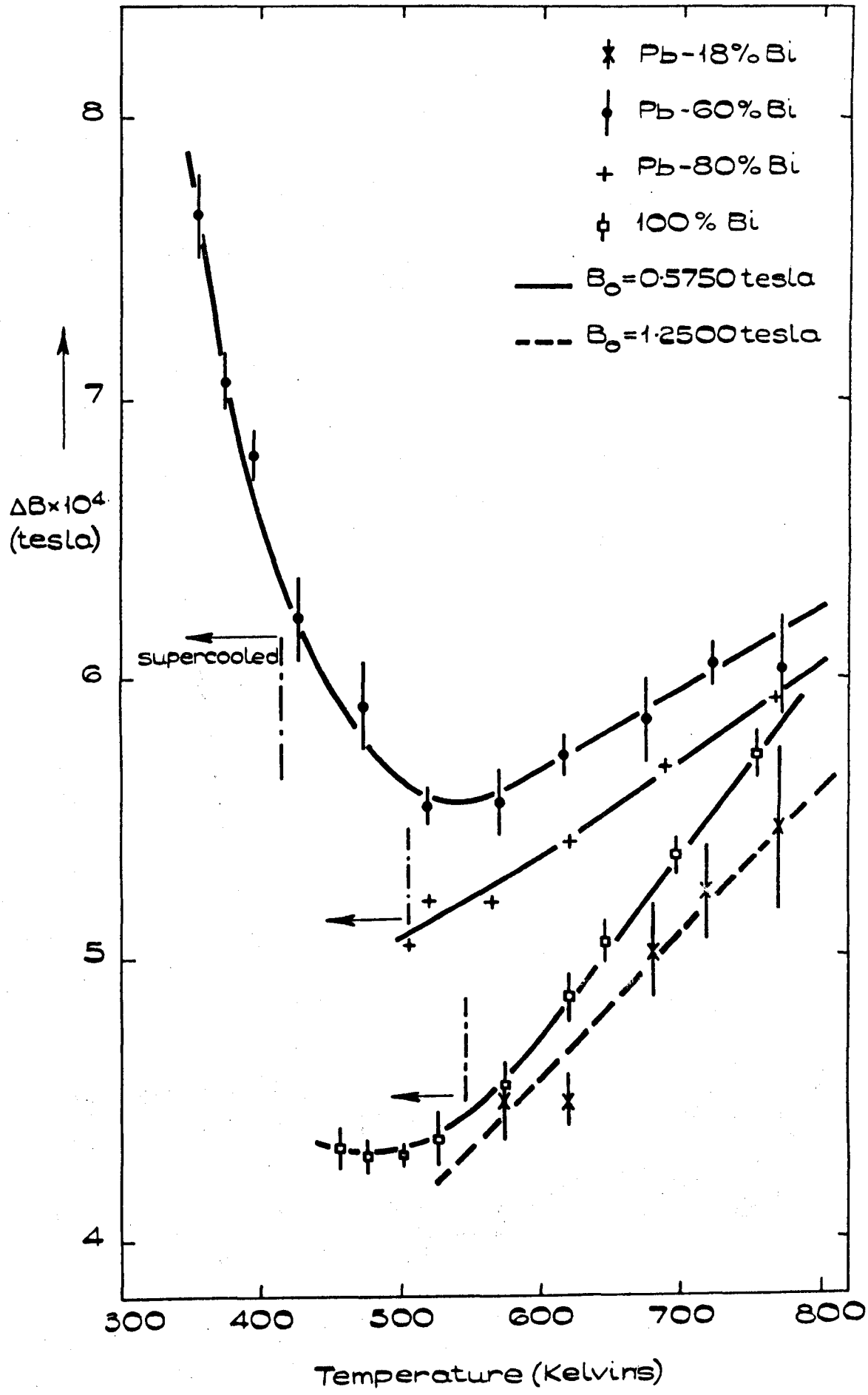

Figure 6.7. VARIATION OF THE LINE WIDTH OF ^{209}Bi RESONANCE WITH TEMPERATURE IN A NUMBER OF Pb-Bi ALLOYS.

^{207}Pb and ^{209}Bi Knight shifts show none of the 'unusual effects' observed earlier, and as Taylor's original samples were available a short subsidiary experiment was performed. Figure 6.8 shows the results (in diagramatic form) of a temperature dependence study of the absorption derivative from Taylor's Pb - 60% Bi sample. At low temperatures a single line was observed which corresponded exactly with the line from the freshly prepared Pb - 60% Bi sample. At higher temperatures a further line, characteristic of 100% Bi, appeared which displaced the apparent line centre giving an apparent increase in the Knight shift with increasing temperature. Thus, inhomogeneity of composition accounts for the reported temperature coefficient and probably also for the sharp change in the concentration dependence of the shift.

It can be said definitely that the Knight shifts of ^{207}Pb and ^{209}Bi show no dramatic changes around the 60% Bi region; there is no correlation between the measured shift and the change in local order reported by Sharrah et al.. Since there is now no known physical property which reflects any sudden change in local order, it is tempting to suggest that the

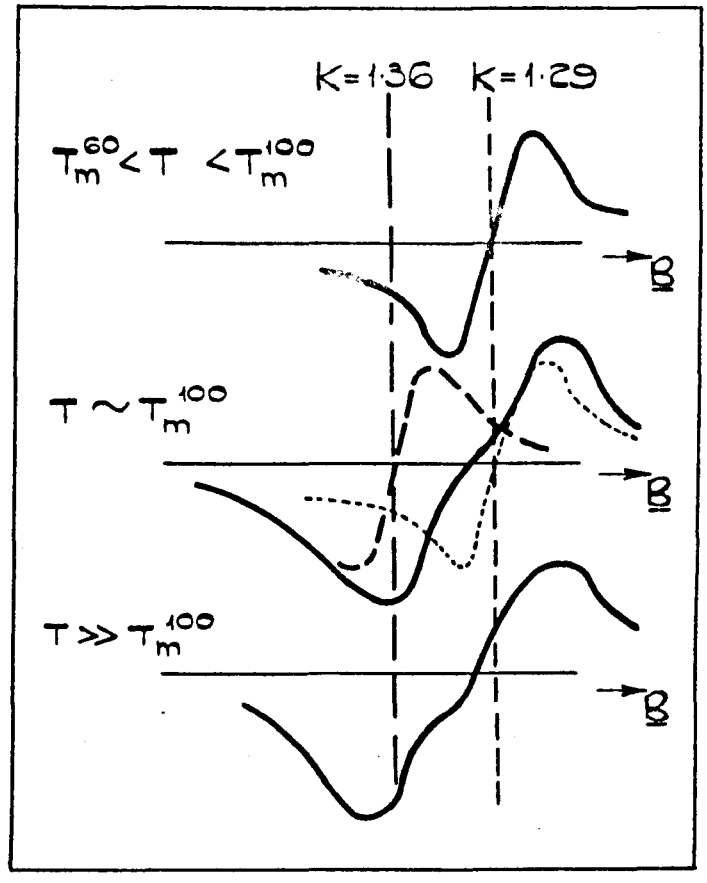

Figure 6.8

interpretation of the X-ray data given by Sharrah is mistaken, and that the coordination number changes smoothly across the system. However, it is interesting to note that a similar negative result has been found by Host (private communication) for the liquid Au-Sn system (which has been reported[4] to show 'structure' in the liquid around the AuSn intermetallic composition); no anomalies in the concentration dependence of the ^{119}Sn Knight shift were observed. Since the interpretation of the X-ray data is less ambiguous in this case, it may be that Knight shifts are not as sensitive to local order as had been suggested by earlier work.

6.04 Discussion of the linewidth

This discussion begins with the Korringa relation. Contributions to the Knight shift and relaxation time other than the hyperfine contact interaction are discussed with reference to bismuth. In particular, quadrupolar relaxation is discussed for pure metals and finally, a general discussion of relaxation in liquid alloys is given with reference to the Pb - Bi observations.

6.04.1 The Korringa relation The Korringa relation in liquid metals has been discussed fully in section 1.04.2 part (ii) the relation was written[13]

$$T_1 \, T(K_s)^2 = \frac{\hbar}{4\pi k} \left(\frac{\gamma_e}{\gamma_n}\right)^2 \times \frac{1}{\mathcal{K}(\alpha)} \qquad 1.10$$

and Pines[14] and Silverstein[15] have shown that $\mathcal{K}(\alpha)$ is a function of a dimensionless parameter r_s. This parameter describes the mean separation of electrons and is defined by $4\pi (a_0 r_s)^3/3 = 1/n$ with a_0 the Bohr radius and n the number

of electrons per unit volume. Silverstein considered the effects of the electron-electron interactions in ~~liquid~~ alkali metals only and for these he finds $\mathcal{K}(\alpha) \sim 0.75$. Rossini[16] has used the same scheme to discuss the relaxation rates $(1/T_1)$ he observed in a series of polyvalent liquid metals. For gallium, rubidium, antimony, and indium he was able to fit his experimental results using the same value of $\mathcal{K}(\alpha)$. In view of this agreement it would seem reasonable to postulate that $\mathcal{K}(\alpha) \sim 0.75$ quite generally for liquid metals. As will be seen, however, this is not the case for pure bismuth if the observed linewidth is taken as a measure of $(1/T_1)_S$. Using eqn. 6.1, the expected width can be calculated as a function of $\mathcal{K}(\alpha)$ (using the measured Knight shift to represent K_s)

$\Delta B = 3.8 \times \mathcal{K}(\alpha)$ $(\times 10^{-4}$ tesla) at 780 K. It was seen in fig. 6.7 that at 780 K the linewidth is $5.9(\pm 0.1) \times 10^{-4}$ tesla. There is thus a clear discrepancy since $\mathcal{K}(\alpha)$ cannot exceed unity.

There are two possible explanations: firstly, the measured linewidth may not be purely that due to spin-lattice relaxation caused by the contact interaction and secondly, the measured Knight shift may be smaller than K_s due to the presence of an additional (negative) contribution. In fact, as is shown presently, it is believed that the full explanation involves both these effects. In the first place it will be shown that there is an additional relaxation mechanism that is important at lower temperatures and is quadrupolar in nature. In the second case, it is concluded, using a value $\mathcal{K}(\alpha) \sim 0.75$, that 'other' contributions to the Knight shift amount to approximately $-0.3_3 K_s$, and that these 'other' contributions are important at all

temperatures.

How does this 'other' negative contribution arise ? Rossini[16] has dealt with this problem for bismuth so let it suffice here to say that there are two, inseparable, possibilities. (i) There can arise an orbital contribution to the shift that may be written[17] as

$$K \sim 2\chi_{orb.} \langle 1/r^3 \rangle \Omega$$

where $\chi_{orb.}$ is the orbital susceptibility, $\langle 1/r^3 \rangle$ is the average value of $1/r^3$ for an atom and Ω is the atomic volume. (ii) There is also the possibility of a contribution from core polarisation[18] In the case of bismuth both effects may be expected to contribute, but evaluation of their magnitudes has not yet been accomplished. (For a number of light metals, calculations[18] have been made to determine the Knight shift contribution from core polarisation and the magnitude is approximately $0.1\,K_s$, see Chapter 4 for further details.) Both these contributions may be temperature dependent, but because the temperature coefficient of the observed shift is so small the effect of temperature is here neglected. As has been shown by Rossini for bismuth, neither of these interactions contributes importantly to the relaxation rate; for a Knight shift contribution from core polarisation of 30% K_s, the additional relaxation rate is only 4% T_{1s}, and this is quite negligible for this discussion. Using the experimentally observed width at 780 K, where there is reason to suppose (see section 6.04.2) that quadrupolar relaxation is also small so that the width is almost entirely due to $(1/T_1)_s$, eqn. 6.1 yields $K_s \sim 2.0\%$ and hence $K_{other} \sim -0.6_7\%$.

It must be emphasised that the above considerations only apply quantitatively when no quadrupolar contribution exists

and when $\mathcal{K}(\alpha) = 0.75$. Should quadrupolar relaxation be important or $\mathcal{K}(\alpha)$ be more nearly unity the estimate of $|K_{other}|$ would be too big. There has been a recent prediction, as yet unconfirmed by experiment, that $\mathcal{K}(\alpha)$ may indeed be more nearly unity at high temperatures for heavy metals, due to 'motional' reduction of the exchange interaction by rapid spin-flip scattering of the conduction electrons[19]; however, even if this suggestion is subsequently confirmed the discussion in the following sections will not be invalidated.

6.04.2 Quadrupolar relaxation It is proposed to continue the discussion of the ^{209}Bi linewidth by looking in detail at the temperature dependence. This has been replotted for 100% Bi in fig. 6.9. At low temperatures there is a distinct flattening and even a hint of a minimum. The linewidth tends asymptotically to a proportionality with absolute temperature as required by a modified Korringa prediction (using $\mathcal{K}(\alpha) = 0.75$ and allowing for K_{other}). The difference between experiment and the Korringa prediction is plotted as ΔB_q and is seen to decrease rapidly with increasing temperature. The direct T_1 measurements of Rossini on bismuth were not sufficiently accurate to show up this effect unambiguously, although there is a hint of such an extra contribution to the relaxation rate.

The most likely source of this extra width is an electric quadrupole interaction. A nuclear spin $I > \frac{1}{2}$ having an electric quadrupole moment Q, can relax by interaction with the fluctuating electric field gradient q, produced by the diffusive motion of surrounding atoms. A simple computation shows that when nuclei have a substantial electric quadrupole

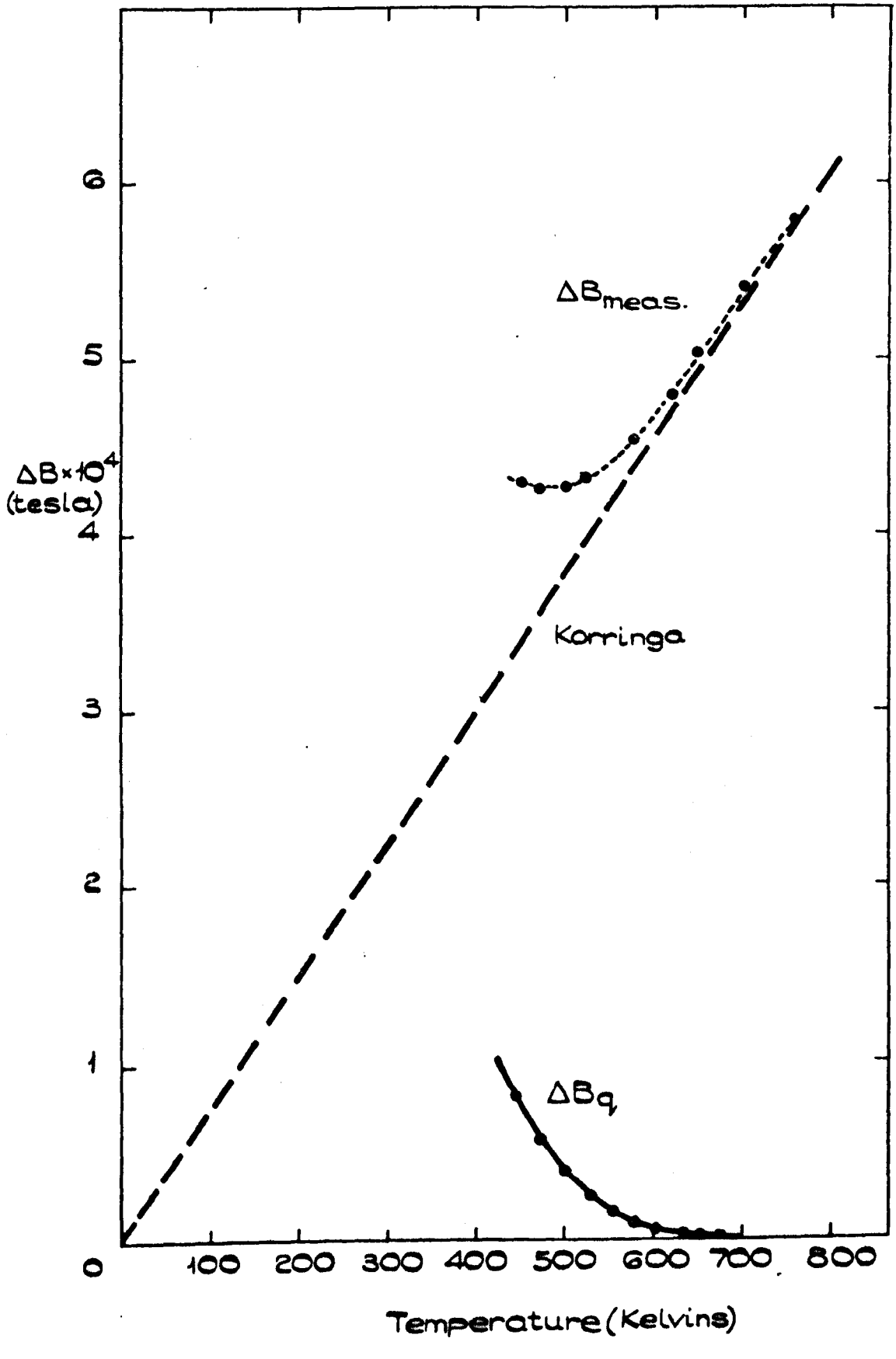

Figure 6.9. ^{209}Bi LINE WIDTH IN 100% Bi AS A FUNCTION OF TEMPERATURE.

moment the relaxation rate produced by the fluctuations of the dipole-dipole interaction is likely to be two orders of magnitude smaller than the quadrupolar induced rate. Similarly. the relaxation rate produced by the pseudo-dipolar interaction is small. Normally in liquids the frequencies of fluctuations of this type extend up to about 10^{12} H_z so that for nuclear spin precession frequencies of the order of 10^7 H_z, one is clearly in the extreme narrowing regime. For this case the relaxation rate is given (Abragam[20]) by

$$\left(\frac{1}{T_1}\right)_q = \frac{3}{80}\,\frac{2I+3}{I^2(2I-1)}\left\{\frac{eQ}{\hbar}\right\}^2 J(0) \qquad 6.2$$

where $J(\omega)$ is the spectral density of the fluctuations of field gradient defined by

$$J(\omega) = \int_{-\infty}^{\infty} e^{-i\omega\tau}\, g(\tau)\, d\tau \qquad 6.3$$

$$g(\tau) = \overline{F(t-\tau)\, F(t)} \qquad 6.4$$

and here $F(t)$ is a function of the second derivatives of the potential at the nucleus evaluated at time t. When $g(\tau)$ is evaluated in the normal correlation time approximation,

$$g(\tau) = \overline{|F(0)|^2}\quad \exp(-\tau/\tau_c) \qquad 6.5$$

the relaxation rate becomes

$$\left(\frac{1}{T_1}\right)_q = \frac{3}{40}\,\frac{2I+3}{I^2(2I-1)}\left\{\frac{eQq}{\hbar}\right\}^2 \tau_c \qquad 6.6$$

For spins $I > \frac{1}{2}$ in non-metallic liquids quadrupolar relaxation has been known for some time[21] to be the dominant mechanism. In the cases where $\{eQq/h\}$ was known eqn. 6.6 gave reasonable values for the correlation time, τ_c. For liquid

metals little work had been published up to 1967. At this time three groups published calculations of the quadrupolar relaxation rates in a number of liquid metals.

Using eqn. 6.6 Rossini et al.[22] discussed T_1 results in liquid indium. They divided q, the electric field gradient, into a part (q_i) due to ions and a part (q_e) due to the effect of these ions on the conduction electrons. Considering liquid indium as a vibrating body-centred-cubic arrangement, they obtained an expression for the r.m.s. field gradient produced by deviations of r, θ and φ from the cubic values. Using the idea of the outer p-electrons as providing directional bonds an expression for q_e was obtained, the value being large compared with that of q_i. The correlation time was derived from diffusion data in terms of an r.m.s. jump distance. The value of the jump distance required to make the result (eqn. 6.6) agree with experiment was found to be a reasonable fit to that deduced from the width of the first peak in the radial distribution function.

Borsa and Rigamonti[23] subsequently calculated quadrupolar relaxation rates on a model of diffusing screened ionic charges. They assumed that an ionic effective point charge Ze produced a screened coulombic potential

$$V(r) = \frac{Ze}{r} \exp(-\alpha_s r) \qquad 6.7$$

where the screening constant α_s is related to the free electron density of states per unit volume by $\alpha_s^2 = 4\pi e^2 \rho(E_F)$. Using eqn. 6.2 and 6.5, with a Sternheimer[24] ionic antishielding factor γ_∞ (see Appendix III), an expression

$$\left(\frac{1}{T_1}\right)_q = \frac{\pi}{90} \frac{2I+3}{I^2(2I-1)} \frac{e^4Q^2}{\hbar^2} \frac{NZ^2(1-\gamma_\infty)^2}{Dd} f(\alpha_s d) \qquad 6.8$$

was obtained. Here D is the diffusion coefficient, d the closest distance of approach, N is the ionic number density and

$$f(x) = \exp(-x)\left\{9 + \frac{37}{4}x + \frac{7}{2}x^2 + \frac{1}{2}x^3\right\}.$$

The essential difference between this treatment and that of Rossini et al. is that here q is assumed to arise solely from charges entirely external to the ion in question, whereas the other model attributes the gradient largely to the conduction electrons in the immediate vicinity of the nucleus concerned. Perhaps the uncertainty inherent in these calculations is shown by the fact that both of the formulations gave values of relaxation rates of the right order of magnitude to explain the experimental results available at the time.

The third contribution to the theory of quadrupolar relaxation rates in liquid metals was more fundamental. Using the screened interatomic potential of amplitude A,

$$V(r) = A \frac{\cos(2k_F r)}{(2k_F r)^3} \qquad 6.9$$

Sholl[25] found the approximate result

$$\left(\frac{1}{T_1}\right)_q = \frac{\pi}{75} \frac{2I+3}{I^2(2I-1)} \left\{\frac{(1-\gamma_{eff.})eQ}{\hbar}\right\}^2 \frac{N}{D} x \int_o^\infty f(r)\, G(r)\, dr \qquad 6.10$$

where

$$f(r) = (2k_F)^2 \left[\frac{7(2k_F r)^2 \sin(2k_F r) + (15-(2k_F r)^2)\cos(2k_F r)}{(2k_F r)^5}\right] \qquad 6.11$$

and

$$G(r) = \frac{g^{\frac{1}{2}}(r)}{r}\left\{\int_0^r f(r_1)\, g^{\frac{1}{2}}(r_1)\, r_1^4\, dr_1 + r^5 \int_r^\infty \frac{f(r_1)\, g^{\frac{1}{2}}(r_1)\, dr_1}{r_1}\right\} \qquad 6.12$$

with $g(r)$ the radial distribution function. Sholl used an almost-neutral-atom antishielding factor $(1 - \gamma_{eff.})$ which he evaluated by fitting his calculated field gradient $q = Aq_0(1 - \gamma_{eff.})$ to the measured quadrupole coupling constant in the solid metal (for the particular cases of indium and gallium).

The three approaches are basically very similar. Sholl is the most fundamental, but it involves evaluation of some very complicated integrals. His treatment of the electronic contribution to the electric field gradient is to include its effect in a modified antishielding factor whilst Rossini approaches the same problem by considering separately directional covalent bonding. Borsa[26] maintains that his expression 6.8, can be shown to be analogous to Sholl's formalism, but he neglected to account for any local electronic contribution to the electric field gradient.

6.04.3 Results for pure bismuth Whatever theory has been developed to discuss quadrupolar relaxation in liquid metals the relaxation rate is always shown to be proportional to $(1/D)$, where D is the diffusion coefficient. Although there are other temperature dependent terms in the expressions it is from D that the major temperature dependence arises. There is much discussion at the present time about the exact form of the temperature dependence of D (for details see Nachtrieb[27]) but for the purposes of this discussion an Arrhenius form will be assumed. This form, $D = D_0 \exp(-Q/RT)$, has been shown to describe the experimental diffusion data for nearly all pure liquid metals, with $Q \sim 3RT_m$, by Saxton and Sherby[28]. It is thus reasonable

to expect

$$\left(\frac{1}{T_1}\right)_q \propto \exp(3T_m/T) \qquad 6.13$$

or $$\ln\left[(1/T_1)_q\right] = 3T_m/T + \text{constant} \qquad 6.14$$

i.e. a graph of $\ln\left[(1/T_1)_q\right]$ or $\ln[\Delta B_q]$ versus 1/T should be a straight line with gradient $\sim 3T_m$. Figure 6.10 shows a semi-logarithmic plot of ΔB_q against 1/T. A straight line will indeed fit the data but the experimental uncertainty is so large that the only conclusion one can draw is that in the temperature range investigated

$$\ln(\Delta B_q) \propto C\ T_m/T$$

where the constant C lies between 3 and 4.5. Thus one can say that the temperature dependence of $(1/T_1)_q$ agrees with that predicted by eqn. 6.14, but is no real test of its validity.

It is tempting to check the applicability of the three approaches by calculating the magnitude of the relaxation rate expected in pure liquid bismuth. However this exercise is not very profitable in view of the large uncertainties in several of the quantities involved. Nevertheless Borsa[23] has attempted to evaluate $(1/T_1)_q$ from eqn. 6.8 using an antishielding factor of $\sim$100, a distance of closest approach of 0.24 nm (determined from Sharrah et al.) and a diffusion coefficient from the literature (Gearzynsky[29]). He obtained a value $17.2 \times 10^3\ s^{-1}$ at 578 K, with an uncertainty which was not stated but may be as high as a factor of 3 in either direction. This is equivalent to an extra linewidth of 4.4×10^{-4} tesla. The observed extra value, ΔB_q, at 578 K is 0.25×10^{-4} tesla. Allowance for any electronic effects by introduction of a modified $(1 - \gamma_\infty)$ increases the discrepancy.

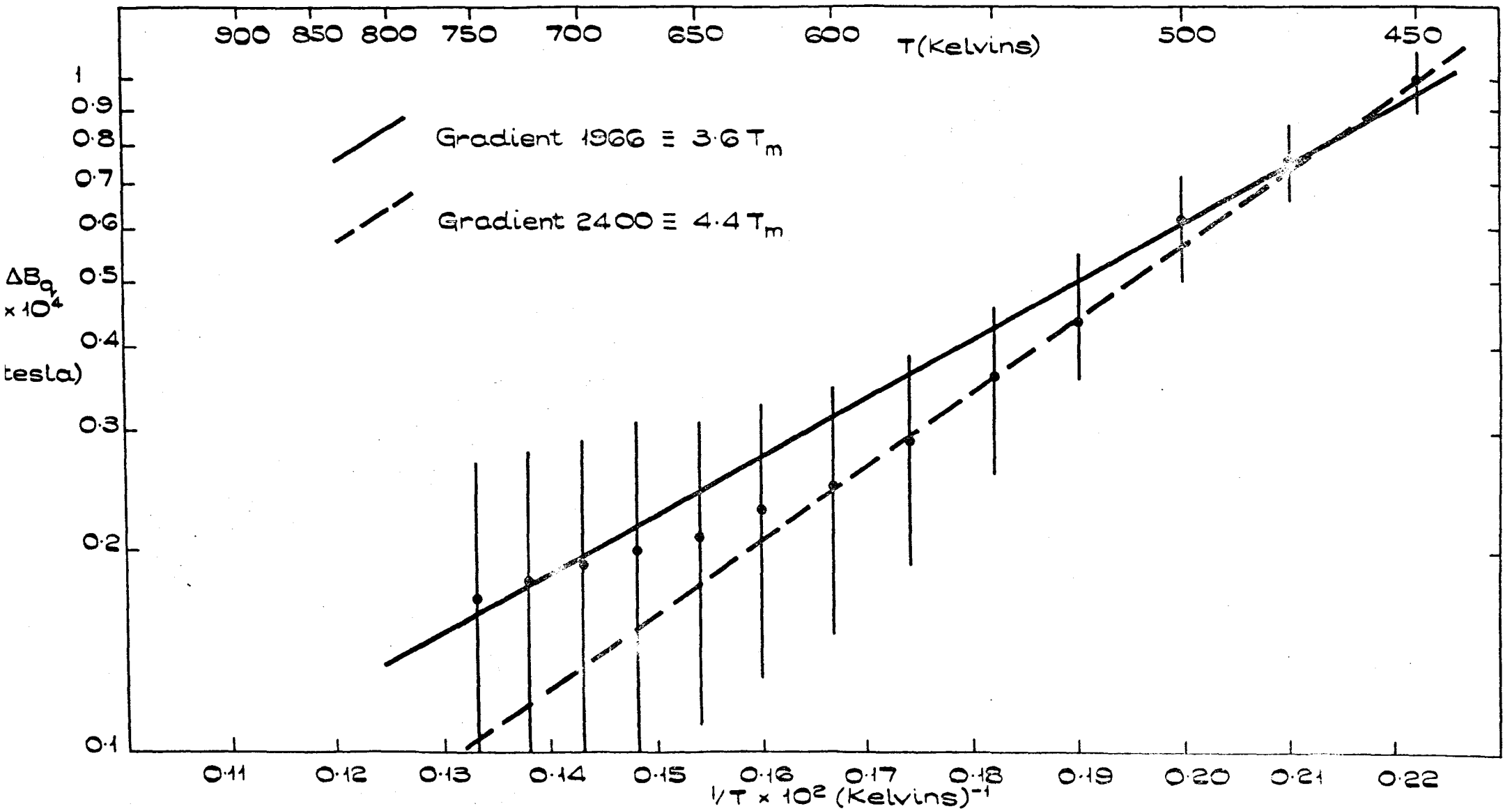

Figure 6.10. SEMI-LOG PLOT OF QUADRUPOLAR CONTRIBUTION TO THE LINE WIDTH.

6.04.4 Conclusions for pure bismuth It is apparent then, that the linewidth results obtained in pure bismuth can be explained on the basis of two contributions.

(i) Spin-lattice relaxation through the contact interaction. Evaluation of this term via the Korringa relation is complicated, in this case, by the effect of 'other' Knight shift contributions. The data suggest that these 'other' contributions have a magnitude of $\sim -0.3_3 K_s$.

(ii) Spin-lattice relaxation through a quadrupolar interaction. This is only appreciable at lower temperatures and its observation was only possible because measurements could be made in the super-cooled region. The temperature dependence of the quadrupolar rate is in qualitative agreement with that predicted theoretically on the basis of diffusing ions. Its absolute magnitude is far smaller than is predicted by eqn. 6.8; the intrinsically more satisfactory theory of Sholl has not been tested in this respect for bismuth but for indium and gallium it gives results within a factor of 2 or 3 of those observed.

6.04.5 Relaxation in liquid alloys Before discussing more fully the results obtained for the ^{209}Bi linewidth in the Pb-Bi system, it is proposed to detail the basic assumptions that will be made, and have been made in the above discussion of pure bismuth.

The whole of the discussion rests on the validity of the Korringa relation. As discussed earlier, the validity of this relation has been proven many times over for pure liquid metals. In an alloy system, however, the problem is more difficult. What is needed is a set of data where the measured

Knight shift is known to be the s-state contact contribution only (suggesting light elements), and where the measured relaxation time is the contact part only (non-quadrupolar nuclei). Such measurements are not at present available. Perhaps then it would suffice to look at linewidths instead of relaxation rates, as we have done in pure bismuth. This incorporates a second assumption, the equality of T_1 and T_2.

All theories of relaxation show that in the liquid phase $T_2 = T_1$, yet up till 1965 the experimental results on liquid sodium showed that the ratio $T_1/T_2 > 1$. This discrepancy was eliminated by Hanabusa[30] who showed that in molten sodium, T_2 was very sensitive to 'solid surface' effects and therefore to the state of oxidation of the particles. By careful distillation and reduction using hydrogen gas he was able to get results for T_1 and T_2 that agreed within the experimental uncertainty. Such contamination problems are unlikely to be as severe for other metals as they are in the highly reactive alkalis and the assumption $T_1 = T_2$ is unchallenged in pure liquid metals. However, in molten sodium - thallium alloys (another highly reactive system) Hanabusa obtained small differences between T_1 and T_2 but with the quoted experimental uncertainties these differences are not considered to be indicative of a breakdown of $T_1 = T_2$ in alloys.

Liquid sodium shows a very large change in the Knight shift on adding thallium. This change, via the Korringa relation in the simple form $T_1TK^2 =$ constant, predicts a decrease in the relaxation rate upon addition of Tl but experimental values show a small increase occurs. Hanabusa[30] corrected his relaxation

rates for 'solid surface' effects and quadrupolar relaxation (assumed to be independent of concentration) but was still unable to fit the experimental data to the Korringa relation. He concluded, after considering many possible relaxation mechanisms, that the Korringa relation should be modified on alloying through the terms

$$\left\{\frac{\rho(E_F)}{\rho^0(E_F)} \quad \frac{\chi_p}{\chi_p}^0\right\} = 1 + \beta c \qquad 6.15$$

where c is the atomic concentration of solute, and β is a constant depending on the alloy system, which for Na - Tl alloys is 3.7. Thus Hanabusa maintains that he has experimental evidence for a modification of the Korringa relation in alloys. This is indeed likely, because $\mathcal{K}(\alpha)$ must be expected to depend on solute concentration since, in general, this will change the electron density and hence the strength of the electron - electron interactions.

There is, however, another possibility here that would not exist were $I = \frac{1}{2}$ for ^{23}Na - the possibility of an increased quadrupolar rate on alloying. Hanabusa dismissed this possibility summarily but it is apparent that his Na - 16% Tl sample shows a definite minimum in the relaxation rate as a function of temperature. This suggests that the quadrupolar relaxation rate has increased on alloying, but without more detailed observations across the whole of the concentration range it is difficult to draw any firm conclusions. Another consideration suggesting that the quadrupolar explanation is more likely is that in the system In - Ga which has been investigated across the whole concentration range the ^{115}In resonance shows a different width variation from the ^{69}Ga. It will be shown later that

this difference is readily explicable on the basis of enhanced quadrupolar relaxation in alloys.

From this brief discussion of the situation we are forced to two conclusions.

(i) The assumption $T_1 = T_2$ is valid in pure liquid metals and in liquid alloys.

(ii) There is doubt as to whether T_1TK^2 is independent of concentration in liquid alloys and it seems intuitively sensible to expect $\int(\alpha)$ to be modified somewhat on alloying.

The position at the time of writing is such that without clarification by further experiment, a discussion of relaxation rates in liquid alloys can only proceed by assuming that T_1TK^2 = constant. This is implicit in all the following discussion.

6.04.6 <u>^{209}Bi linewidths in liquid alloys - Identification of quadrupolar component</u> There are a number of reports of relaxation rates in liquid alloy systems where quadrupolar relaxation is possible. The results of these are summarised in fig. 6.11. This is not intended to contain all the linewidth (and relaxation rate) data but it does contain the results of the more reliable and complete investigations. In this figure, all the data have been converted (where necessary) to linewidths and the Korringa prediction is shown dotted. Too much importance should not be attached to the absolute magnitudes because in most cases the results have been taken from published figures; however the trends in the variations have been retained. It is perhaps worth noting that the effects shown for Na and Ga would not be detectable using wide-line continuous wave n.m.r. because they represent such small changes

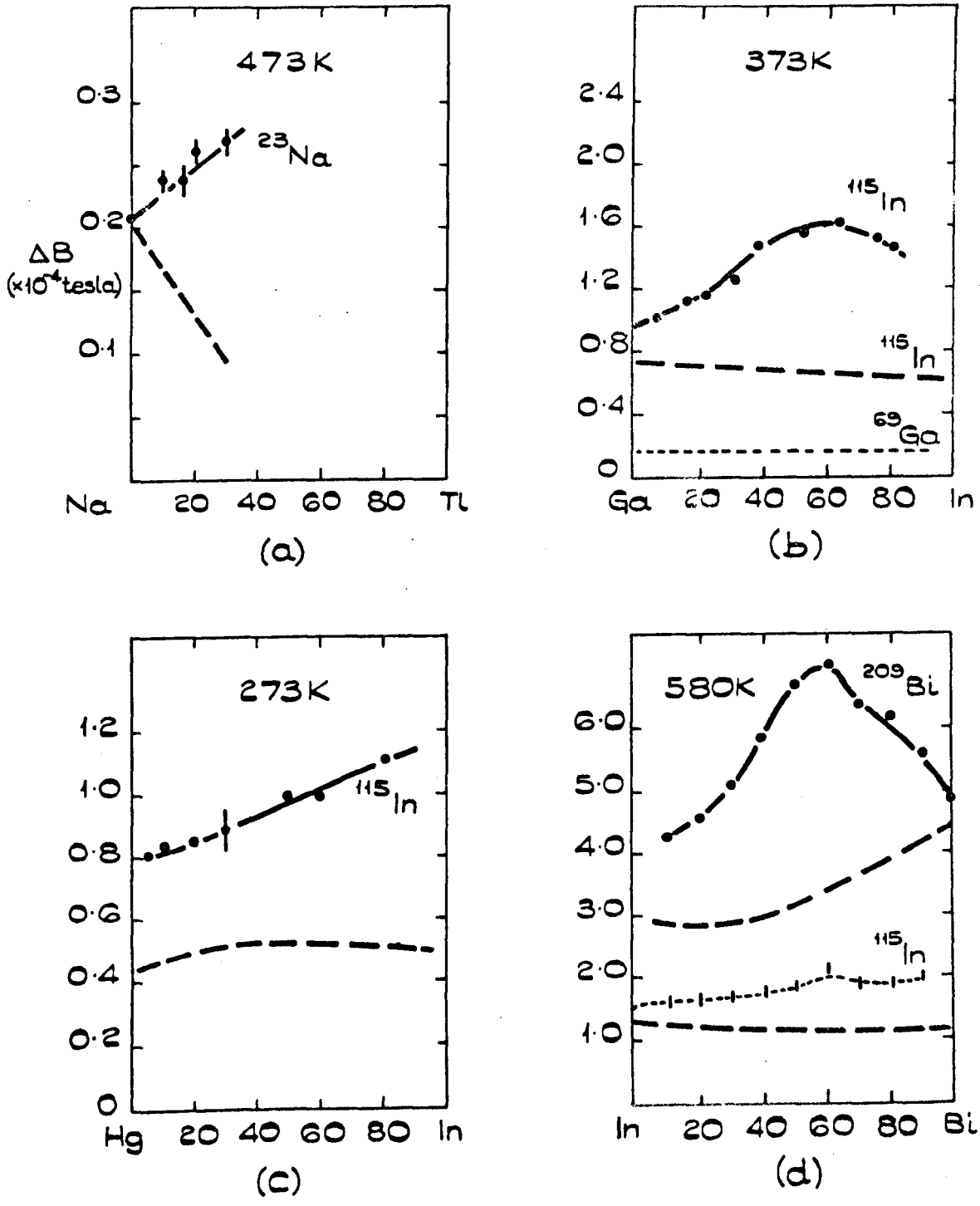

Figure 6.11.

SUMMARY OF LINE WIDTH (AND RELAXATION ~~NOTE~~ RATE) DATA IN QUADRUPOLAR LIQUID ALLOY SYSTEMS

(a) ^{23}Na - Tl : HANABUSA[28] T_1 DATA USED.

(b) ^{115}In - ^{69}Ga : BORSA ET AL.[24] $1/T_1$ DATA USED.

(c) ^{115}In - Hg : BORSA ET AL.[24] $1/T_1$ DATA USED.

(d) ^{115}In - ^{209}Bi : STYLES[1]. LINE WIDTH DATA USED.

to small linewidths.

In the Pb - Bi system the ^{209}Bi linewidth shows a definite maximum at approximately 50% Bi. Figure 6.12 shows the ^{209}Bi width as a function of concentration together with the Korringa prediction. The difference between the Korringa value (calculated on the basis of the measured Knight shift change) and the observed value is plotted as ΔB_q in the same figure. This contribution goes through a sharp maximum at 50%. These results are surprisingly similar to those of Styles[1] in the In - Bi system, and to those of Borsa[26] on the ^{115}In resonance in the In - Ga system. (The In - Hg system behaves atypically as it does in many other respects.) Thus there is something rather striking to explain in these alloy systems.

In fig. 6.13 the temperature dependence of the ^{209}Bi width for Pb - 60% Bi is shown, again with the Korringa prediction

$$(T_1TK^2)_{100\%\ Bi} = (T_1TK^2)_{60\%\ Bi} \qquad 6.16$$

and the difference, ΔB_q. Following an argument similar to that employed for pure bismuth $\ln(\Delta B_q)$ has been plotted in fig. 6.14 against reciprocal temperature. The result is a surprisingly good straight line with gradient 2.3 T_m, and it is maintained that this is very strong evidence for the suggestion that the increased width on alloying is due to an increased effectiveness of quadrupolar relaxation. There seems little doubt that the results obtained in this alloy conform to eqn. 6.14 and therefore to quadrupolar relaxation induced by ionic diffusion i.e. fig. 6.12 indicates that by alloying Bi with Pb the quadrupolar relaxation rate has been increased by approximately an order of magnitude. It was found that such a good straight line could not be obtained

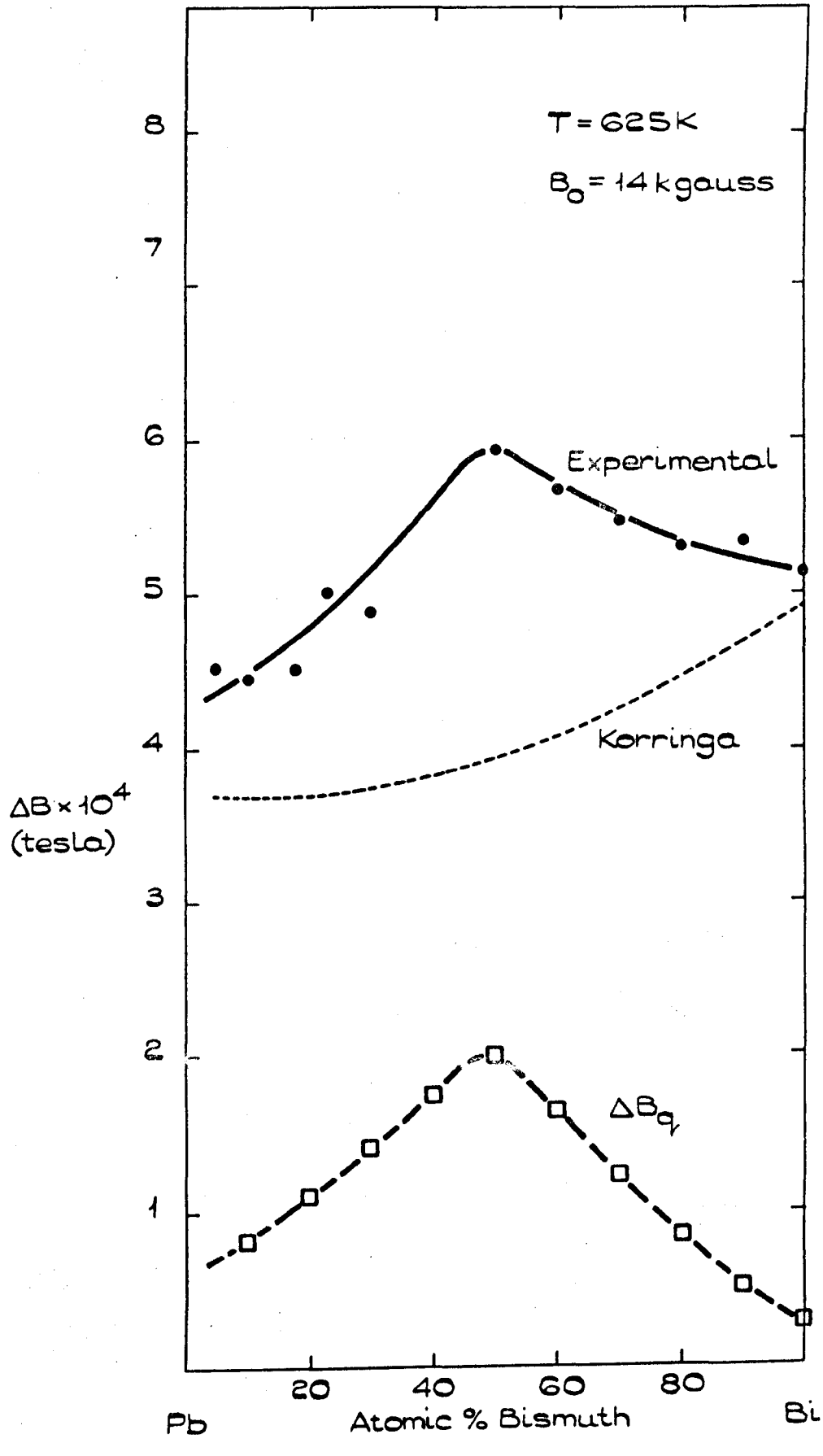

Figure 6.12. SHOWS THE COMPARISON OF EXPERIMENT AND KORRINGA PREDICTION FOR THE LINE WIDTH OF ^{209}Bi IN Pb-Bi ALLOYS.

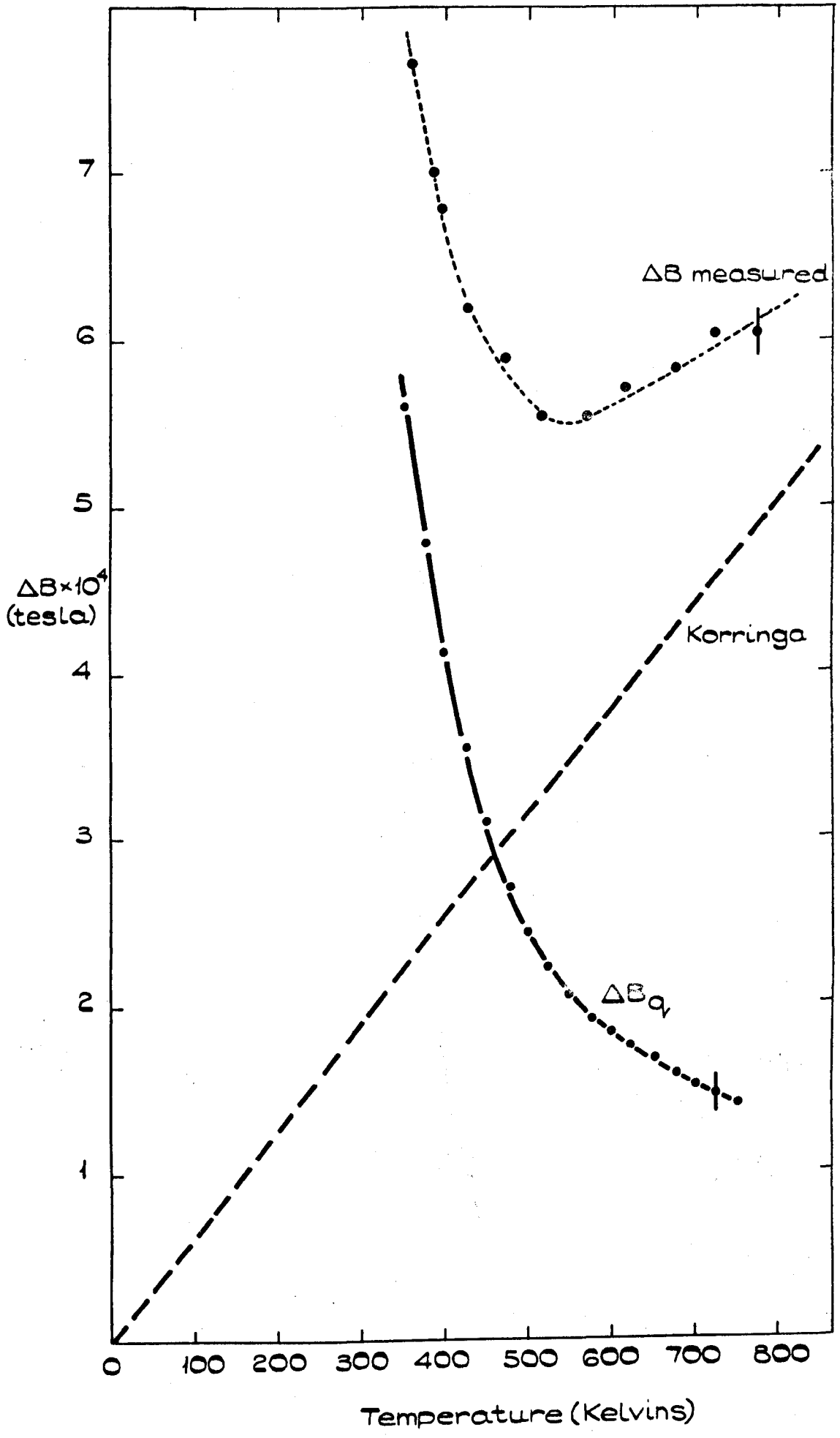

Figure 6.13. LINEWIDTH VARIATION OF ^{209}Bi IN Pb-60%Bi AS A FUNCTION OF TEMPERATURE.

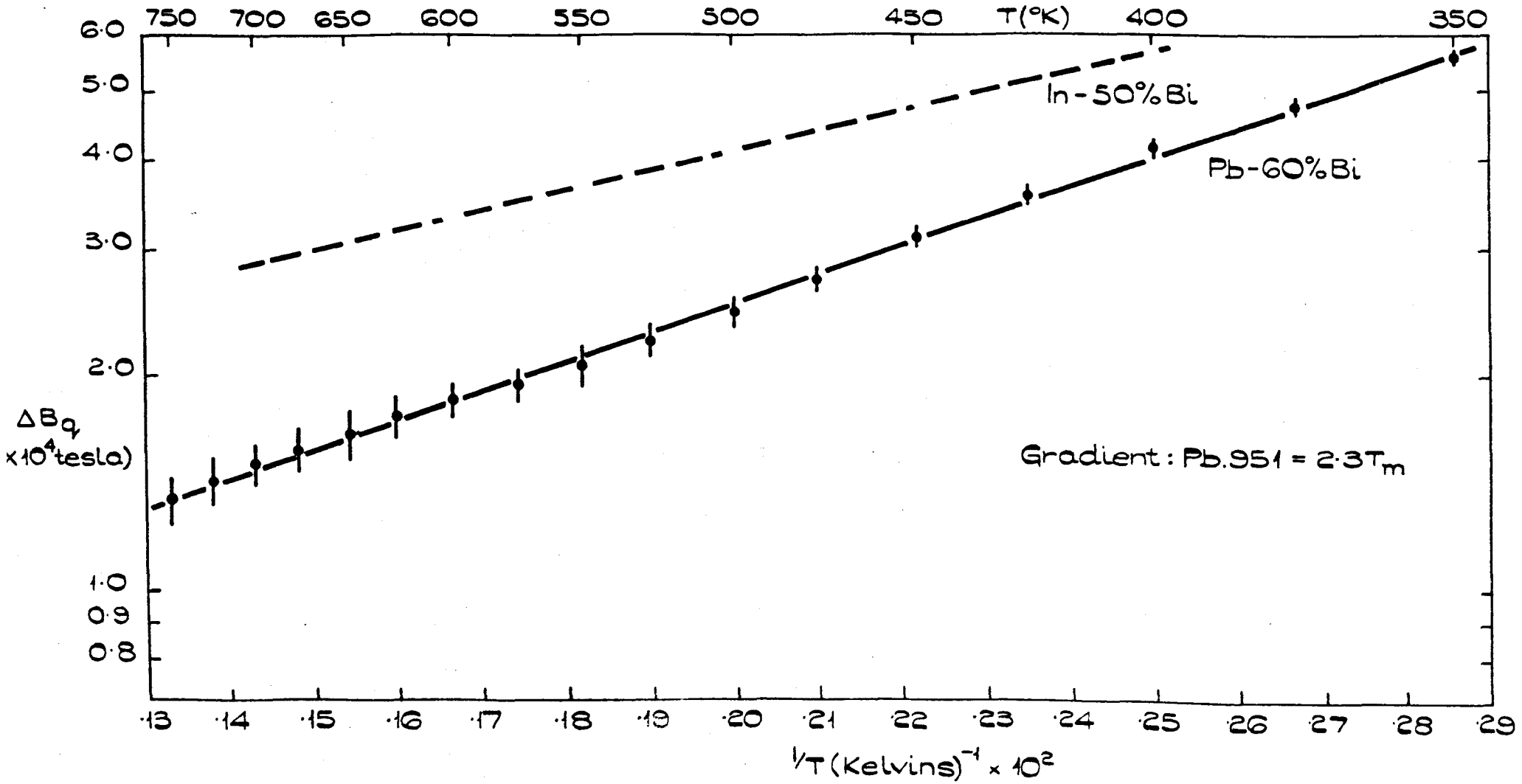

Figure 6.14. SEMI-LOG PLOT OF THE QUADRUPOLAR CONTRIBUTION TO THE LINE WIDTH OF ^{209}Bi IN Pb-60% Bi, In-50% Bi AS A FUNCTION OF THE RECIPROCAL TEMPERATURE.

if the Korringa equality (eqn. 6.16) was not assumed; even a 10% change in the Korringa product between metal and alloy would produce a significant deviation from linearity.

If the observed effect is indeed due to an enhanced quadrupolar rate it would be expected to occur for all quadrupolar nuclei in all liquid alloys. It would, of course, occur to differing extents because of the basic differences in the strength of the interaction for different nuclei in different environments. In particular the interaction depends on the nuclear spin and quadrupole moment and on the Sternheimer antishielding factor (as well as on the diffusion coefficient and the radial distribution function). On the basis of eqn. 6.6, Table 6.1 has been constructed to show the relative magnitudes of the quadrupolar relaxation rates predicted for nuclei in a common environment. It is interesting to compare these predictions with the experimental 'extra' widths ΔB_q plotted in fig. 6.15.

Firstly ^{209}Bi, as predicted, shows a larger effect than ^{115}In in In - Bi, and ^{115}In shows a larger effect than ^{69}Ga in In - Ga. The 'observed' ΔB_q are difficult to assess accurately but they certainly do not disagree with the predicted ratios 4 : 1 for Bi : In and 4 : 1 for In : Ga. Of course these ratios could be affected if the liquid alloys are not ideally substitutional, when differences in partial structure factors could affect different nuclei in different ways. It does not appear to be necessary to call on any drastic effect of this sort to explain the observations.

Secondly, it would seem from the comparison of ^{209}Bi widths in Pb - Bi and in In - Bi at closely similar temperatures,

Table 6.1

Relevant quadrupolar parameters for Eqn. 6.6

Nucleus	I	eQ [a]	$(1-\gamma_\infty)$ [b]	$\frac{2I+3}{I^2(2I-1)} e^2Q^2(1-\gamma_\infty)^2$
^{209}Bi	9/2	-0.4	80(±20) [c]	80
^{115}In	9/2	0.8	20(±5)	20
^{69}Ga	3/2	0.2_3	8(±2)	4.5
^{23}Na	3/2	0.1	4.5(±0.5)	0.3

(a) Varian Associates, n.m.r. Table, 5th Edition.

(b) Taken from a survey of the literature. The uncertainties are the mean deviation from the mean of the available theoretical estimates, references to which are contained in Appendix III.

(c) For details of the method used to estimate γ_∞ for Bi see Appendix III.

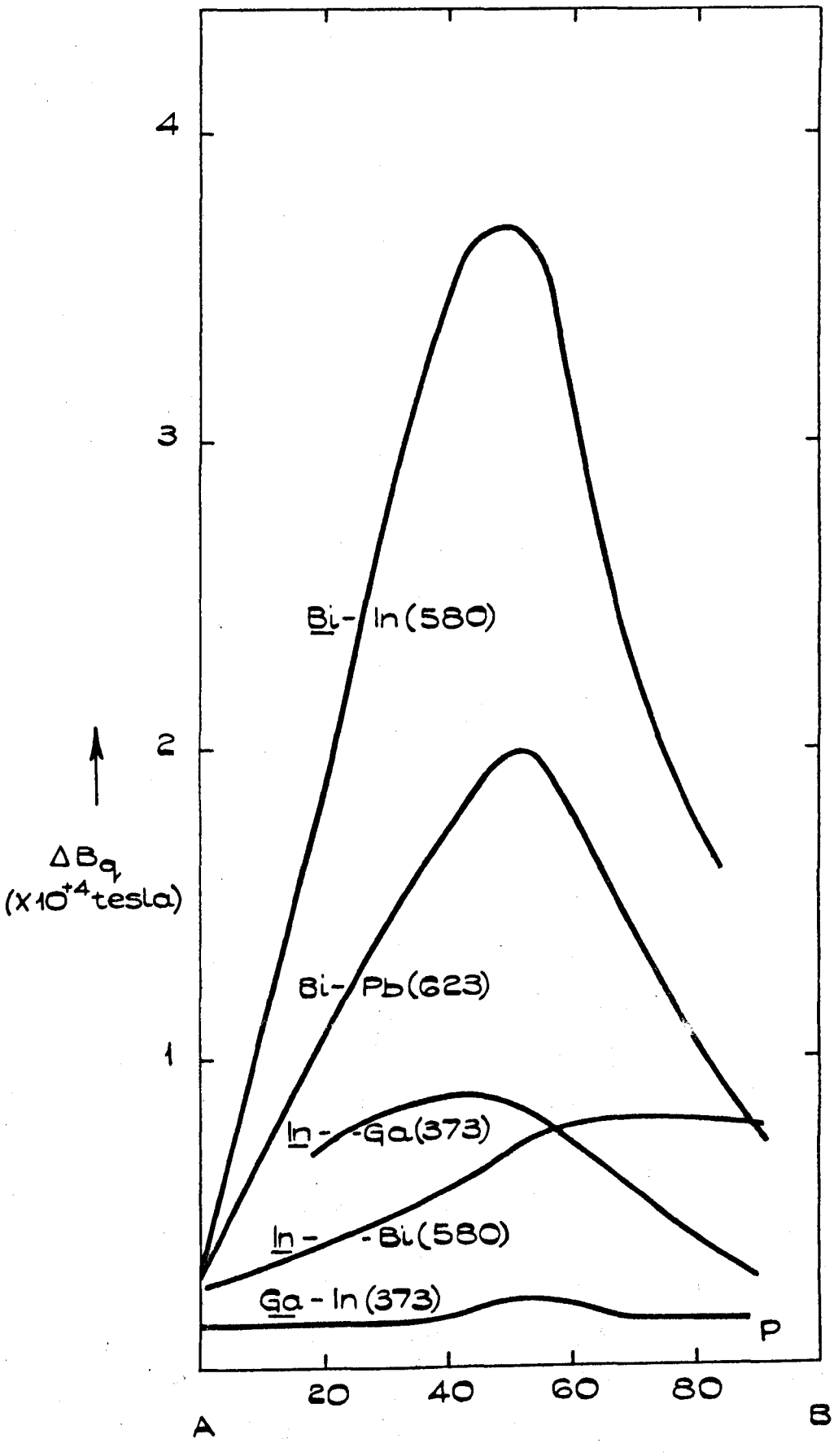

Figure 6.15. SCHEMATIC VARIATION OF EXTRA LINE WIDTH WITH CONTRATION IN A SERIES OF ALLOYS.

that solute-solvent valence difference is an important factor in the increase of the field gradient with increase of solute concentration. This conclusion appears to be supported by the measurements of Moulson[31] on the Sb - Bi system, where there is no valence difference, and within an uncertainty of $\sim 0.8 \times 10^{-4}$ tesla no maximum in the linewidth; however these measurements were made at 800 K where the effect would in any case be smaller. The presence of a maximum in Ga - In shows clearly that valence difference is not the only factor, but a really meaningful comparison of the observed ^{115}In widths in Ga - In and in Bi - In is prevented by the wide difference between the temperatures used. It is, therefore, maintained that the agreement between experiment and the relative magnitudes predicted on the basis of quadrupolar effects is strong additional evidence that the increased width is indeed due to an enhanced quadrupolar rate,

6.04.7 ^{209}Bi linewidths in liquid alloys - Origin of the enhanced quadrupolar component It has been pointed out in the last section that valence differences cannot be the source of the whole of the linewidth increase in these alloy systems. Other possible sources of the increase are now examined.

Styles[1] suggested that the maximum in the ^{209}Bi width at In - 50% Bi was due to an enhanced quadrupolar interaction caused by preferential bonding between unlike atoms with a life-time of an InBi grouping of about 1μs - a relic of the solid intermetallic compound. Such a suggestion is ~~untenable~~ unlikely in general since, in the Pb - Bi system for instance, no intermetallic compounds exist in the solid phase. Moreover the fact that the temperature dependence in In - 50% Bi gave an activation energy

of $\sim 1.8\,T_m$ (shown dotted in fig. 6.14), rather than $2.3\,T_m$ may have been a result of the uncertainty in the modulation correction used. Thus it is possible even in this case that a normal diffusion activated process without any preferential bonding may be adequate to explain the observations; the possible existence of such bonding will not be considered further.

Another possibility, tentatively suggested by Borsa[26] for In - Ga, is that the diffusion coefficient could pass through a minimum half way across the concentration range. There seems no reason to suppose either that this would occur consistently in all three systems discussed, or that the required order of magnitude change in D is to be expected. Moreover, although no diffusion measurements are available, Arpi[8] has measured the viscosity coefficient η for the Pb - Bi system and this shows an almost monotonic increase from Bi to Pb. Since D is inversely proportional to η (see for instance Saxton and Sherby[28]), this trend is far too small in magnitude, and has the wrong concentration dependence, to explain the observations. This possibility will also be discarded, therefore.

It is clear, then, that attention must be concentrated on the factor q^2. In principle it is possible to extend the theory of Sholl to alloys by including partial structure factors. This would produce an extremely involved expression and in addition care would be necessary to ensure that the ensemble averaging was done at the correct stage of the computation. This latter point has been missed by Bonera et al.[26]; in extending their expression 6.8 to alloys they merely added the separate contributions to q^2. Each of these contains an ensemble average,

and in essence therefore they assumed that $\overline{q_1^2} + \overline{q_2^2} = \overline{(q_1 + q_2)^2}$ In order to discuss the possible effect of alloying upon the mean square field gradient a very crude model will thus be used. By this means it is possible to show simply, why an enhancement of the quadrupolar rate might be expected in alloys with a maximum at about 50%. It will be assumed that the only important contribution to the mean square field gradient comes from nearest neighbours and that the ions other than nearest neighbours have the same effect in the alloy as they do in the pure liquid metal. For simplicity a model with twelve nearest neighbours will be assumed (this is reasonable for most liquid metals, but is perhaps not so good for bismuth) the neighbours being arranged on an f.c.c. lattice. These ions (represented by point charges) vibrate and diffuse causing an electric field gradient, fluctuating about zero, at the central nucleus. It is the non-zero mean square value of this field gradient that causes the quadrupole relaxation in pure liquid metals. If one of the surrounding point charges Z, is replaced by a different charge Z′, then in addition to the fluctuations already discussed there will be a further field gradient due to just a single charge (Z - Z′) in one of the nearest neighbour positions. Similarly if more impurities are considered, different field gradients are possible. Figure 6.1b shows schematically the situation for a random substitutional model.

This figure represents a series of random pulses of heights determined by the number of impurities in the nearest neighbour positions, and length determined by the time an impurity spends in the nearest neighbour position. Following an early

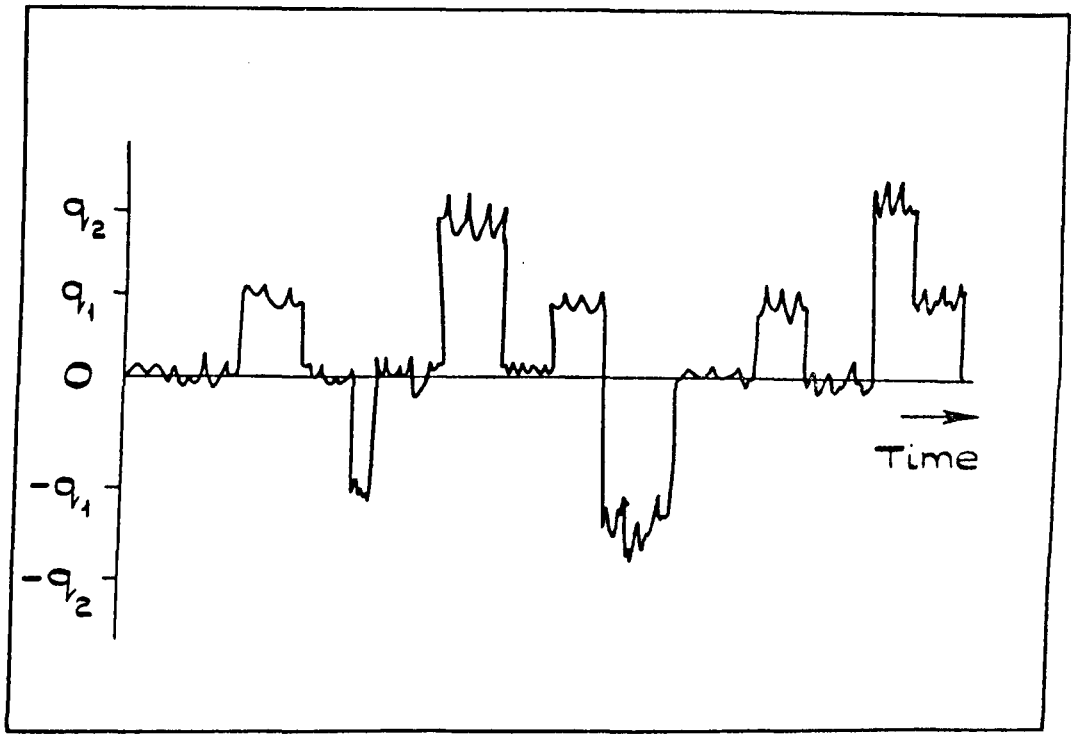

Figure 6.16

discussion of diffusing vacancies (Bloembergen[32]), the probability of one impurity being in a nearest neighbour position is denoted P_1, of two impurities is denoted P_2 ..... The corresponding field gradients are q_1, q_2 ..... where q_2, for instance, can take a series of values depending on the relative positions of the two impurity atoms. Neglecting the small fluctuations due to the motions of like ions the correlation function is given by

$$\overline{F(t)\,F(t-\tau)} = \left\{ \sum_{i=0}^{12} P_i \overline{[q_i]^2} \right\} \exp(-\tau/\tau_c) \qquad 6.17$$

and the quadrupolar rate by,

$$\left(\frac{1}{T_1}\right)_q \simeq \frac{3}{40} \frac{2I+3}{I^2(2I-1)} \frac{e^4Q^2}{\hbar^2} (1-\gamma_\infty)^2 \left\{ \sum_{i=0}^{12} P_i \overline{[q_i]^2} \right\} \tau_c \qquad 6.18$$

In fact only terms i = 1 → 11 contribute to the summation because in this approximation no field gradient is produced by a nearest neighbour shell completely filled with either host or impurity. The evaluation of the field gradient from a distribution of charges randomly placed on f.c.c. lattice is not a trivial

problem. The field gradient produced is a 3 by 3 tensor with in general 5 independent coefficients. The tensor must be diagonalised to give the field gradient components along the principal axes of the system, and all three diagonal elements enter into the effective field gradient

$$q_{eff.} = \left[1 + \frac{\eta^2}{3}\right] \frac{\partial^2 V}{\partial z'^2}$$

where η is the asymmetry parameter difined by $\frac{V_{x\,x'} - V_{y\,y'}}{V_{z\,z'}}$.

This has been neglected in all the foregoing because in general $\eta \ll 1$ (typically 0.05 for Gallium[25]). A full evaluation of the field gradient would be a very complicated problem, not warranted by the crudeness of the model. As an approximation, the $\langle 100 \rangle$ direction has been taken to be a principal axis and the summation (for all possible configurations of impurity ions in near neighbour positions) gives

$$\sum_{i=1}^{11} P_i \overline{[q_i]^2} = (z - z')^2 \frac{e^2}{r^6} \left[A_1 x y^{11} + A_2 x^2 y^{10} \ldots\ldots A_{11} x^{11} y\right] \qquad 6.19$$

where $x \equiv c$, the concentration of impurities, $y \equiv 1 - c$ and the constants

$$A_1 = A_{11} = 6$$
$$A_2 = A_{10} = 84$$
$$A_3 = A_9 = 270$$
$$A_4 = A_8 = 560$$
$$A_5 = A_7 = 1380$$

and $A_6 = 840$. If the quantity inside the square bracket of eqn. 6.19 is evaluated then the curve of fig. 6.17 is obtained i.e. this crude model succeeds in predicting a maximum at c = 0.5.

The shape of the curve does not agree quantitatively with the observed dependence and the predicted proportionality of the peak height with $(z - z')^2$ is not completely borne out in practice either. However it is easy to see how the model could be extended so as to yield a maximum even when host and impurity ions carry the same charge; account could be taken of an ionic size difference, and hence of a difference in distance of nearest approach (the lattice points being effectively displaced inwards or outwards when occupied by an impurity). The calculation carries through in a completely analogous fashion, so that the occurrence of the maximum is independent of the particular feature by which the two types of ion differ.

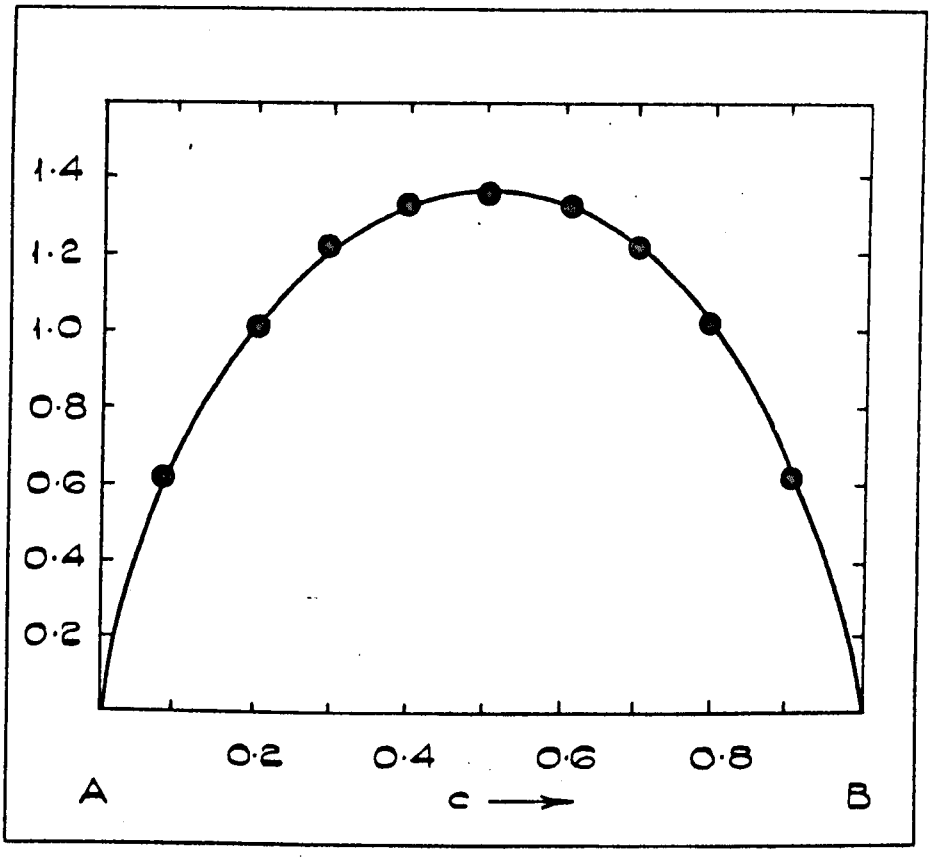

Figure 6.17

6.04.8 Conclusions It has been shown for pure bismuth that there is a temperature dependent quadrupolar contribution to the linewidth. The variation of this 'extra' width with temperature follows a relation.

$$\Delta B_q \propto \exp(-C\, T_m/T) \qquad 6.20$$

where $C \simeq 3$. This type of temperature variation was shown to

be due to an ionic diffusion activated process. Previous experimenters had attributed such 'extra' widths to a quadrupolar mechanism but the experimental data left doubt as to the origin of the effect. Clark[33] maintains that in liquid indium, antimony and InSb the 'extra' relaxation rate (i.e. width) could be proportional to the absolute temperature and explains this in terms of scattering of the conduction electrons on the Fermi surface. Such effects had been considered by Mitchell[34] for Bloch electrons, and did produce a small quadrupolar rate proportional to temperature. From the temperature dependence in pure bismuth it is deduced that Fermi surface scattering is not an important mechanism.

The temperature dependence of the 'extra' width in liquid alloys has also been shown to decrease with increasing temperature as described by eqn. 6.20 with C = 2.3, and the good straight line obtained suggested that any modification of the Korringa relation on alloying was not greater than 10% for the liquid Pb - Bi system.

Further, the 'peaking' of the ^{209}Bi linewidth about 50% was discussed in terms of a crude diffusing impurity ion model which gave qualitative agreement with the observations. The relative magnitudes of this effect in a series of liquid alloys was shown to be in accord with that expected for a quadrupolar interation.

In order to substantiate these conclusions on the alloy linewidths, further experimental results are required. An interesting possible experiment is a complete systematic investigation of the Cd - Sn, In - Sn and Sb - Sn systems. In

the first system both nuclei have $I = \frac{1}{2}$ and would be expected to show no maximum and follow, roughly, the Korringa prediction. The second system should give a maximum for the ^{115}In nucleus and no maximum for the ^{119}Sn. The final system is perhaps the most attractive possibility because the existence of the isotopes ^{121}Sb and ^{123}Sb should allow accurate separation of the quadrupolar relaxation rates, and, in addition, a large interaction would be expected. With the availability of these data a more detailed and complete understanding of relaxation processes in liquid alloys is anticipated.

References

(1) Styles G. A., Adv. in Phys., 16, (1967), 275.

(2) Hanabusa M. and Bloembergen N., J. Phys. Chem. Sol., 27, (1966), 363.

(3) Dutchak Ya. I. and Klym N. M., Phys. Met. and Metall, 19b, (1965), 128.

(4) Kaplow R., Strong S. L. and Averbach B. L., Local Atomic arrangement studied by X-ray diffraction (ed. Cohen & Hilliard, N.Y., pub. Gordon and Breach, 1966).

(5) Sharrah P. C., Petz J. I. and Kruh R. F., J. Chem. Phys., 32, (1960), 241.

(6) Seymour E. F. W., Styles G. A. and Taylor B., Proc. XIth Colloque Ampère, (1962), 612.

(7) Kubaschewski O. and Catterall J. A., Met. Phys. and Phys. Mettall., 3, (Perg. Press 1956), 124.

(8) Arpi R., Z. Metallographie, (1914), 156.

(9) Honda K. and Endo H., J. Inst. Met., 37, (1927), 447.

(10) Matuyama Y., Sci. Rep. Tohoku Univ., 16, (1927), 447.

(11) Furukawa K., Rep. Prog. Phys., 25, (1962), 395.

(12) Smith G. W., J. Appl. Phys., 35, (1964), 1218.

(13) Narath A., Hyperfine Interactions, (A.P. 1967), ed. Freeman and Frankel, 330.

(14) Pines D., Sol. State Phys., 1, (A.P. 1955), 367.

(15) Silverstein D., Phys. Rev., 128, (1962), 631; ibid, 130, (1963). 912.

(16) Rossini F., Tech. Report No. 10, (1968), Univ. of California, Berkeley.

(17) Noer R. J. and Knight W. D., Rev. Mod. Phys., 36, (1964), 177.

(18) Shyu W. M., Das T.P. and Gaspari G. D., Phys. Rev., 152, (1966), 270.

(19) Warren W. W., Clark W. G. and Pincus P., Sol. State Commun., 6, (1968), 371.

(20) Abragam A., Princ. of Nuc. Mag., (O.U.P. 1961), 314.

(21) Pound R. V., Phys. Rev., 72, (1947), 1273.

(22) Rossini F. A., Geissler E., Dickson E. M. and Knight W. D., Adv. in Phys., 16, (1967), 287.

(23) Borsa F. and Rigamonti A., Nuovo Cimento, 48, (1967), 194.

(24) Sternheimer R. M., Phys. Rev., 146, (1966), 140.

(25) Sholl C. A., Proc. Phys. Soc., 91, (1967), 130.

(26) Bonera G., Borsa F. and Rigamonti A., XV Colloque Ampère, (1968).

(27) Nachtrieb N. H., Adv. in Phys., 16, (1967), 309.

(28) Saxton J. and Sherby O. D., Amer. Soc. Met. Quart., 55, (1962), 826.

(29) Gearzynsky J., Proc. Phys. Soc., 81, (1963), 745.

(30) Hanabusa M., Tech. Rept. 470, Cruft Lab., Harvard Univ., (1965).

(31) Moulson D., Ph.D. Thesis, Univ. of Leeds, (1966).

(32) Bloembergen N., Defects in Solids - Rept. of Bristol Conference, (1954), 1.

(33) Warren W. W. and Clark W. G., Phys. Rev., 177, (1969), 600.

(34) Mitchell A. H., J. Chem. Phys., 26, (1957), 1714.

CHAPTER SEVEN

SYNOPSIS

The experimental and theoretical situation in liquid metal physics at the beginning of this work was discussed in Chapter 1. It was shown that the free-electron theory seemed adequate for a discussion of most electronic properties of liquid metals and that changes in these properties on freezing indicated a departure from free-electron ideas. The Knight shift data appeared to contradict information derived from other electronic properties although some suggestions had been made to explain the discrepancy. In addition the variation of the Knight shift with temperature and with alloying had in general been treated from, on the one hand, the Faber pseudopotential approach and, on the other hand, the Friedel scattering theory. It was hoped that the work involved in the thesis might cast some light on the general position of the Knight shift in liquid metal physics and enable a consistent approach to be used in discussing shifts in alloys.

We have seen that the absolute value of K in a metal (solid or liquid) can be calculated to a good approximation on the basis of a zero-order pseudopotential technique. The expression given by Holland has been extended to take account of non-constancy of the assumed pseudowavefunction over an ion core and in general excellent agreement with experiment obtained. This calculation is based on a single O.P.W. and a free-electron situation. We note that Holland has shown that, for the

evaluation of the electron density at a nuclear site, using linear combinations of O.P.W.'s the expression for P_F reduces to that obtained for a single O.P.W. The approach is thus general and this fact suggests that P_F will not be sensitive to band structure effects and therefore will be constant with temperature. The extension of his scheme to take account of non-constancy does introduce some temperature dependence but we have seen that this is a very small effect. We have, then, an explanation of why the Knight shift is constant with temperature for many metals. In addition, the calculation suggests that any large observed changes in K with temperature are due to changes in χ_p rather than in the factor P_F. Of course, the situation is not quite as simple as this suggests because relativistic core functions are not generally available (and we have shown that they are necessary for heavier elements) and core-polarisation and orbital contributions to the observed shift cause difficulties. However, in general the Knight shift is better understood than seemed the case at the beginning of the work.

Perhaps the only notable exception to the agreement between the calculated value of K and the observed value is that of mercury. We can take refuge here in the fact that Hg shows a number of anomalous properties and has been the subject of much discussion in the literature. In general the proffered explanation of the strange properties of Hg has been a low density of states at the Fermi surface. From the results of Chapter 4 it seems that the real explanation is more complicated than this for if $\rho(E_F)$ were considerably below the free-electron value a much larger discrepancy between the calculated value of K and the observed value would occur. In this context it seems that the

Knight shift may well be interpreted as an indication of whether χ_p is free-electron like or not. Certainly χ_p should be sensitive to any deviation from free-electron behaviour and the Knight shift ought to be a sensitive test. This presents a further complication in the discussion of alloys and in the present work the free-electron expression for χ_p has been assumed to apply.

During the course of this work the strange situation has arisen where the absolute value of K is determined by the term to zero-order in the pseudopotential whilst any change (with temperature or alloying) is dominated by the term to first-order in the pseudopotential. As far as temperature effects are concerned the first-order term has been directly shown to contain the dominant temperature dependence. The evidence in the case of alloying is less direct. For reasons discussed in Chapter 5 (notably the uncertainty in U(K) and the lack of precise knowledge of the partial structure factors) the Faber expression has not been used to evaluate the dependence of K on solute concentration. The coarser, though similar, method of Friedel has been used and has given encouraging results if the somewhat empirical Flynn-type phase shifts are used. This method evaluates the 'screening' effects just as does the Faber expression and therefore, indirectly, supports the suggestion that first-order effects dominate the concentration dependence of K. In essence, then, little really useful progress has been made when discussing alloying effects but we can conclude that with improved energy dependent pseudopotentials and partial structure factors an explanation may be available. Nearly-free-electron ideas are adequate within the existing uncertainties, not the least of which is the variation of the core-polarisation Knight shift with alloying.

With regard to the particular case of lead, the advent of liquid alloy results has eliminated the discrepancies between theory and experiment giving a particularly illustrative demonstration of the relative simplicity of the liquid state. In considering how the differences arose a qualitative discussion in terms of overlapping bands was given, but no quantitative work is possible at the moment. It is however possible to conclude that susceptibility effects are much more important in the solid than in the liquid and far more detailed investigation of solid solutions is necessary before an understanding will be available.

The investigation of the Pb - Bi system has cleared part of the situation and in addition has illustrated a certain lack of definite knowledge. The latter point concerns the Korringa relation in alloys; the conclusions of Chapter 6 suggest avenues for further research and an understanding of how the Korringa relation is modified on alloying must be obtained before really conclusive discussions of linewidths in alloys are possible. The first point above concerns the sensitivity of the Knight shift to local order. It now seems that K is perhaps not as sensitive to the state of local order as was supposed at the beginning of this work. Certainly it is not sensitive to any changes in local order that may exist in the Pb - Bi system and in addition does not appear to be sensitive to local order in the noble metal-tin systems.

We must conclude, therefore, that the detailed dependence of the Knight shift on solute concentration in binary liquid alloys is not fully understood at the present although there are signs that an understanding may be available with improved 'input' functions. The situation in pure liquid metals

is far better understood. The Knight shift value and its temperature dependence has been explained and with the advent of improved core functions, pseudopotentials and structure factors it seems likely that even better agreement with experimental results will be available.

APPENDIX I

The tables given are numbered so as to indicate the figures to which they refer.

Tables 3.1 and 3.2

The temperature dependence of the Knight shift K and the line width H of ^{207}Pb in pure lead

Conditions	Temp.(K)	$\delta K/K$ (%)	$\Delta B \times 10^4$ (tesla)
^{207}Pb	292	0	$3.9_5(\pm 0.1_0)$
Solid state	323	$0.25(\pm 0.1_5)$	$4.3_0(\pm 0.1_7)$
B_0 = 1.4 tesla	362	$0.75(\pm 0.1_5)$	$4.4_4(\pm 0.0_9)$
	391	$0.73(\pm 0.1_5)$	$4.5_6(\pm 0.1_2)$
	433	$1.08(\pm 0.1_8)$	$5.2_3(\pm 0.2_9)$
	454	$1.24(\pm 0.1_6)$	$5.0_0(\pm 0.3_0)$
	487	$1.49(\pm 0.0_9)$	$5.2_4(\pm 0.2_4)$
	520	$1.66(\pm 0.1_5)$	$5.0_0(\pm 0.2_3)$
	546	$2.01(\pm 0.1_5)$	$4.7_6(\pm 0.2_0)$
	565	$2.01(\pm 0.1_5)$	$4.7_6(\pm 0.1_4)$
^{207}Pb	558	$2.3_9(\pm 0.2_5)$	$4.9(\pm 0.3)$
Liquid state	588	$2.3_0(\pm 0.1_0)$	$5.0(\pm 0.4)$
	623	$1.7_6(\pm 0.2_5)$	$5.0(\pm 0.7)$
	675	$1.6_3(\pm 0.1_0)$	$4.5(\pm 0.5)$
	722	$1.3_8(\pm 0.2_6)$	$5.6(\pm 0.5)$
	781	$0.7_1(\pm 0.2_6)$	$5.0(\pm 0.3)$

Table 3.3

Relative change of the Knight shift with concentration of solute in Pb-Ag alloys

Nucleus	Conditions	Conc$^{n.}$ (At.%)	$\delta K/K$(%)
^{207}Pb	B_0 = 1.4 tesla	1	$+0.08(\pm 0.3_2)$
	T = 625 K	2.5	$+0.28(\pm 0.3_2)$
	T = 675 K	5	$+0.41(\pm 0.1_6)$

Table 3.4

Relative change of the Knight shift with concentration of solute in Pb-Cd alloys

Nucleus	Conditions	Conc$^{n.}$ (At.%)	$\delta K/K$(%)
^{207}Pb	B_0 = 1.4 tesla	5	$-0.41(\pm 0.1_0)$
	T = 625 K	10	$-0.65(\pm 0.2_0)$
		28	$-0.74(\pm 0.1_8)$
^{113}Cd		28	$-5.3(\pm .2)$

Table 3.5

Relative change of the Knight shift with concentration of solute in Pb-h alloys

Nucleus	Conditions	Conc$^{n.}$ (At.%)	$\delta K/K$(%)
^{207}Pb	B_0 = 1.4 tesla	5	$+0.08(\pm 0.3_2)$
	T = 625 K	10	$-0.14(\pm 0.1_6)$
		15	$-0.14(\pm 0.1_6)$

Table 3.6

Relative change of the Knight shift with the concentration of solute in Pb-Sb alloys

Nucleus	Conditions	Conc$^{n.}$ (At.%)	$\delta K/K$ (%)
^{207}Pb	B_0 = 1.4 tesla	5	$0.41(\pm 0.1_4)$
	T = 625 K	10	$1.07(\pm 0.3_0)$
		17.5	$1.4(\pm 0.0_7)$
			K(%)
^{121}Sb		5	0.657(±0.001)
		10	0.655(±0.002)
		17.5	0.651(±0.001)

Table 3.7

Relative change of the Knight shift with the concentration of solute in Pb-Au alloys

Nucleus	Conditions	Conc$^{n.}$ (At.%)	$\delta K/K$ (%)
^{207}Pb	B_0 = 1.4 tesla	5	$0.74(\pm 0.2_5)$
	T = 625 K	10	$1.1_5(\pm 0.40)$
		15	$2.4_0(\pm 0.2_5)$

Table 3.8

Relative change of the Knight shift with the concentration of solute in Pb-Hg alloys

Nucleus	Conditions	Conc$^{n.}$ (At.%)	$\delta K/K$ (%)
^{207}Pb	B_0 = 1.4 tesla	5	$-1.0_0(\pm 0.2_0)$
	T = 625 K	10	$-1.2_2(\pm 0.4_0)$
		20	$-4.3_0(\pm 0.2_0)$

Table 3.9

Relative change of the Knight shift with the concentration of solute in Pb-Tl alloys

Nucleus	Conditions	Conc$^{n.}$ (AT.%)	$\delta K/K$(%)
^{207}Pb	B_0 = 1.4 tesla	5	$-1.24(\pm 0.1_6)$
	T = 625 K	10	$-2.46(\pm 0.2_5)$
		20	$-4.8_5(\pm 0.4_0)$

Table 3.10

Relative change of the Knight shift with the concentration of solute in Pb-Bi alloys

Nucleus	Conditions	Conc$^{n.}$ (AT.%)	$\delta K/K$(%)
^{207}Pb	B_0 = 1.4 tesla	5	$1.0(\pm 0.3)$
		10	$1.8(\pm 0.3)$
		18	$3.2(\pm 0.1_5)$
^{209}Bi		5	$-4.3_3(\pm 0.2_3)$
		10	$-4.4_1(\pm 0.0_6)$
		18	$-4.5_5(\pm 0.0_7)$

Table 3.12

The temperature dependence of the Knight shift and linewidth in Pb - 18% Bi

Nucleus	T(K)	$\delta K/K(\%)$	$\Delta B \times 10^4$ (tesla)
^{207}Pb	293	$-3.1_0(\pm 0.3_0)$	28.4(±1.0)
Solid state	358	$-1.9_0(\pm 0.6_0)$	24.0(±0.5)
B_0 = 1.4 tesla	433	$-1.3_0(\pm 0.2_5)$	24.0(±0.9)
	453	$-1.1_0(\pm 0.7_0)$	18.2(±1.6)
	473	$-0.5_7(\pm 0.1_7)$	11.0(±1.4)
	493	$+0.0_8(\pm 0.4_4)$	7.6(±1.0)
Liquid state	573	$3.7_2(\pm 0.1_0)$	5.2(±0.2)
	623	$2.9_8(\pm 0.1_5)$	4.9(±0.4)
	673	$2.7_2(\pm 0.1_6)$	5.2(±0.4)
	726	$2.2_2(\pm 0.2_6)$	4.5(±0.5)
^{209}Bi	577	$-11.3_0(\pm 0.1_0)$	
Liquid state	620	$-11.9_0(\pm 0.1_0)$	
	680	$-12.2_5(\pm 0.1_0)$	
	718	$-12.5_5(\pm 0.1_0)$	
	765	$-12.9_0(\pm 0.2_0)$	

Table 3.13

The temperature dependence of the Knight shift and linewidth in Pb - 20% Tl

Nucleus	T(K)	$\delta K/K(\%)$	$\Delta B \times 10^4$ (tesla)
^{207}Pb	293	$-0.5_0(\pm 0.3_0)$	10.5(±1.0)
Solid state	445	$-0.5_7(\pm 0.4_0)$	10.5(±1.0)
B_0 = 1.4 tesla	519	$-1.2_0(\pm 0.6_0)$	8.6(±1.0)
	567	$-1.0_7(\pm 0.2_1)$	5.0(±0.5)
	600	$-0.8_2(\pm 0.4_0)$	5.0(±1.0)
Liquid state	639	$-5.0_0(\pm 0.2_0)$	
	708	$-5.7_5(\pm 0.4_0)$	5.0(±0.8)
	745	$-5.7_5(\pm 0.3_0)$	7.0(±0.8)
	791	$-6.5_0(\pm 0.2_0)$	

Table 6.2

Relative change of the Knight shift of ^{207}Pb and ^{209}Bi in Pb - Bi alloys

Nucleus	Conditions	Composition	$\delta K/K$ (%)
^{207}Pb	T = 625 K	100% Pb	0
	B_0 = 1.4450 tesla	Pb - 5% Bi	$0.9_5(\pm 0.0_2)$
	$(B/\nu)_{ref}$	Pb - 10% Bi	$1.6_5(\pm 0.0_3)$
	= 1.1237217	Pb - 18% Bi	$3.1_0(\pm 0.0_6)$
		Pb - 23% Bi	$4.4_0(\pm 0.0_9)$
		Pb - 30% Bi	$6.8_0(\pm 0.1_2)$
		Pb - 50% Bi	$13.3_0(\pm 0.3_0)$
		Pb - 60% Bi	$15.2_0(\pm 0.3_0)$
		Pb - 70% Bi	$18.0_0(\pm 0.2_0)$
^{209}Bi	$(B/\nu)_{ref}$	Pb - 5% Bi	$-11.7_0(\pm 0.2_0)$
	= 1.14615609	Pb - 10% Bi	$-11.8_2(\pm 0.0_8)$
		Pb - 18% Bi	$-11.9_5(\pm 0.0_4)$
		Pb - 23% Bi	$-10.8_7(\pm 0.1_5)$
		Pb - 30% Bi	$-10.7_2(\pm 0.1_0)$
		Pb - 50% Bi	$-8.6_0(\pm 0.0_4)$
		Pb - 60% Bi	$-7.4_8(\pm 0.0_4)$
		Pb - 70% Bi	$-5.5_8(\pm 0.0_4)$
		Pb - 80% Bi	$-3.2_3(\pm 0.0_4)$
		Pb - 90% Bi	$-2.1_0(\pm 0.0_4)$
		100% Bi	0

Table 6.3

Fractional change in ^{209}Bi Knight shift with temperature

Composition	Conditions	T(K)	$\delta K/K(\%)$
100% Bi	B_0 = 0.5750 tesla	457	$1.4_3(\pm 0.0_7)$
		465	$1.3_9(\pm 0.0_3)$
		474	$1.3_6(\pm 0.0_3)$
		483	$1.3_2(\pm 0.0_7)$
		501	$1.1_8(\pm 0.0_7)$
		523	$0.8_5(\pm 0.0_8)$
		573	$0.5_1(\pm 0.0_7)$
		587	$0.3_3(\pm 0.0_4)$
		619	$0.1_5(\pm 0.0_7)$
		644	$-0.2_2(\pm 0.0_4)$
		694	$-0.5_9(\pm 0.0_7)$
		753	$-1.1_8(\pm 0.0_7)$
Pb -80% Bi	B_0 = 0.5750 tesla	476	$-2.8_0(\pm 0.0_9)$
		503	$-2.4_2(\pm 0.0_8)$
		521	$-2.4_2(\pm 0.1_2)$
		563	$-2.8_6(\pm 0.0_3)$
		619	$-3.2_1(\pm 0.0_8)$
		687	$-3.7_5(\pm 0.0_4)$
		767	$-4.3_2(\pm 0.0_8)$

... continued ...

Table 6.3 continued

Composition	Conditions	T(K)	$\delta K/K(\%)$
Pb - 60% Bi	B_0 = 0.5750 tesla	357	$-5.8_7(\pm 0.0_3)$
		375	$-5.9_5(\pm 0.0_3)$
		394	$-6.1_0(\pm 0.0_4)$
		428	$-6.4_6(\pm 0.0_7)$
		473	$-6.4_6(\pm 0.0_6)$
		518	$-6.7_5(\pm 0.0_7)$
		570	$-7.1_2(\pm 0.0_7)$
		678	$-7.8_0(\pm 0.0_7)$
		722	$-8.1_0(\pm 0.0_7)$
		773	$-8.5_2(\pm 0.0_7)$
Pb-18% Bi	B_0 = 1.2500 tesla	578	$-11.3\ (\pm 0.0_7)$
		622	$-12.0\ (\pm 0.0_4)$
		673	$-12.3\ (\pm 0.0_4)$
		717	$-12.6\ (\pm 0.0_4)$
		765	$-13.0\ (\pm 0.1_0)$

Table 6.4

Fractional change in the ^{207}Pb Knight shift with temperature in some Pb - Bi alloys

Sample	Conditions	T(K)	$\delta K/K(\%)$
Pb - 60% Bi	B_0 = 1.4000 tesla	438	$16.8(\pm 0.1_0)$
		483	$16.2(\pm 0.1_5)$
		558	$15.6(\pm 0.3_0)$
		627	$15.0(\pm 0.1_7)$
Pb - 18% Bi	B_0 = 1.2500 tesla	573	$3.6_2(\pm 0.0_7)$
		623	$2.8_8(\pm 0.1_6)$
		673	$2.6_3(\pm 0.1_5)$
		725	$2.1_4(\pm 0.2_4)$

Table 6.5

^{209}Bi linewidths in a series of Pb - Bi alloys

Conditions	Composition	Temperature	$\Delta B \times 10^4$ (tesla)
B_0 = 1.4450 tesla	Pb	—	—
Modulation (p - p)	Pb - 5% Bi	623	$4.5_6(\pm 0.3_1)$
= 3.6×10^{-4} tesla	Pb - 10% Bi	585	$4.6_4(\pm 0.6_5)$
	"	623	$4.4_1(\pm 0.3_5)$
	Pb - 18% Bi	623	$4.5_1(\pm 0.1_0)$
	Pb - 23% Bi	623	$5.0_0(\pm 0.0_7)$
	Pb - 30% Bi	512	$4.9_8(\pm 0.1_0)$
	"	623	$4.8_5(\pm 0.1_7)$
	Pb - 50% Bi	431	$6.6_0(\pm 0.1_2)$
	"	623	$5.9_2(\pm 0.0_7)$
	Pb - 60% Bi	423	$6.3_2(\pm 0.1_2)$
	"	623	$5.6_5(\pm 0.1_5)$
	Pb - 70% Bi	444	$6.0_6(\pm 0.1_5)$
	"	623	$5.4_5(\pm 0.0_4)$
	Pb - 80% Bi	506	$5.1_6(\pm 0.1_5)$
	"	623	$5.3_1(\pm 0.1_0)$
	Pb - 90% Bi	538	$4.8_9(\pm 0.0_6)$
	"	623	$5.4_1(\pm 0.2_4)$
	Bi	565	$4.6_6(\pm 0.1_5)$
	"	623	$5.0_6(\pm 0.1_5)$

Table 6.6

^{209}Bi linewidth, concentration dependence at 625 K and 0.5750 tesla

Composition	$\Delta B \times 10^4$ tesla
Pb	—
Pb - 18% Bi	$4.5_3(\pm 0.2_1)$
Pb - 30% Bi	$4.9_5(\pm 0.1_0)$
Pb - 50% Bi	$5.7_3(\pm 0.1_2)$
Pb - 60% Bi	$5.7_1(\pm 0.1_2)$
Pb - 70% Bi	$5.6_1(\pm 0.1_2)$
Pb - 80% Bi	$5.4_1(\pm 0.1_2)$
Bi	$4.7_7(\pm 0.0_8)$

Table 6.7(a)

Variation of the ^{209}Bi linewidth with temperature in a series of Pb - Bi alloys

Sample	Conditions	Temperature (K)	$\Delta B \times 10^4$ (tesla)
100% Bi	B_0 = 0.5750 tesla	458	4.3_3 ($\pm 0.1_4$)
		465	4.4_1 ($\pm 0.1_0$)
		474	4.3_1 ($\pm 0.1_2$)
		483	4.3_0 ($\pm 0.0_5$)
		501	4.3_1 ($\pm 0.1_2$)
		523	4.3_6 ($\pm 0.1_5$)
		573	4.5_7 ($\pm 0.1_2$)
		645	5.0_7 ($\pm 0.1_2$)
		753	5.7_4 ($\pm 0.1_2$)
Pb - 80% Bi	B_0 = 0.5750 tesla	476	5.5_3 ($\pm 0.1_5$)
		503	5.0_5 ($\pm 0.0_4$)
		521	5.2_5 ($\pm 0.0_6$)
		563	5.2_4 ($\pm 0.1_2$)
		620	5.4_1 ($\pm 0.0_6$)
		688	5.6_8 ($\pm 0.1_4$)
		768	5.9_2 ($\pm 0.1_5$)
Pb - 60% Bi	B_0 = 0.5750 tesla	357	7.6_5 ($\pm 0.2_4$)
		375	7.0_6 ($\pm 0.1_5$)
		395	6.8_0 ($\pm 0.1_0$)
		427	6.2_1 ($\pm 0.2_0$)
		473	5.9_0 ($\pm 0.2_0$)
		518	5.5_4 ($\pm 0.0_5$)

... continued ...

Table 6.7(a) continued

Sample	Conditions	Temperature (K)	$\Delta B \times 10^4$ (tesla)
		570	5.5_6 ($\pm 0.1_5$)
		613	5.7_2 ($\pm 0.0_7$)
		677	5.8_4 ($\pm 0.2_5$)
		721	6.0_6 ($\pm 0.1_3$)
		773	6.0_2 ($\pm 0.3_0$)
Pb - 18% Bi	B_0 = 1.2500 tesla	577	4.5_1 ($\pm 0.1_8$)
		620	4.5_1 ($\pm 0.1_0$)
		680	5.0_2 ($\pm 0.2_5$)
		718	5.2_3 ($\pm 0.2_2$)
		765	5.4_5 ($\pm 0.4_5$)

Table 6.7(b)

^{209}Bi linewidth variation with magnetic field

Composition	B_0 (tesla)	$\Delta B \times 10^4$ (tesla)
Pb - 60% Bi	0.3210	6.3_4 ($\pm 0.2_3$)
	0.4753	6.3_5 ($\pm 0.1_6$)
438 K	0.8410	6.2_3 ($\pm 0.1_5$)
	1.0005	6.2_0 ($\pm 0.1_5$)
	1.1894	6.3_0 ($\pm 0.2_3$)
	1.4530	6.1_8 ($\pm 0.1_4$)
100% Bi	0.3210	4.4_6 ($\pm 0.1_2$)
	0.8400	4.4_1 ($\pm 0.1_7$)
570 K	0.9970	4.3_2 ($\pm 0.0_9$)
	1.1893	4.3_4 ($\pm 0.0_3$)
	1.4520	4.4_3 ($\pm 0.0_6$)

APPENDIX II

Evaluation of the terms b_n, Θ^1_{nk} and Θ^2_{nk} of Chapter 4.

The evaluation of these terms was performed using the University of Warwick Elliott 4100 computer and the radial functions needed were obtained from Herman F. and Skillman S. Atomic Structure Calculations, Prentice-Hall Inc., New Jersey, 1963.

The program to evaluate b_n etc. is given below; firstly in block diagram form and then fully; the language used was ALGOL 60.

$$\alpha = \Psi(0)$$

$$b_n = \int d^3\underline{r}\, \Psi^*(\underline{r})$$

$$\Theta^1_{nk} = -\int d^3\underline{r}\, \Psi^*(\underline{r})\, i(\underline{k}.\underline{r})$$

$$\Theta^2_{nk} = -\tfrac{1}{2}\int d^3\underline{r}\, \Psi^*(\underline{r})(\underline{k}.\underline{r})^2$$

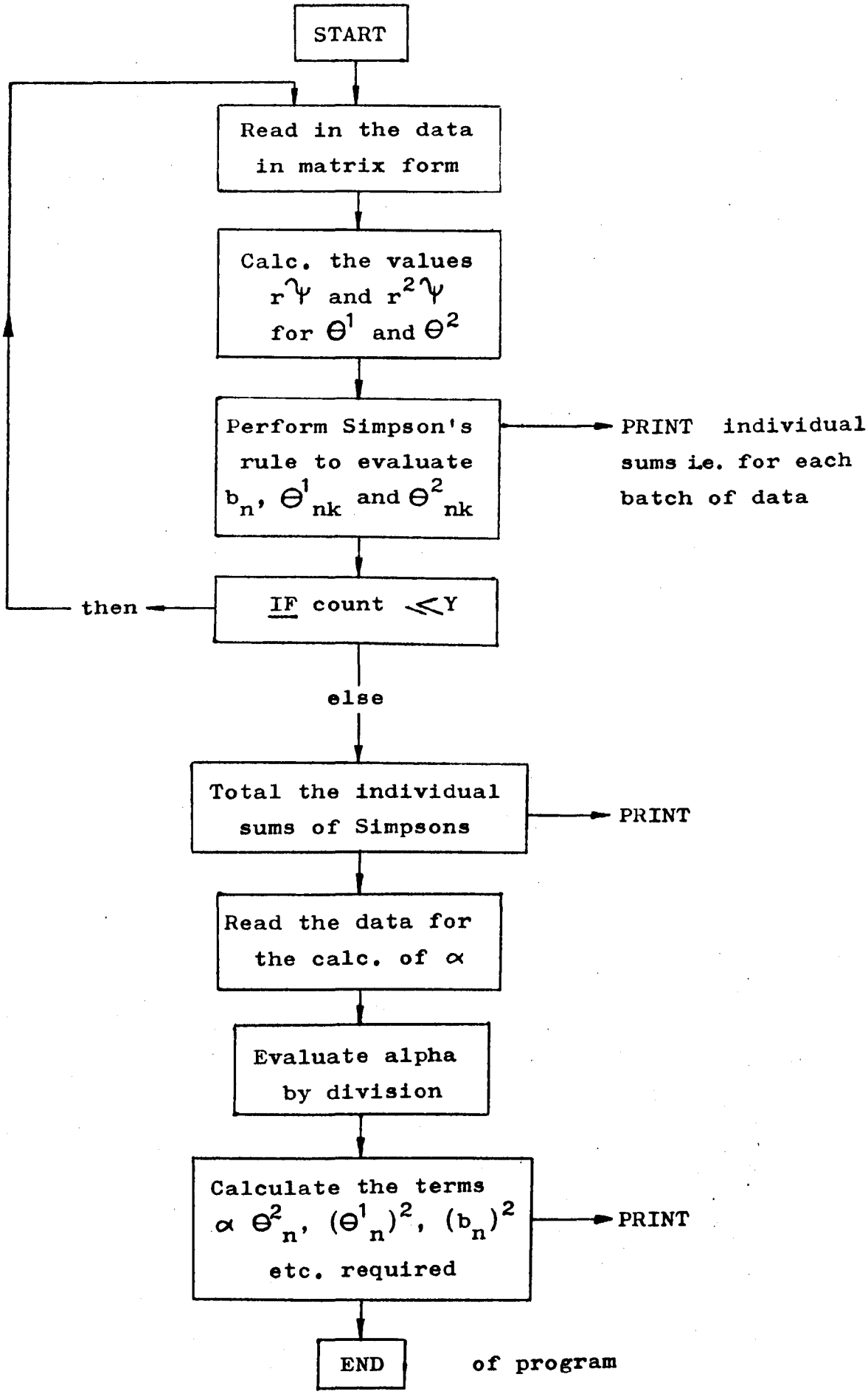
START
Read in the data in matrix form
Calc. the values $r\hat{\psi}$ and $r^2\hat{\psi}$ for θ^1 and θ^2
Perform Simpson's rule to evaluate b_n, θ^1_{nk} and θ^2_{nk}
PRINT individual sums i.e. for each batch of data
IF count $\ll$ Y
then
else
Total the individual sums of Simpsons
PRINT
Read the data for the calc. of α
Evaluate alpha by division
Calculate the terms $\alpha\ \theta^2_n$, $(\theta^1_n)^2$, $(b_n)^2$ etc. required
PRINT
END
of program

```
& JOB;  PH/R007/01;
& ALGOL;
  LIBRARY
  ALGOL
& LIST;
  KNIGHT SHIFT PROGRAM TO EVALUATE OVERLAP INTEGRALS
  "BEGIN" "REAL" COUNT,ST1,ST2,ST3,SA1,SA2,SA3,SB1,SB2,SB3,SC1,
                 SC2,SC3,SF1,SF2,SF3,S1,S2,S3,M,H,X,P,R,
                 A1,AB,BB,T1T1,AT2,BT2;
        "REAL" "ARRAY"  XP[1:2,1:11],R2,R1,OV1,OV2,OV3[1:11];
        "INTEGER"       I,J,K,Y,N;
        "COMMENT"       We have M for 0.88534138 divided by the
                        cube root of the atomic number.  Y is
                        the number of Simpsons to be done for the
                        orbital minus one.  N is the number of
                        S-states of the atom.  Data cards start
                        by giving M, Y and N, the X for one
                        Simpson followed by P values, then the
                        step H.  Repeat for all Simpsons.  Then
                        one card with X of 0.01 and the P value
                        for all S-states to calc. alpha;
        "READ"          M,Y,N;
         COUNT:=0;  ST1:=0;  ST2:=0;  ST3:=0;
         RESTART:   "FOR" I:=1 "STEP" 1 "UNTIL" 2 "DO"
        "BEGIN" "FOR" J:=1 "STEP" 1 "UNTIL" 11 "DO" "READ" XP[I,J];
        "END";  "READ" H;
         SA1:=0;  SA2:=0;  SA3:=0;  SB1:=0;  SB2:=0;  SB3:=0;
         SC1:=0;  SC2:=0:  SC3:=0;  SF1:=0;  SF2:=0;  SF3:=0;
         S1:=0;  S2:=0;  S3:=0;
```

```
"FOR" J:=1 "STEP" 1 "UNTIL" 11 "DO"
"BEGIN"      R2[J]:=(XP[1,J])xM;
             R1[J]:=(R2[J])xM;
             OV1[J]:=R1[J]x(XP[2,J]);
             OV2[J]:=OV1[J]x(R2[J]);
             OV3[J]:=OV2[J]x(R2[J]);
"END";
"FOR" K:=2 "STEP" 2 "UNTIL" 10 "DO"
"BEGIN"      SA1:=SA1 + OV1[K];
             SA2:=SA2 + OV2[K];
             SA3:=SA3 + OV3[K];
"END";
"FOR" K:=3 "STEP" 2 "UNTIL" 9 "DO"
"BEGIN"      SB1:=SB1 + OV1[K];
             SB2:=SB2 + OV2[K];
             SB3:=SB3 + OV3[K];
"END";
 SC1:=OV1[1] + OV1[11];
 SC2:=OV2[1] + OV2[11];
 SC3:=OV3[1] + OV3[11];
 S1:=(SA1)x4 +(SB1)x2 + SC1;
 S2:=(SA2)x4 +(SB2)x2 + SC2;
 S3:=(SA3)x4 +(SB3)x2 + SC3;
 SF1:=((S1)xH)/3;
 SF2:=((S2)xH)/3;
 SF3:=((S3)xH)/3;
"PRINT"      FREEPOINT(5), 'SF1=',
             SAMELINE, SF1, 'SF2=', SF2, 'SF3=', SF3;
```

```
        ST1:=ST1 + SF1;
        ST2:=ST2 + SF2;
        ST3;=ST3 + SF3;
        COUNT:=COUNT + 1;
      "IF" COUNT "LE" Y "THEN" "GO TO" RESTART;
      "COMMENT"    We have calculated the values of the
                   overlap integrals and those are given by
                   ST1, ST2, ST3, they are not yet normalised;
      "PRINT"      FREEPOINT(5), 'ST1=',
                   SAMELINE, ST1, 'ST2=', ST2, 'ST3=', ST3;
      "FOR" I:=1 "STEP" 1 "UNTIL" N "DO"
      "BEGIN" "READ" X, P;
                   R:=MxX;
                   A1:=(P/R)x(1/(4x3.1418)↑(1/2));
                   AB:=(A1)x(ST1);
                   AT2:=(A1)x(ST3);
      "PRINT"      FREEPOINT(5), 'A1=',
                   SAMELINE, A1, 'AB=', AB, 'AT2=', AT2;
      "END";
        BB:=(ST1)↑2;
        T1T1:=(ST2)↑2;
        BT2:=(ST1)x(ST3);
      "PRINT"      FREEPOINT(5), 'BB=',
                   SAMELINE, BB, 'T1T1=', T1T1, 'BT2=', BT2;
      "END" OF PROGRAM;
& RUN;
        Data Cards

& END;
```

APPENDIX III

Sternheimer Antishielding Factors

The Sternheimer antishielding factor is introduced because the core electrons modify the nuclear quadrupole moment and thus alter the quadrupole coupling with an external electric field gradient i.e. for an external field gradient V_{kl} and an induced quadrupole moment γQ_{kl} the total energy of the system is

$$H_Q = \frac{1}{6}(1 + \gamma) \sum_{kl} Q_{kl} V_{kl}$$

Sternheimer has obtained numerical values of γ by using a first order perturbation technique to solve the Schrödinger equation.

These calculations have not been performed for all metals and, importantly, have very rarely been performed for almost neutral atoms, authors' prefering to do the calculations for fully ionised atoms. It is thus necessary to interpolate from the values in the literature and the interpolation procedure adopted is illustrated in the figure.

The shaded areas in this figure represent transition element groups, the dots are calculated values (taken from the literature) for fully ionised atoms. The two heavy lines give the approximate dependence of Sternheimer factors on Z for (I) elements before the transition set in each row of the periodic table and (II) elements after the transition set. The value for bismuth is based on the value in the literature for Bi^{3+} and is deduced via ratios, determined from data where the calculation

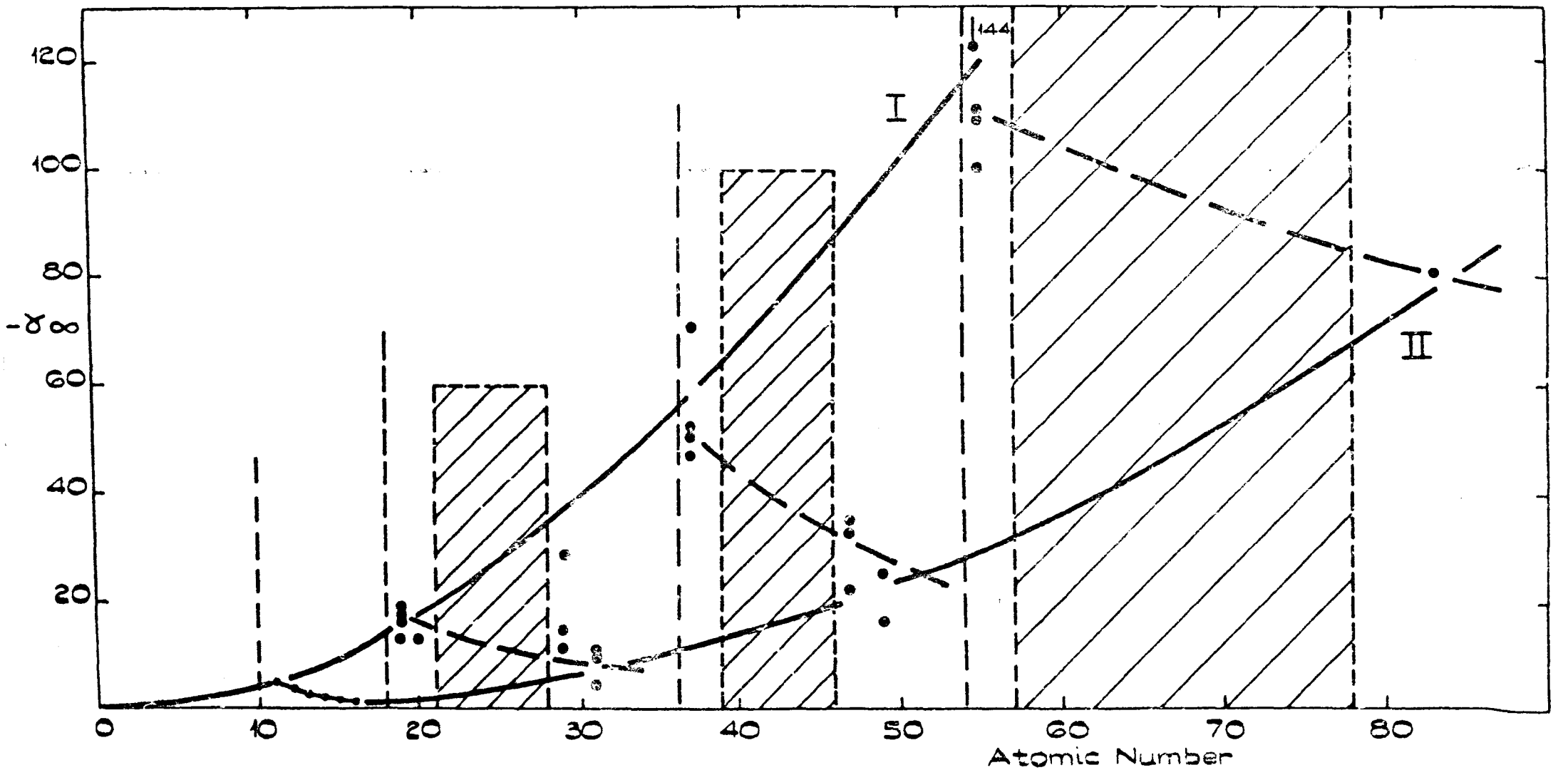
120
100
80
60
40
20
-α∞
0
10
20
30
40
50
60
70
80
Atomic Number
144
I
II

has been performed for all ionisation states.

The ratio of $\frac{\text{fully ionised}}{(n-1)\text{ ionised}} \sim 1.26$ and

the ratio of $\frac{\text{fully ionised}}{(n-2)\text{ ionised}} \sim 1.9$

for details see Clementi below

References

Sternheimer Phys. Rev., 102, (1956), 731.
Na^+, Cl^-, Cu^+, Rb^+, Cs^+ ions.

Das and Bersohn Phys. Rev., 102, (1956), 733
H^-, He, Li^+, Be^{++} and B^{+++}. Na^+ and Al^{+++}.

Wikner and Das Phys. Rev., 109, (1958), 360.
Cl^-, K^+, Cu^+, Ga^{+++}, Br^-, Rb^+, I^-, Cs^+.

Sternheimer Phys. Rev., 115, (1959), 1198.
Na^+, K^+, B^+, H^-, He, Li^+, Be^{++}.

Schwartz Ann. Phys., 6, (1959), 170.
H^-, He, Li^+, Be^{++}.

Burns and Wikner Phys. Rev., 121, (1960), 155.
Cu^+, Ga^{+++}, Kr, Ag^+, In^{+++}, Mn^{++}, Fe^{+++}.

Sachs Phys. Rev., 124, (1961), 1283.
Na^+.

Khubchandani, Sharma and Das Phys. Rev., 126, (1962), 594.
K^+, Cl^-.

Sternheimer Phys. Rev., 130, (1963), 1423.
Fe^{+++}, Mn^{++}, Ga^{+++}, Ag^+, Na^+, K.

Ingalls Phys. Rev., 130, (1963), 517.
Fe^{++}.

Watson and Freeman Phys. Rev., 132, (1963), 706.
Ce^{+++}.

Clementi J. Chem. Phys., 38, (1963), 996.
All ionisation states of all atoms up to Cl.
See also Roothan et al..

Roothan, Sachs and Weiss Rev. Mod. Phys., 32, (1960), 186.
Table VI.

Watson and Freeman Phys. Rev., 135A, (1964), 1209.
Br^-, Rb^+, I^-, Cs^+, La^{+++}, Ce^{+++}, Yb^{+++}.

Langhoff and Hurst Phys. Rev., 139A, (1965), 1415.
Li^+, Na^+, Cl^-, Be, Al^{+++}, Mg^+, Mg^{++}.

Lahiri and Mukherji Phys. Rev., 141, (1966), 428.
Li^+, Be^{++}, B^{+++}, C^{4+}, N^{5+}, O^{6+}, F^{7+}, Ne^{8+}.

Sternheimer Phys. Rev., 146, (1966), 140.
Be^{++}, Al^{+++}, Cs^+, Pr^{+++}, Tm^{+++}.

Sternheimer Phys. Rev., 159, (1967), 266.
In^{+++}, Bi^{+++}.

THE CALCULATION OF KNIGHT SHIFTS

J. HEIGHWAY, E. F. W. SEYMOUR and G. A. STYLES
University of Warwick, Coventry, England

Abstract: Holland has recently pointed out that values of Knight shifts may be very simply calculated to zero order in the pseudopotential. His results are calculated with the approximation that the pseudowavefunction for a conduction electron at the Fermi level does not vary appreciably over an ion core. This approximation is now removed and a correction to the shift evaluated for sodium, thereby improving agreement with experiment. This correction gives rise to a dependence of solvent shifts on solute concentration in alloys; the effect is less important for alkali metals as solvents than it is for copper and silver (Watson et al., 1968).

Holland [1] has recently pointed out that values of Knight shifts for pure metals may be very simply calculated to zero order in the pseudopotential. His results are obtained with the approximation that the pseudowavefunction for a conduction electron at the Fermi level does not vary appreciably over an ion core; this approximation is not essential and indeed Holland (private communication) has discussed the effect of its removal. The calculation without the approximation proceeds in the following way. The wavefunction $\psi(r)$ for a conduction electron can be expressed in terms of the pseudowavefunction $\phi(r)$ as

$$\psi(r) = C\{\phi(r) - \sum_{j,n} \psi_n(r-R_j) \int d^3r\, \psi_n^*(r-R_j)\, \phi(r)\} \qquad (1)$$

where C is a normalization constant and $\psi_n(r-R_j)$ is the nth core state of the jth ion. The integral occurring in this expression can be approximated as

$$\phi(R_j)\{b_n + \theta_n^{(1)} + \theta_n^{(2)}\}\,, \qquad (2)$$

where

$$b_n = \int d^3r\, \psi_n^*(r)\,, \qquad \theta_n^{(1)} = \int d^3r\, \psi_n^*(r)\, i\boldsymbol{k}\cdot\boldsymbol{r}\,, \qquad \theta_n^{(2)} = -\tfrac{1}{2}\int d^3r\, \psi_n^*(r)(\boldsymbol{k}\cdot\boldsymbol{r})^2$$

and $\phi(r)$ has been taken to be $V^{-\frac{1}{2}}\exp(i\boldsymbol{k}\cdot\boldsymbol{r})$ where V is the volume of the metal; the terms in eq. (2) arise from a series expansion of $\phi(r)$ about R_j; the first term only was retained by Holland [1]. Substitution of (2) into (1) and neglect of all terms containing powers of k higher than k^2 leads eventually to

$$\psi^*(R_j)\psi(R_j) = \frac{\phi^*(R_j)\phi(R_j)\gamma^2}{\beta}\{1-\delta\}\,, \qquad (3)$$

Colloque Ampère XV, North-Holland, Amsterdam, 1969

where

$$\delta = \frac{2}{\gamma}\sum_n \theta_n^{(2)}\alpha_n - \frac{1}{\beta\Omega}\sum_n (\theta_n^{(1)*}\theta_n^{(1)} + 2b_n\theta_n^{(2)}) ,$$

$\alpha_n = \psi_n(\boldsymbol{R}_j)$, the amplitude of the nth core function at the nucleus,

$$\beta = 1 - \frac{1}{\Omega}\sum_n b_n^* b_n$$

$$\gamma = 1 - \sum_n b_n\alpha_n ,$$

and Ω is the atomic volume. It will be noted that the new correction term δ is quadratic in k, the term linear in k being identically zero.

Eq. (3) with $k = k_F$ can be used in evaluating the Knight shift. The quantity δ represents a correction to Holland's expression for the shift itself; its dependence on k_F and on Ω introduces contributions to the change in shift on melting, to its temperature coefficient and to its change on alloying. The contribution to the change with electron-to-atom ratio of the type of effect we are concerned with here was first considered by Watson et al. [2]; they showed that the effect could explain the greater part of the observed changes in the shifts of copper and silver on alloying. We now consider the question of the magnitudes of the other effects we have mentioned, and evaluate them for the case of sodium.

Core state wavefunctions for sodium were taken from Tubis [3]. Using $\Omega = 37.9$ Å^3 and $k_F = 0.91$ Å^{-1} we find $\delta = -0.22$. Of this the term in $\theta_{2S}^{(2)}\alpha_{2S}$ contributes by far the greater part; indeed a rough estimate of δ can be obtained from this term alone (or in general for the corresponding term evaluated for the outermost core s-state), yielding

$$\delta \simeq -\frac{2\theta_{2S}^{(2)}}{b_{2S}} \simeq \tfrac{1}{5}k_F^2\,\overline{r_{2S}^2} , \qquad (4)$$

where $\overline{r_{2S}^2}$ is the mean square radius of the 2S core function. The resultant correction to the Knight shift as calculated by Holland improves the agreement between his result and experimental somewhat; his result of 0.12-0.13% (the uncertainty arising from lack of precise knowledge of the electron spin susceptibility) becomes 0.10-0.11%, compared with the experimental value of 0.11%.

The contribution, $\Delta K/K$, to the fractional change in shift on melting is readily evaluated from the known increase in atomic volume (2.5%) and the free-electron relation $k_F \propto \Omega^{-1/3}$. We find $\Delta K/K \sim +3.0 \times 10^{-3}$, this again arising largely from the factor k_F^2 within $\theta_{2S}^{(2)}\alpha_{2S}$; this result represents only a small part of the observed change of $+22 \times 10^{-3}$ (McGarvey and Gutowsky [4]).

In a similar way the contribution to the temperature coefficient $(1/K)(dK/dT)$ can be obtained from the expansion coefficient; for solid sodium we find $+2.5 \times 10^{-5}$ deg^{-1}C and for liquid sodium $+3.5 \times 10^{-5}$ deg^{-1}C,

compared with an observed value of about $+20 \times 10^{-5}$ deg^{-1}C for both solid and liquid (McGarvey and Gutowsky [4]).

The effect of increasing the electron-to-atom ratio by adding an atomic fraction c of Z-valent solute is found from $dk_F/dc = \frac{1}{3}(Z-1)(k_{F_{c=0}})$ to be $(1/K)(dK/dc) = -0.19(Z-1)$, neglecting volume changes. For mercury and cadmium as solutes in sodium, therefore, the contribution is -0.19, compared with observed values of -0.59 and -0.92, respectively (Kellington and Titman [5]).

Thus the contributions to changes in K due to change of state, temperature and electron-to-atom ratio are all smaller than the observed effects for sodium, though the last at least is not negligible. It is concluded that the dominant contributions to these changes must in this case arise from the first order term in the pseudopotential (Lackman-Cyrot [6], Watabe and Tanaka [7], and Faber [8]), but evaluation of this term will not be attempted here because the local pseudopotentials and model potentials currently available are not adequate for the purpose. That the contributions we have considered appear to be of less importance for sodium than for copper and silver may be due to the smaller size of the sodium ion compared with that of the sodium unit cell (and therefore with k_F^{-1}), than is the case for the other two metals.

Detailed calculations for the other alkali metals have not yet been completed, but it seems clear that in all cases the contribution to ΔK on melting is positive, that to $(1/K)(dK/dT)$ is positive, and that to $(1/K)(dK/dc)$ is negative for solutes with valence greater than unity. Since the observed effects do not always conform to these rules, e.g. $(1/K)(dK/dT)$ for cesium is negative (an estimate from eq. (4) gives a value of about $+5 \times 10^{-5}$ deg^{-1}C), it is concluded that the effect here considered is not the most important one for the alkali metal series as a whole.

We are indebted to Dr. B. W. Holland for many helpful discussions, to The Science Research Council for a research grant and a maintenance award (J. H.), and to Imperial Chemical Industries for the provision of a fellowship (G. A. S.).

REFERENCES

[1] B. W. Holland, Phys. Stat. Solidi, 28 (1968) 121.
[2] R. E. Watson, L. H. Bennett and A. J. Freeman, Phys. Rev. Letters 20 (1968) 653.
[3] A. Tubis, Phys. Rev. 102 (1956) 1049.
[4] B. R. McGarvey and H. S. Gutowsky, J. Chem. Phys. 21 (1953) 2114.
[5] S. H. Kellington and J. M. Titman, Phil. Mag. 15 (1967) 1045.
[6] F. Lackman-Cyrot, Physik Kondens Materie 3 (1964) 75.
[7] M. Watabe and M. Tanaka, Phil. Mag. 12 (1965) 347.
[8] T. E. Faber, Advances in Physics 16 (1967) 637.

ELECTRONIC STRUCTURE OF IMPURITIES IN LIQUID LEAD

J. HEIGHWAY and E. F. W. SEYMOUR
School of Physics, University of Warwick, Coventry, UK

Received 25 March 1969

The ^{207}Pb Knight shift has been measured in eight binary lead-base liquid alloy systems. The results differ radically from the corresponding results in the solid state.

No completely satisfactory explanation of the variation Γ ($= dK/K\ dc$) of the solvent Knight shift K with solute concentration c is available even for dilute alloys. However Blandin et al. [1], on the basis of a free electron model, accounted semiquantitatively for the values of Γ of monovalent solvents through oscillations of electron charge density around impurity atoms. The oscillations were described by phase shifts η_l for electrons at the Fermi surface, calculated by representing impurities by square-well potentials. Such a scheme is less successful for polyvalent solvents [2]. Rigney and Flynn [3] suggested an alternative choice of phase shifts based on the idea that the s-wave content of the displaced charge cannot cause the total s-electron content of the solute cell to exceed two. This led to a qualitatively correct description of the dependence of Γ on solute-solvent valence difference for solvents of all valences. To obtain quantitative agreement Flynn called on a scaling factor typically between 0.25 and 1 attributed to electron-electron interactions. However, the factor required for lead in solid lead alloys at room temperature [4] is about -0.08. To distinguish between the occurrence of a factor so different from

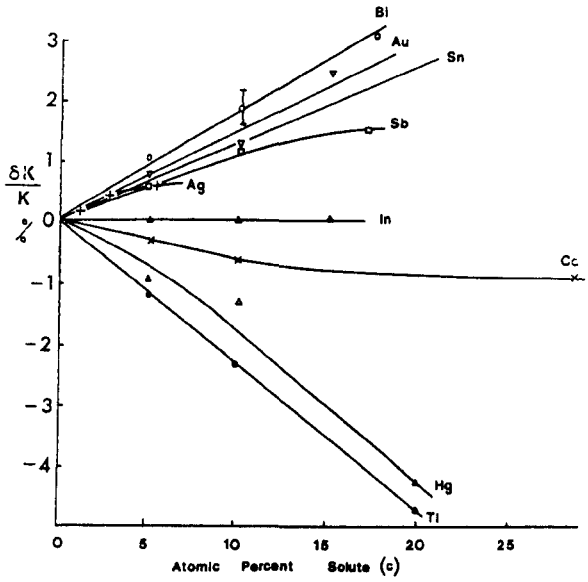

Fig. 1. Fractional change of ^{207}Pb Knight shift with solute concentration at 625°K. The data for tin are taken from [5].

unity and the possible effect of the ignored band structure in the solid, measurements of Γ have been made in liquid lead alloys where we believe the free electron basis to be more appropriate.

Fig. 1 shows $\delta K/K$ for ^{207}Pb at 14 kG as a function of solute concentration in several liquid alloys. The results are strikingly different from those in the solid at room temperature, the sign of Γ having reversed and its magnitude increased in almost every case. In order to compare the values of Γ with the theoretical expression [1]

$$\Gamma = \sum_l \{A_l \sin^2 \eta_l + B_l \sin 2\eta_l\}$$

we have calculated values of the coefficients A_l and B_l from the experimental radial distribution function [6] for pure liquid lead. The values obtained are $A_0 = -0.04$, $B_0 = -0.20$, $A_1 = -0.24$, $B_1 = +0.49$. For a tetravalent solvent the model [3] requires $\eta_0 = 0$ for solutes which leave the s-electron content of a cell equal to two, so that $\eta_1 = \frac{1}{6}\pi x$ (valence difference) if higher order partial waves are neglected. We consider here the predictions for p-wave scattering only, for the simplest cases viz. Hg, Tl and Bi, omitting the more complex cases of monovalent solutes (where s-wave scattering enters) and solutes not in the same row of the periodic table as lead (since differing core structures are not described by phase shifts derived solely from valence differences). The calculated Γ values, with experimental values in brackets, are: Hg, -0.60(-0.18); Tl, -0.48(-0.24); Bi, +0.36(+0.18). Thus a scaling factor of +0.3 to +0.5, rather than -0.08, seems to be required - a factor of the same sign and order as those required for solvents of other valences. Further, since the change in the radial distribution function on melting is far from sufficient to explain the differences between the results for the solid at room temperature and those for the liquid, we suggest that the results in the solid are affected by its band structure.

We have investigated how the differences in behaviour of solid and liquid arise, by following the variation with temperature of $\delta K/K$ for ^{207}Pb in pure lead and in a typical alloy, Pb-18%Bi. The change from negative to positive Γ is a progressive one, occurring partially as the temperature of the solid is increased, and partially on melting. There is no feature of this theory which would account for such a large temperature coefficient of Γ in the solid. By contrast there is no further change in Γ with temperature in the liquid state. This relative simplicity of the behaviour in the liquid reinforces our view that the free-electron-based considerations used here are more appropriately applied to the liquid state than the solid.

We wish to acknowledge the receipt of a research grant and a maintenance award (J.H.) from the Science Research Council.

References

1. A. Blandin, E. Daniel and J. Friedel, Phil. Mag. 4 (1959) 180.
2. E. F. W. Seymour and G. A. Styles, Proc. Phys. Soc. 87 (1966) 473.
3. D. A. Rigney and C. P. Flynn, Phil. Mag. 15 (1967) 1213.
4. R. J. Snodgrass and L. H. Bennett, Phys. Rev. 134 (1964) A1294.
5. D. J. Moulson and E. F. W. Seymour, Adv. in Phys. 16 (1967) 449.
6. R. Kaplow, S. L. Strong and B. L. Averbach, Phys. Rev. 138 (1965) A1336.